Design and Optimization of Resorbable Silk Internal Fixation Devices

A thesis submitted by
Dylan S. Haas

In partial fulfillment of the requirements for the degree of

Master of Science
In

Biomedical Engineering

TUFTS UNIVERSITY

February 2015

Advisor: David L. Kaplan

Abstract

Limitations of current material options for internal fracture fixation devices have resulted in a large gap between user needs and hardware function. Metal systems offer robust mechanical strength and ease of implantation but require secondary surgery for removal and/or result in long-term complications (infection, palpability, sensitivity, etc.). Current resorbable devices eliminate the need for second surgery and long-term complications but are still associated with negative host response as well as limited functionality and more difficult implantation. There is a definitive need for orthopedic hardware that is mechanically capable of immediate fracture stabilization and fracture fixation during healing, can safely biodegrade while allowing complete bone remodeling, can be resterilized for reuse, and is easily implantable (self-tapping). Previous work investigated the use of silk protein to produce resorbable orthopedic hardware for non-load bearing fracture fixation. In this study, silk orthopedic hardware was further investigated and optimized in order to better understand the ability of silk as a fracture fixation system and more closely meet the unfulfilled market needs. Solvent-based and aqueous-based silk processing formulations were cross-linked with methanol to induce beta sheet structure, dried, autoclaved and then machined to the desired device/geometry. Silk hardware was evaluated for dry, hydrated and fatigued (cyclic) mechanical properties, *in vitro* degradation, resterilization, functionalization with osteoinductive molecules and implantation technique for fracture fixation. Mechanical strength showed minor improvements from previous results, but remains comparable to current resorbable fixation systems with the advantages of self-tapping ability for ease of implantation, full degradation in 10 months, ability to be resterilized and reused, and ability to release

molecules for osteoinudction. *In vivo* assessment confirmed biocompatibility, showed improved bone deposition and remodeling with functionalization and showed promising feasibility of fracture fixations with minor adjustments to geometry. The proposed silk orthopedic hardware exhibits high potential as a resorbable fixation system that can bridge the gap between the current materials for internal fixation devices.

Acknowledgements

I would like to thank my advisor Dr. David Kaplan for your guidance, motivation and support in all that I have done over the past year. I would also like to thank the rest of my committee members, Dr. Sam Lin and Dr. Fiorenzo Ominetto for your advice and support in the pursuit of my research. As a group your passion for research and willingness to provide endless support, knowledge and resources allowed me to accomplish my goals and gain a wide breadth of knowledge and research experience.

I am also very grateful for all the help from my collaborators at Beth Israel Deaconess Medical Center and Children's Hospital for all the help with in vivo procedures from performing surgeries to providing invaluable advice.

I would like to express endless gratitude to all of you at Tufts for the help, support and friendship. Thank you to Jon Kluge, Jodie Moreau, Rod Jose, Roberto Elia, Joe Brown, Jeannine Coburn, David Wilbur, Dan Smoot and the rest at 200 Boston Ave for advice and help with everything from tests/analysis to daily frustrations. A special thanks to Scott MacCorkle for all the work with machining of silk devices and to Gabe Perrone for all the initial work he accomplished with this project and affording me the opportunity to continue it.

I would like to thank my coworkers at Silk Therapeutics Inc for their endless support and their tolerance of my crazy schedule.

Lastly I would like to thank my parents, brother, and the rest of my friends and family. Without your love, support and encouragement, nothing I do would be possible.

Contents

List of Figures

List of Tables

Chapter 1. Introduction

1.1 Orthopedic Hardware for Fracture Fixation

Until the 1900's, bone fractures were often considered life-threatening, permanent injuries due to the lack in medical technology of a system to fix a fractured bone in such a way that it could heal properly. The development of orthopedic hardware has enabled the ability to not only restore normal anatomy after a fracture but also achieve recovery of function [1]. The goal of fixation devices is to stabilize fractured bone enabling rapid bone healing and remodeling to restore full function and mobility. Orthopedic hardware for fixation is composed of two main classes: external and internal fixation devices. External fixation devices are based on the idea of splinting and include systems composed of splints, casts, rods, wires and pins. Internal fixation devices are used when the fractured bone must be exposed through open reduction and includes wires, pins, screws, plates and intramedullary nails or rods [1,2]. Internal fixation devices will be the focus of the work in this investigation. Fixation devices can also be categorized into two classes of biomaterials: metal and resorbable hardware. Metal systems such as titanium and stainless steel, have been considered the gold standard for decades due to their robust mechanical properties, biocompatibility, ease of fitting and implantation and ability to be resterilized [3][4][5]. These systems were able to address what was considered to be the requirements of a fixation material; sufficient strength to maintain fracture stabilization and resist physiologic stresses until healing was complete, while being sufficiently malleable to allow in situ plate placement and thin enough to minimize palpability, visibility and discomfort [6]. However, key disadvantages including permanence or need for removal, atrophy and poor bone remodeling of underlying bone, corrosion, loosening

and implant migration and complications with cold and medical imaging spawned questions of long term safety and efficacy, particularly for facial fractures [3,4,6,7][8][9]. With the advancement of biodegradable polymers, resorbable fixation devices became an attractive option to provide strength when necessary for bone healing and then degrade safely over time, eliminating long term complications or need for removal. Bioabsorbable materials also have elasticity much closer to bone than metals, which would minimize stress complications and potentially improve bone remodeling [4,7][10][9]. The challenge in use of resorbable materials for fracture fixation involves the ability to provide sufficient strength and rigidity over time, ease of implantation and safe biodegradation. Related to the issue of strength, resorbable biomaterials have thus far mainly been applied to non-load bearing applications such as craniomaxillo facial fractures (CMF). Lead candidates for resorbable devices include polylactic acid (PLA), poly-L-lactic acid(PLLA), poly-DL/L-lactic acid (P(L/DL) LA), poly glycolic acid and copolymers of these families [6,7]. The work presented here will focus on a new candidate biomaterial for open reduction and internal rigid fixation of non-load bearing areas such as the CMF complex.

Chapter 2. Background

2.1 Fracture Fixation: Open Reduction and Internal Fixation

Bone fractures are one of the most commonly seen injuries with a wide range of type, location and severity. Fractures can be complete or incomplete, open or closed, can occur in a variety of bone types and locations and therefore require a wide range of fixation techniques and devices [2]. Internal fixation devices for open reduction and internal fixation will be highlighted in the present work. Open reduction and internal

fracture fixation refers to the fixation of a bone fracture by opening of the patient to expose the fractured bone and fixation of the fracture through the use of an internal device implanted into the patient [2].

The first use of a fixation device was in 1775 by Lapeyode and Sicre in which a long bone fracture was stabilized through the use of iron wire. In 1847, the first metallic fixation device for craniomaxillofacial was created using interosseous wire for a mandibular fracture. Dr. Carl Hansmann is credited with the first use of rigid internal fracture fixation in 1858 with the use of a plate and screw system. It was not until the early 20th century that internal fixation became widespread due to the development and advancement of corrosion resistant materials such as Vitallium in 1936. Stainless steel became a popular metal option and was the implant of choice until the mid 1980s. In 1983 Branemark provided insight into titanium as the best option for metallic internal fixation devices due to superior biocompatibility and favorable mechanical properties. Biodegradable orthopedic hardware first emerged in the mid 1990s [3,6]

Open reduction and internal fracture fixation has been used clinically since the late 1950's and provides the ability to overcome limitations of external fixators such as casts, in regards to restoration of function and speed of healing or mobilization. The primary goal is to achieve full function with rapid rehabilitation. Internal fixation devices include wires, pins, screws, plates and intramedullary nails or rods [2].

2.2 Indication Area: Craniomaxillofacial complex

The proposed system of orthopedic hardware will initially target non-load bearing applications with a primary focus on the craniomaxillofacial complex (CMF) (Figure 1). The CMF is the anatomical area consisting of the skull, mouth, jaw and face. The CMF

is a primary example of non-load bearing fixation location and can therefore be fixated with devices of lesser strength and stiffness than metallic systems. Currently, resorbable systems are primarily approved for CMF procedures, with the majority of clinical experience in elective pediatric procedures [6]. The initial proposed indication for the silk orthopedic hardware will be CMF fixation by plates and screws. Other applications may be feasible with the production of silk intramedullary nails but will not be investigated past fabrication feasibility.

Figure 1. Craniomaxillofacial Complex representation from Biomet Microfixation [11]

2.3 Current Fixation Device Systems

2.3.1 Market

Bone fracture requiring osseous fixation and orthopedic repair is a prevailingly frequent injury with 60-65% of nearly 40 million annual ER visits involving orthopedic injuries. A total of 40-45% of these visits require fracture repair techniques and devices

[12,13]. These numbers do not take into account additional non-ER repairs and the possible need for multiple fixations in a single case. The American Society of Plastic Surgeons reported 209,000 CMF surgical procedures, which is a 164% increase from 2010 and a 7% increase from 2011[14]. Millennium Research Group reports that the increase in volume of CMF procedure along with the adoption of premium priced devices will lead to modest expansion in the US CMF device market through 2017. The CMF device market that includes plate and screw fixation, intramedullary(IM) nails, cannulated screws, bone graft substitutes (BGS), cranial flap fixation devices, CMF distraction devices, temporomandibular joint (TMJ) replacement devices and more, is dominated by plates and screws with a 75% share (MRG CMF devices 2013). The growth and demand of this market and industry are self-sustaining due to the non-elective nature of bone fractures and associated necessary repair. The gold standard for fixation devices are metals, particularly titanium alloys, due to the delivery of robust mechanical properties for secure fixation, ease of implantation and ability to be resterilized for reuse [3,5]. Due to major limitations in bone remodeling and need for second surgery removal, there is potential in a biodegradable fixation system able to meet the mechanical requirements of bone fixation while slowly degrading, reducing complications and improving long term outcomes. For this reason, there has been interest into bioresorbable orthopedic hardware in the past few decades. The family of polyesters including poly-lactic acid (PLA) and poly-glycolic acid (PGA) has been the lead candidate for these systems.

2.3.2 Metal Hardware

Metal orthopedic hardware systems have always been the primary internal fixation device option, even for adult CMF (Figure 2, Figure 3). Metal systems have

robust mechanical properties with strength and stiffness sufficient to fix fractures even in load-bearing extremities. Metallic systems are also associated with easy implantation technique. For screw placement, a pilot hole is drilled and screws can be immediately inserted due to the self-tapping capabilities of these systems. The ductility of metal also allows for easy shaping and adjusting of plates intra-operatively to fit the specific conformation of the fracture area. Metal orthopedic hardware can be resterilized and reused if opened in the operating room and not implanted into a patient [3]. The mechanical integrity of the hardware can be maintained even after 50 autoclave cycles [5].

Figure 2. Synthese Titanium MatrixMIDFACE. [15]

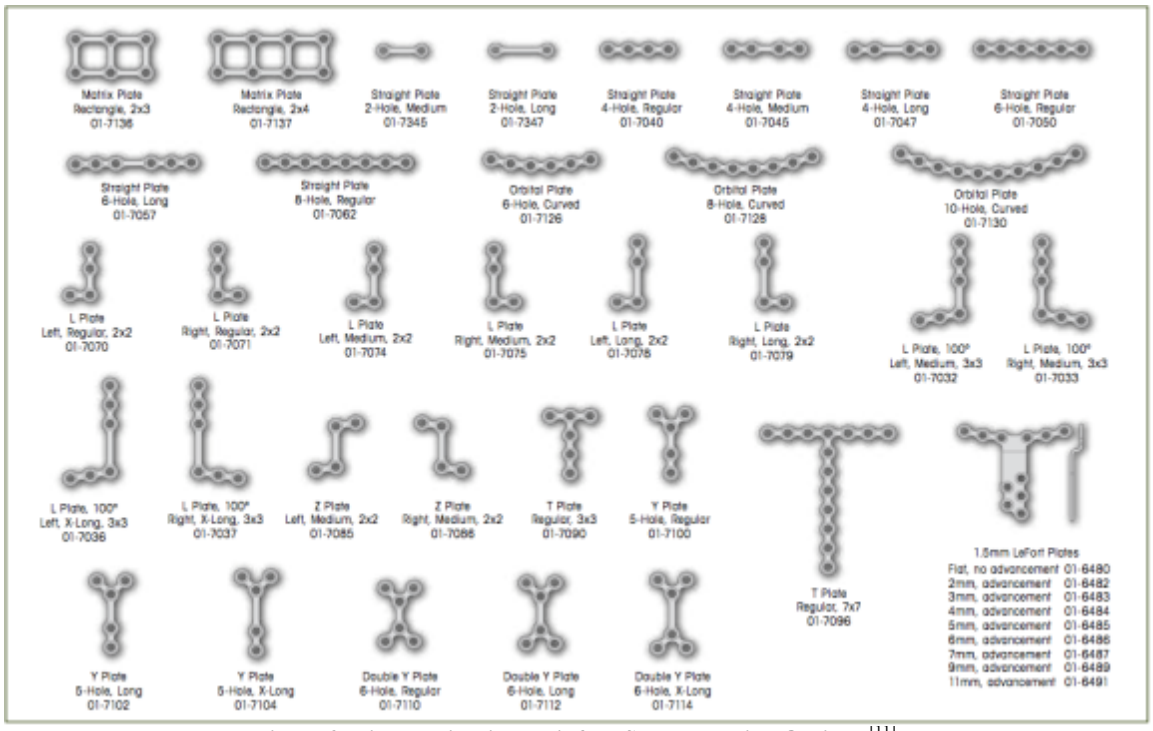

Figure 3. Biomet Titanium Midface System Plating Options [11]

Although metal systems are often regarded as the gold standard, there are significant drawbacks and disadvantages associated with them. One of the biggest concerns with metallic hardware is the permanence of the device. Once fracture healing is complete, the fixation systems are effectively useless. Therefore, any negative complication from palpability or sensitivity to cold or inflammation due to corrosion will potentially affect patients for their lifetime unless removed [3]. Hardware removal presents a number of negatives issues including cost, scarring, risk of infection (particularly hospital acquired infections), increased recovery time and general risk and patient fear of another surgery. The reason for hardware removal is rarely by choice but rather related to one or more of the other possible complications of metal internal fixation devices. Some of the potential problems include wound dehiscence, temperature sensitivity, poor bone remodeling, stress shielding due to mismatch in modulus with bone, poor wound healing and plate exposure, palpability, device migration, pain, various

infections, corrosion (sometimes causing renal failure), limited radiological imaging and therapy, growth disturbance in children, loosening of hardware and more [3,6,8,10,16–21]. The most commonly used metals for orthopedic hardware are stainless steel, cobalt based alloys and titanium. Comparison of these metal options is detailed in Table 1.

Table 1. Comparison of options for metallic fixation devices [3,6,22]

Metal	Description
Stainless Steel	• Contains variable amounts of nickel, chrome, manganese, vanadium and/or molybdenum • Possible issues with corrosion resistance in vivo. Corrosion products may lead to tissue granulation or infection • High elastic modulus causes stress shielding • Tensile Strength: 250 MPa • Bending Strength: 280 MPa
Cobalt Based Alloys	• Vitallium is the most common cobalt based alloy and was popularly used until the shift toward titanium • Twice the tensile strength, 50% more yield strength and twice the hardness than some other metals such as other cobalt alloys and even stainless steel • Corrosion products can lead to health issues
Titanium	• Biocompatible and corrosion resistant • Closer elastic modulus to bone for less stress shielding • Creation of 10 micron thick layer of titanium-oxide in vivo offering corrosion resistance and adhesion of glycoproteins for better bone remodeling • Some osseointegration with bone to prevent screws becoming loose • Expensive

2.3.3 Resorbable Hardware

Development and advances in the medical use of biodegradable materials has led to the development of bioabsorbable orthopedic hardware systems to overcome the shortcomings of metallic systems. Bone healing of a fracture site can take up to 12 weeks in load bearing areas and as little as 4 weeks in non load bearing areas. Fracture

stabilization by rigid internal fixation devices is only necessary until fracture healing is complete, after which the devices is rendered useless [23]. The use of resorbable hardware obviates the need for second surgery removal and limits complications such as thermal sensitivity, issues with radiological imaging and stress shielding due to extreme stiffness of metals [3,6]. The use of biodegradable hardware (Figure 4) has been supported by clinical use showing that sufficient strength for fixation of non-load bearing fractures can be achieved with resorbable systems that do not require removal and provide a more gradual transfer of stress from device to bone allowing improved bone remodeling [10,17,19,21,24–28]. Although load bearing applications require the mechanical properties of metallic systems, areas such as the CMF do not require such strength and rigidity and thus weaker resorbable hardware can be used. The development of bioresorbable orthopedic hardware began in the 1960s but it was not until the 1990s that these devices gained clinical significance and use. Biomaterials that have been used for resorbable systems mainly include polyesters such as polylactic acid (PLA), polyglycolic acid (PGA), poly-lactic-co-glycolic acid, polycaprolactone, polyhydroxybutyrate, polytrimethylcarbonate, polydioxanone and polyurethane. The most commonly used materials include the group of PLA, PGA and PLGA that include different ratios and stereoisomers of these polymers [3,6].

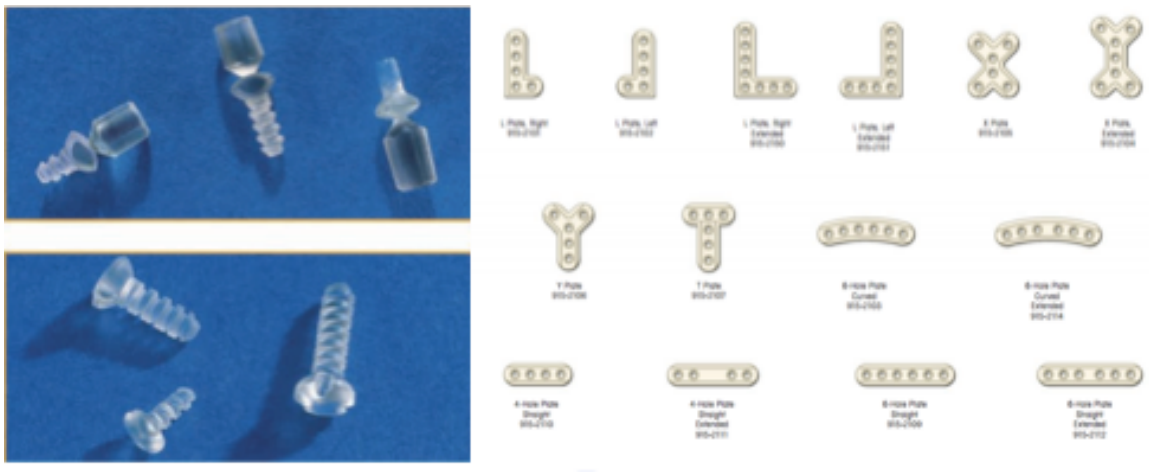

Figure 4. Biomet Lactosorb Resorbable Plates and Screws [11]

Polylactic acid is a polymer of the monomer lactic acid, which has two enantiomeric forms, L-lactic acid and D-Lactic acid. Poly-L-lactic acid (PLLA) refers to the pure L-lactic acid polymer. PLLA has the highest strength but can take up to 4-6 years to degrade. For this reason, copolymers of the L- and D- sterioisomers are more common. Biosorb FX (Bionx Implants Inc., Tampere, Finland) uses a 70L:30D ratio that shows adequate strength and degrades in 2-3 years. Polyglycolic acid is a polymer with units of glycolic acid. PGA is usually self-reinforced in order to obtain strong mechanical properties but will degrade in about 1 year. However, pure PGA is associated with inflammation in about 60% cases[7]. More commonly used is a copolymer of PLLA and PGA referred to as PGA. By copolymerizing L-lactic acid and glycolic acid units in different ratios, properties such as degradation time and mechanics can be tailored. There is usually a trade-off between the strength and degradation. Lactosorb (Walter Lorenz Surgical, Jacksonville, FL) is an 82 PLLA:18 PGA ratio that is currently commercialized. These devices retain most of their strength for the first 2 months and degrade in a year or more. Swelling and inflammation has remained an issue due to the use of PGA [3,6,7][19].

Table 2 and Table 3 summarize the characteristics and properties of PLA, PGA, PLGA and current commercialized systems.

Table 2. Mechanical and Degradation Characteristics of PLA/PGA/PLGA Resorbable Fixation Systems [8]

Monomer	Glass Transition Temperature, °C	Flexural Strength, MPa	In Vivo Degradation Time	
			Strength	Mass
Polyglycolic acid	35-40	320	4-6 wk	6-12 mo
Poly L-lactic acid	60-65	190	6 mo	1-6+ y
Poly DL-lactic acid	55-60	150	8-12 wk	12-16 mo
Polydioxanone	16	120	4-6 wk	6-12 mo

System; Manufacturer (Date of Introduction)	Polymer Composition (%)	In Vivo Time	
		Remaining Strength (%)	Complete Resorption
LactoSorb; W. Lorenz Surgical Inc, Jacksonville, Fla (February 1996)	PLLA (82); PGA (18)	8 wk (70); 12 wk (30)	6-12 mo
Macropore; Medtronic, Minneapolis, Minn (July 1998)	PLLA (70); PDLLA (30)	6 mo (90); 12 mo (50)	1-3 y
Bionx; Bionx Implants Inc, Bluebell, Pa (December 1998)	PLLA (70); PDLLA (30)	8 wk (90); 6 mo (30)	1-2 y
Resorbable Fixation System; Synthes, Paoli, Pa (February 2000)	PLLA (70); PDLLA (30)	8 wk (68); 6 mo (30)	1-6 y
DeltaSystem; Styker-Leibinger, Kalamazoo, Mich (March 2000)	PLLA (85); PDLLA (5); PGA (10)	8 wk (81); 6 mo (50)	1.5-3 y

Table 3. Characteristic Summary of Current Commercial Resorbable Internal Fixation Systems[6]

	Stryker Inion CPS*	Synthes Rapid†	Biomet LactoSorb SE‡	KLS Martin Resorb X and SonicWeld Rx§
Composition	Varying combinations of L-polylactic acid; D,L-polylactic acid; polyglycolic acid; trimethylene carbonate	85:15 poly (L-lactide-*co*-glycolide)	82:18 poly L-lactic acid: polyglycolic acid	Both systems are 100% poly (D,L-lactic acid)
Degradation characteristics	BABY: strength retention 6–9 weeks; resorbed in 1–2 years ADULT: strength retention 9–14 weeks; resorbed 2–3 years	85% strength at 8 weeks; resorbed within 12 months	70% strength at 8 weeks, resorbed within 12 months	Strength retention to 10 weeks; resorbed in 1–2 years
Available sizes for craniomaxillofacial use	BABY system: 1.5 mm ADULT system: 1.5, 2.0, 2.5 mm 2.8/3.1-mm (screws only)	1.5-mm system 2.0-mm system	1.5-mm system 2.0-mm system 2.5/2.8-mm (screws only)	Both Resorb X (screws) and SonicWeld Rx (pins): 1.6-mm system; 2.1-mm system
Plate profile (thickness)	1.5-mm system: 1.0 mm 2.0-mm system: 1.3 mm 2.5-mm system: 1.7 mm	1.5-mm system: 0.8 mm 2.0-mm system: 1.2 mm	1.5-mm system: 1.0 mm 2.0-mm system: 1.4 mm	Resorb X and SonicWeld Rx: all plates shapes 1.0 mm
Screw placement	Self-drilling tap or separate tap	Self-drilling tap or separate tap	Self-drilling tap or separate tap; push screws (no tapping required)	Resorb X: screws with self-drilling tap SonicWeld Rx: drill hole for pins and secure with ultrasonic frequency welder (no tapping required)
Indicated for mandible fractures	Yes (with IMF only)	No	No	No

As previously stated, resorbable devices currently are used for non-load bearing CMF applications for which the weaker mechanical properties are sufficient. Although the strength requirements are met for fixation, there are limitations in implantation and handling. The current materials are softer than bone and thus require pre tapping before screw insertion. For plate shaping and implantation, the polymeric material must be heated passed its glass transition temperature in order to become flexible. In the case of PLA, PGA and PLGA the glass transition occurs at about 40-60ºC meaning that plates must be preheated by pads or probes before placement. Heating the plates also introduces the risk of effecting structure and stability if over heated. If screws are opened in the operating room and not used, they can not be resterilized by autoclaving like the metal counterparts due to instability at such high temperatures above the glass transition [3,8]. Once the plate is

shaped and screw holes are drilled and threaded, there is still a risk of fracture of the screw upon insertion due to poor torsional properties [3,27].

2.4 Bone

2.4.1 Morphology

Bone tissue is morphologically diverse and consists of a hierarchy of structures (Figure 5). At the top of the hierarchy is the macrostructure consisting of cortical and cancellous bone. All types of bones (location, flat vs. long bone) are composed of different quantities and orientations of these two categories of bone with cortical bone being the outer shell to cancellous bone. Cortical bone is dense and has low porosity while cancellous bone is sponge-like with low density and high porosity. The second level of hierarchy is the microstructure which is composed of osteons, Haversian systems and trabecullae. Osteons and haversian systems are prominent in cortical bone while trabecullae are the building block of cancellous bone structure. Below the microstructure is the sub-microstructure which consists of lamellae. Lamellae are planar arranged sheets of mineralized collagen fiber, that provide both structure (cortical or cancellous) and mechanical properties based on orientation. The fourth level of hierarchy in bone is the nanostructure consisting of the collagen fibers that make up lamellae. Last is the sub-nanostructure comprised of bone mineral crystals, collagen molecules and non collagenous proteins. This hierarchy systems provides for a very complex composite material capable of a wide range of mechanical properties, form and function (biological, chemical, structural) [29].

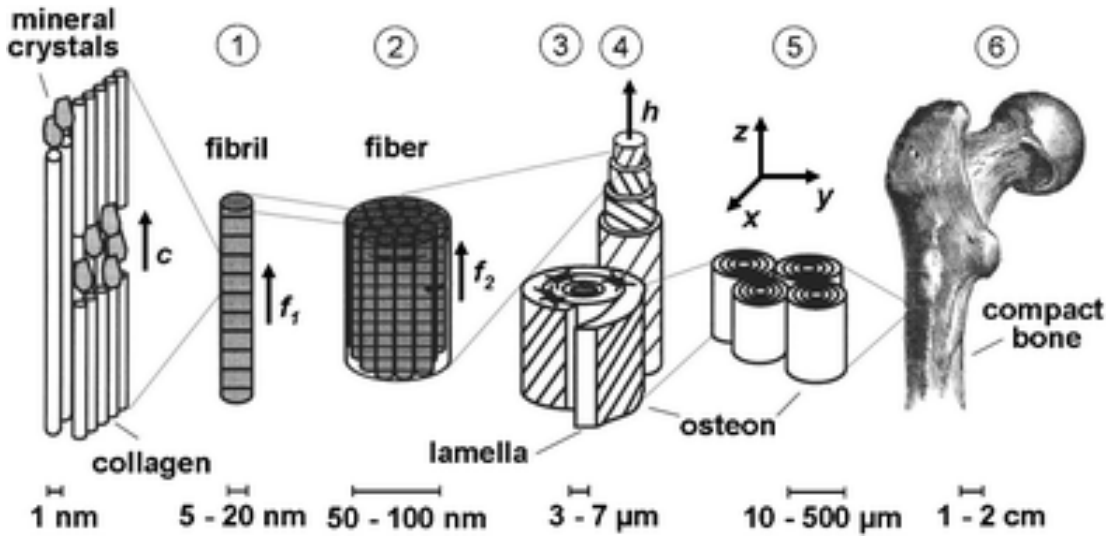

Figure 5. Hierarchial Structure of Bone: (1) Collagen Fibril composed of bone mineral crystals, collagen molecules, and non-collagenous proteins (2) Collagen Fiber (3,4)Lamella/ Haversian System (5) Osteon (6) Compact Bone (Cortical or Cancellous) [29]

2.4.2 Remodeling

Bone remodeling is a common, ongoing process for the body that is consistently carried out throughout life. Normal remodeling of bone can be broken down into a few steps: bone resorption during which osteoclasts remove and digest old bone; congregation of bone cells or osteocytes on the resorbed bone surface; new bone formation by osteoblasts to replace bone digested by osteoclasts; mineralization of the newly deposited bone [30]. Fracture healing adds another layer of complexity. Repair of fractured bone is characterized by an initial inflammatory response, soft callus formation, hard callus formation, bony union and bone remodeling. There are many different types of cells and molecules that are involved in this process. At the cellular level, inflammatory cells, vascular cells, progenitors, osteoclasts, osteoblasts and osteocytes all play major roles. At a molecular level, pro-inflammatory cytokines and growth factors, pro-osteogenic factors and angiogenic factors are the main classes involved [31]. One of the most prominent class of factors in the repair process are bone morphogenic proteins which

have a major role in osteoinducton in all stages of repair. In particular, bone morphogenic protein 2 (BMP-2) has been studied extensively for its natural role in bone induction as well as the ability to induce bone by external delivery of BMP-2 molecules [31,32]. Bone will remodel differently in response to mechanical stimuli. The more mechanical load applied to bone, the stronger and more dense it will be [31]. This is important with regard to resorbable internal fixation since the transfer of stress from device to bone will play a major role in how well the bone will remodel as the device degrades.

2.4.3 Relevant Biomechanical Properties

Bone is a very complex system and therefore mechanical properties vary greatly. It will be important to note some general biomechanical properties for this work. The elastic modulus of bone is directly related to the risk of stress shielding that an implant will cause. The bigger the mismatch in modulus, the more stress shielding will occur. Bone elastic modulus will vary but is about 20 GPa [6]. With regard to animal studies that will be used for proof of concept, the bone mineral density is important. If bone mineral density is very different than in human bones, the animal model may not be applicable. Rats will be used as the proof of concept model in this study. Table 4 summarizes bone mineral density in different animals compared to human. Bone mineral density is the density of mineral content such as calcium in the bone and is a reflection of bone health and strength. It can be seen that bone mineral density of rat is comparable to that of human in the femur [33]. Bone mineral density is not to be confused with density of bone. In the current application parietal bone density of humans will be most applicable as it is most widely used for mechanical testing of orthopedic hardware. Human parietal bone has a bone density of ~1.75-1.85 g/cm3 [34]. Compared to rat bone which has a bone

density of ~0.4-0.9g/cm^3, human bone is more dense [35]. Rats are commonly used for proof of concept studies for implant materials but are not considered ideal models for implant biomaterial research due to mismatches in physical properties [36]. However, rats are commonly used as an animal model for bone/bone implant research particularly for models of bone modeling/remodeling [37,38]. The present work will use a rat model for investigation into bone remodeling with BMP-2 loaded silk implants.

Table 4. Comparison of Bone Mineral Density of Human and Animal Models [33]

Species [Reference]	Mean BMD of controls ± SD/SEM	Mean difference osteoporotic vs control	Anatomical location
Human [20]	0.47 g/cm^3	−19%	Femur head
Human [21]	0.160 ± 0.034 g/cm^3 (SD)	−42%	Cancellous bone distal radius
Human [22]	1.079 ± 0.110 g/cm^2(SD)	−26% (2.5 SD)	Spine
Primate [23]	0.569 g/cm^2	−5%	Spine
Primate [24]	1.140 g/cm^2	−11%	Spine
Primate [14]	1.33 ± 0.09 g/cm^3	−2%	Femur head
Sheep [25]	0.62 ± 0.07 g/cm^3 (SD)	−13%	Spine
Sheep [25]	0.63 ± 0.08 g/cm^3 (SD)	−33%	Radius
Dog [13]	0.578 ± 0.020 g/cm^2 (SEM)	No change	Spine
Dog [12]	No information	No change	Tibia
Rat [26]	0.328 ± 0.01 g/cm^2(SEM)	−8%	Femur
Rat [27]	0.254 ± 0.006 g/cm^2 (SEM)	−7%	Femur
Mice [28]	0.069 ± 0.003 g/cm^2	−14%	Whole body

2.5 Silk Background

The use of silk as a biomaterial dates back centuries to ancient Egypt where physicians used silk fibers as a suture material. The use of silk in other formats has since been extensively studied in the last few decades. As seen in Figure 6 silk cocoons can be reformulated into a variety of formats including sponges, gels, films, microspheres and more through the use of different processing techniques and conditions. In Table 5, the wide range of applications for silk is depicted. The various formats of silk allow for applications from tissue engineering of varying tissues such as bone and tendons, to applications in drug delivery by microspheres and films [39].

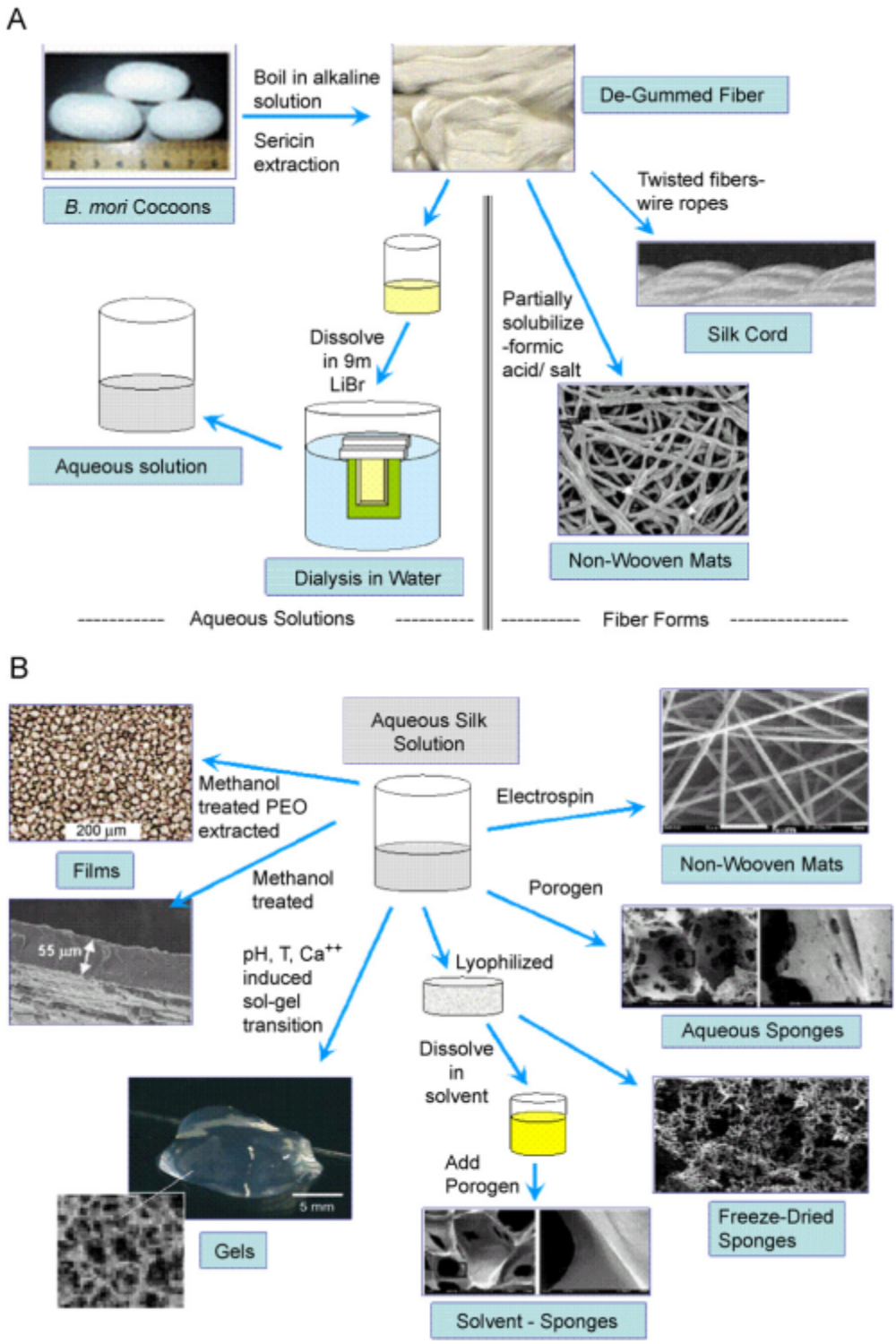

Figure 6. (A) Sericin is removed from Silk Fibroin. The purified silk can then be dissolved into an aqueous solution or processed into silk cords or non-woven mats. (B) Aqueous silk solution can be processed and reformatted into films, gels, non-woven mats and a variety of sponges. [40]

Table 5. Applications of Various Silk formats. [41]

Application	Tissue type	Material format
Tissue engineering		
	Bone	HFIP sponges
		Aqueous sponges
		Electrospun fibers
	Cartilage	HFIP sponges
		Aqueous sponges
		Electrospun fibers
	Soft tissue	HFIP sponges
		Aqueous sponges
		Hydrogels
	Corneal	Patterned silk films
	Vascular tissues	Tubes
		Electrospun fibers
	Cervical tissue	Aqueous sponges
	Skin	Electrospun fibers
Disease models		
	Breast cancer	HFIP sponges
		Aqueous sponges
	Autosomal dominant polycystic kidney disease	Aqueous sponges
Implant devices		
	Anterior cruciate ligament	Fibers
	Femur defects	HFIP sponges
	Mandibular defects	Aqueous sponges
Drug delivery		
	Drug delivery	Spheres
	Growth factor delivery	Spheres
	Small molecule	Spheres

Note: The sources for the reagents and equipment described in these protocols are given only as examples. Equivalent materials can be used unless otherwise noted.

Silk is a fibrous protein polymer that is spun by Lepidoptera larvae such as spiders, silkworms and flies [42]. Silk proteins are produced in specialized epithelial cells and secreted in specialized glands. The most widely studied and used silk is that of *Bombyx mori* silk worms. Silk from *B. mori* is composed of two proteins, the silk fibroin and a glue like protein called sericin. Sericin is a globular protein that coats the silk fibroin and acts as glue for the fibers. This provides structure and support for the silk cocoon. However, sericin has been immunogenic and for this reason is removed from the silk fibroin before processing in biomedical applications [42,43]. The silk fibroin fibers consist of two silk proteins. The light chain (~26 kDa) and the heavy chain (~390kDa) which are linked by a disulfide bone. The amino acid sequence of these proteins is composed primarily of glycine, alanine and serine. These sequences can be broken down further into domains with varying characteristics such as being crystalline or hydrophobic/hydrophilic.. The silk proteins form into three main physical structures: random coil, α-helix (Silk I), and anti-parallel β-sheets (Silk II). Different properties and characteristics of silk have been observed based on the variability in these structural levels. For example, high β-sheet content is indicative of high order and tight structural packing providing better mechanical properties [40,42–44].

2.5.1 Benefits of Silk as a Biomaterial

Silk is widely used in biomedical applications due to its robust mechanical properties, biocompatibility, biodegradation and the ability to tune such properties. Comparison of mechanical properties including modulus, ultimate tensile strength and percent strain at break can be seen in **Error! Reference source not found.**, where *B.*

mori silk has favorable strength in all of these properties compared to collagen, PLLA, tendon and other biomaterials.

Table 6. Summary of Mechanical Properties of Silk and other Biomaterial Fibers [42]

Material	UTS (MPa)	Modulus (GPa)	% Strain at break	Authors
B. mori silk (w/ sericin)[a]	500	5–12	19	Perez-Rigueiro et al. [68]
B. mori silk (w/o sericin)[b]	610–690	15–17	4–16	Perez-Rigueiro et al. [68]
B. mori silk[c]	740	10	20	Cunniff et al. [13]
Spider silk[d]	875–972	11–13	17–18	Cunniff et al. [13]
Collagen[e]	0.9–7.4	0.0018–0.046	24–68	Pins et al. [69]
Collagen X-linked[f]	47–72	0.4–0.8	12–16	Pins et al. [69]
PLA[g]	28–50	1.2–3.0	2–6	Engelberg and Kohn [70]
Tendon (comprised of mainly collagen)	150	1.5	12	Gosline et al. [71]
Bone	160	20	3	Gosline et al. [71]
Kevlar (49 fiber)	3600	130	2.7	Gosline et al. [71]
Synthetic Rubber	50	0.001	850	Gosline et al. [71]

[a] *Bombyx mori* silkworm silk—determined from bave (multithread fibers naturally produced from the silk worm coated in sericin).
[b] *Bombyx mori* silkworm silk—determined from single brins (individual fibroin filaments following extraction of sericin).
[c] *Bombyx mori* silkworm silk—average calculated from data in Ref. [13].
[d] *Nephila clavipes* silk produced naturally and through controlled silking.
[e] Rat-tail collagen Type I extruded fibers tested after stretching from 0% to 50%.
[f] Rat-tail collagen dehydrothermally cross-linked and tested after stretching from 0% to 50%.
[g] Polylactic acid with molecular weights ranging from 50,000 to 300,000.

Silk and its degradation products are biocompatible. Unlike the bulk hydrolysis of the polyester family to acidic products, silk degrades by proteolytic surface degradation to amino acids [45,46]. Degradation by surface erosion helps prevent the loss of bulk mechanical properties allowing continued mechanical support of the implant. Degradation to amino acids results in a lower inflammatory response than other common degradable biomaterials including PLA, PGA, PLGA and collagen [40,45,47]. The tunability of silk degradation from days to years offers potential in achieving the target degradation profiles for different applications [48].

Functionalization of silk with a vast array of molecules offers yet another advantage as a biomaterial. Growth factors, cytokines, anti-inflammatory drugs, antibiotics and other molecules can easily be incorporated into silk implants for drug delivery, obviating the need for additional material or procedures. The processing versatility enables a variety of functionalization methods while inherent stabilization features of silk allow for high stability of the additives [49–53]. For the current application,

stabilization and delivery of compounds such as bone morphogenic protein for improved osseointegration or vancomycin for reduced infection would be highly desirable. Stabilization and delivery of BMP-2 has been successfully shown in various silk formats [54–56].

2.5.2 HFIP Silk

The primary silk format in the present work is a dense, non-porous scaffold prepared with the organic solvent 1,1,1,3,3,3 hexafluro-2-propanol (HFIP). HFIP and other fluorinated solvents are highly effective stabilizers of the α-helix structures in peptides, which is a common conformation of silk. HFIP acts by denaturing the native state (unfolded or β-sheet) and then re-stabilizes the unfolded peptides in an α-helix. HFIP induces this conformational change more effectively than other alcohols including tetrafluoroethylene, isopropanol, ethanol and methanol. This is related to HFIP requiring the lowest concentration to induce a change in free energy ΔG_H of the transition to the helical state [57,58]. HFIP has been previously used with regenerated silk fibers to promote high strength. This has been achieved through stabilization of silk in the α-helical conformation and then a transition to a β-sheet structure through physical cross-linking with methanol [59,60]. The high strength with ability to degrade render HFIP silk solutions a promising format for silk orthopedic hardware.

2.5.3 "Aqueous" Based Silk Scaffolds

3D silk scaffolds generated from aqueous silk solutions were investigated for feasibility. Any "aqueous based silk scaffold" will refer to a scaffold that is generated from aqueous silk solution without the use of an organic solvent such as HFIP. Silk cocoons can be processed to aqueous silk solution using protocols outlined Rockwood et

al. (2011). It is important to distinguish between aqueous based silk scaffolds and organic solvent based scaffolds due to inherent differences. Organic solvents have posed problems once the scaffolds are introduced to cells due to toxicity and/or reactivity. For this reason, research has been done to transition processes that require organic solvents to aqueous silk based processes. An aqueous process for producing silk orthopedic hardware will enable better biocompatibility and safer/less costly manufacturing [61,62].

Chapter 3. Objective

There is a significant clinical need for fully degradable orthopedic hardware that can overcome current limitations in bone remodeling and integration, degradation kinetics, complication rates and ease of use. Current material options for orthopedic devices consist of nondegradable metals and degradable polymers, mainly poly-L-lactic acid (PLLA) and polyglycolic acid(PGA). While both classes have shown success and/ or potential in the treatment of fracture healing, an ideal system has yet to be realized. Metal systems reside on one end of the orthopedic hardware spectrum with great mechanical properties, ease of implantation, resterilization and ability to be used in almost any indication area with the associated downfalls of being a permanent system and a possible need for removal surgery, poor bone remodeling and a number of common complications. Resorbable systems are on the opposite side of the spectrum with the ability to biodegrade, promote improved bone remodeling and limit long term complications while facing major disadvantages in weaker mechanical properties limiting applications and more difficult use/implantation. Orthopedic hardware that could bridge the gap between current material options would revolutionize orthopedic repairs in

combining improved long-term patient outcomes, reduced second surgeries and complication rates, ease of use and re-use. Table 7 details the properties of current options for fracture fixation as well as desired traits of an ideal system that will be pursued in this work. Silk orthopedic devices will be pursued as a candidate system with the hypothesis that the combined strength, biocompatibility, and tunability of silk will render it an ideal biomaterial to meet the desired ideal traits for the proposed application. The initial goal will be to meet the specifications for non-load bearing applications such as the craniomaxillofacial complex. Previous work has been done on silk orthopedic hardware and is summarized in Table 8. The work presented here will involve design and optimization of the initial proof of concept and improve the system to better meet the goals of the ideal system (Table 8). This will be done by: optimizing fabrication and system design/geometry; exploration of processing effects on degradation and mechanical properties/characteristics; functionalization of silk hardware with osteoinductive proteins (BMP-2) and exploration and feasibility of different aqueous based silk solutions.

Table 7. Properties and Characteristics of Current and Target Systems for Orthopedic Hardware [3,6–8,18,22,24,46,48,63–71]

Category	Metal		Resorbable		Ideal New System
Implantation	Self Tapping (pilot hole)		Pre-drill pilot hole and tapping required		Self Tapping (pilot hole)
	In situ plate shaping		Heat to shape plates		In situ plate shaping
Mechanical Properties	Pullout:	~ 400 N [69]	Pullout:	95-175 N ([63],[69])	Pullout:~100-200N (non-load bearing, >200N (load bearing)
	Shear:	~550Mpa [68]	Shear:	100-185MPa ([63-66])	Shear: ~100-200 Mpa (non-load bearing), > 200MPa (load-bearing)
	Bending Mod:	~7GPa [18,24]	Bending Mod:	~7GPa [18,24]	Bending Mod:
Degradation	N/A, Permanent		Time: PLLA (over 1 year), PGA (6-12 months), PLGA (~1 year to more than 1.5 years), P(L/DL)LA (2-3 Years) (c,k,r)		Time: Maintain strength for ~3 months, degrade quickly after (~6-12 months)
			Degradation Products: acidic components (inflammatory response) (l,m)		Degradation Products: Biocompatible/biodegradable with no inflammatory response
Biocompatability	yes		yes		yes
Resterilization	yes (any method)		no		yes
Elastic Modulus	> 105 Gpa [6]				Close to bone (20 Gpa) [6]
Complications/ Weaknesses (a,q)	Stress Shielding		Inflammatory reaction		None
	Temperature Sensitivity		Sterile sinus formation		
	Plate Exposure or Migration		Osteolysis		
	Corrosion		Incomplete bone remodeling		
	Growth Disturbance in Children		Limited applications		
	Palpability				
	Interference with medical imaging				
	Infection				
	Cold sensitivity				
	Possible need for hardware removal				
Benefits	Robust Mechanical Properties		Biodegradable/obviate need for hardware removal		Robust Mechanical Properties
	Ease of Implantation		Avoid stress shielding with close modulus to bone		Ease of Implantation
	Resterilization				Resterilization
					Biodegradable/obviate need for hardware removal
					No complications
					Match degradation to strength required for fixation

Table 8. Summary of previous work on silk orthopedic hardware

Category	Previous Results	Goals
Fabrication	30 minute boil HFIP silk process	Screws with bone screw threads
	Machinable silk blanks	Bone plates (various geometry)
	1-72 mechanical screws	New application/device
	Proof of concept plates (strips of silk material)	Minimize material waste
		Minimize Palpability
		Aqueous process
Silk Structure	High beta sheet content confirmed (49.3%)	N/A
Mechanical Properties	Shear (dry): 90.0±11.8 MPa	Shear (dry, hydrated), optimization
	Shear (hydrated): 19.3±0.51 MPa	Pullout (dry, hydrated), optimization
	Pullout (dry): 80.7±9.38N	Bending properties of plates
	Pullout(hydrated): 19.18 ± 5.98 N	Fatigue testing (cyclic)
		Elastic Modulus
Swelling	Swell ratio: 0.22±0.03	Optimize (decrease) swell ratio/water uptake
	Water uptake: 17.9±1.99%	
	No significant swelling in first 15 min	
Degradation	31% by week 23 (by surface erosion), ~ 7 months	Further investigate degradation with different treatments
		Shear strength after degradation
Ease of implantation	Proved self tapping (Vickers microhardness=40 kg/mm2)	N/A
Resterilization	Dimensional stability proven after 1st autoclave	Determine feasibility of resterilization by dimensional stability and mechanics
	Some decrease in shear strength	
In vivo characterization and implantation technique	Plates malleable with spray of water	Fracture fixation: implantation of silk screw and plate
	Self tapping in rat femur and human cadaver skull	Fracture fixation: implantation of silk IM nail
	Rats implanted with a screw were mobile post surgery on all 4 legs	
	Implanted rats showed minimal signs of complication/infection	
	Osteoclast/osteblast formation	
Functionalization	N/A	In vitro functionalization and release of BMP-2
		In vivo implantation and release of BMP-2

Chapter 4. Experimental Methods

4.1 Preparation of Silk Solution

Silk solution was prepared under established silk processing and purification protocols (Figure 7)[41]. The starting raw material for all silk solutions was Taiwanese *B. mori* cocoons. Cocoons were cut into four pieces and boiled for either 20, 30, 40 or 60 minutes in 0.02 M Na2CO3 (sodium carbonate). The purpose of the boiling process is to extract the sericin protein from the silk fiber protein. The longer the boil time, the longer the silk is exposed to the heat and salt resulting in more sericin removal and a higher degree of silk degradation. After boiling, the silk was rinsed 3 times for 30 minutes in distilled water to remove sericin and sodium carbonate. The resultant silk mat was allowed to dry for no less than 24 hours to ensure residual moisture had evaporated. Once

dry, the silk was dissolved in a 9.3 M LiBr solution at 60°C for 4-6 hours to produce a 20% w/v silk solution. The solution was then dialyzed in distilled water for 2 days with a minimum of 6 water changes in order to remove the LiBr and create an aqueous silk solution. The solution was dialyzed in Slide-a-Lyzer dialysis cassettes (MWCO 3,500) from Pierce Protein and Biology Products (Rockford, IL, USA). The aqueous silk solution was centrifuged in a Sorvall RC-5B Refrigerated Superspeed Centrifuge (Dupont Instruments, Wilmington, DE, USA) at 18,000 RPM and 2-10°C for 2, 20-minute cycles. The final concentration was determined by weighing the remaining silk after drying a measured volume of silk solution. The final solution was determined to be 6-8% w/v silk and could be stored at -4°C until further use.

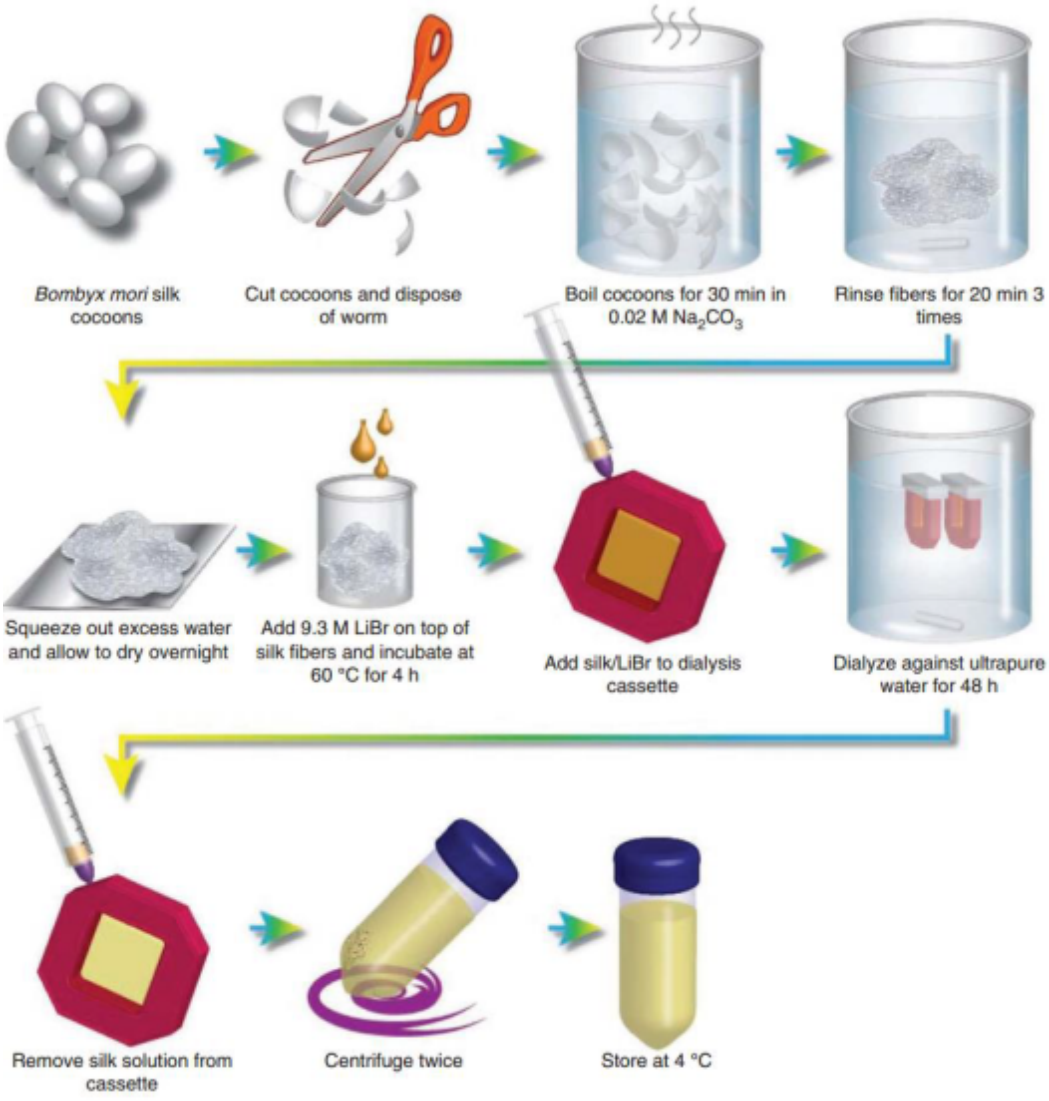

Figure 7. Stepwise process diagram of silk solution preparation. Note that boiling cocoons was done at 20, 30, 40 or 60 minutes. [41]

4.2 Preparation of HFIP Silk Blanks

4.2.1 Preparation of 1,1,1,3,3,3 Hexafluro-2-propanol (HFIP) Silk Solutions

The 6-8% w/v silk solution was frozen for 3-5 days and subsequently lyophilized to sublimate the frozen water. Lyophilization removes the bulk of water resulting in a Styrofoam-like form of silk that could be stored at ambient conditions and covered to prevent rehydration. The lyophilized silk was then chopped into small pieces with the use

of a Waring blender (Stamford, CT. USA) and packed into a syringe. 1,1,1,3,3,3 hexafluoro-2-propanol (HFIP) (≥ 99.0%(GC) from Sigma Aldrich (St. Louis, MO, USA) was added to the chopped silk-filled syringe in order to resolubilize the silk and produce a 25% w/v silk in HFIP solution. The HFIP silk solutions were stored sealed at ambient temperatures until fully dissolved and ready to be used for molding. For certain variations of HFIP silk molds, the HFIP silk solution was heated at 60°C for one week. Heating the HFIP silk results in a darker, amber colored solution as opposed to a golden yellow color that is normally seen. A heated HFIP silk solution was pursued in hopes that the darker color was due to crystallization of the silk and would prevent swelling and improve hydrated mechanics. The HFIP silk solution process along with molding and machining is illustrated in Figure 2.

4.2.2 Molding and Preparation of HFIP silk blanks for machining

Silk screw and silk intramedullary nail blanks were prepared using wax molds from MachinableWax.com (Traverse City, MI, USA), as shown in Figure 8A. The machinable wax cylinders were machined to molds of 1.3 in (3.30 cm) height with 6 through holes of 0.30 in (0.76 cm) diameter accompanied by a thin wafer of 0.10 in (0.25 cm) that would act as a base for the mold. Prior to injection of HFIP silk solution, the thin wafer of wax was attached to the base of a mold by melting both edges of the wafer and base and allowing it to dry together. Once HFIP silk was injected from a syringe into the 6 hole-molds, the open side of the mold was covered with a small circular petri dish and parafilm (Figure 8B). Upon exposure to air, the surface of the HFIP silk will become tough and rubbery. Covering the mold prevents formation of the rubbery surface and allows any bubbles created during injection to escape. If bubbles are not allowed to

escape, large defects will be created in the silk blank rendering unusable and wasteful material. Molds were allowed to sit for 1 day to ensure escape of bubbles. Silk plate molds (Figure 8 A) were machined from Teflon with inner dimensions of 60 mm, 60 mm and 3 mm. The molds consist of two pieces of Teflon that can be screwed together for molding and taken apart to remove the final mold. A small inlet hole was machined into one side with a diameter equal to that of a syringe tip. A syringe was stuck into the hole and HFIP silk was injected to fill the mold from bottom to top in order to minimize bubbles (Figure 8B). Once filled, the molds were wrapped with parafilm and allowed to sit for one day to ensure all bubbles escaped. After injection and bubble release, molds (screw, IM nail and/or plate) were placed into 100% methanol (Certified ACS Reagent Grade) from Thermo Fischer Scientific Inc (Pittsburgh, PA, USA) for 4 days to induce crosslinking, beta sheet formation and to displace HFIP. The methanol bath was then slowly transitioned to deionized water through 4 additions of deionized water at 1-hour intervals to create a methanol to water gradient. Once the bath was transitioned to 100% water, 6 subsequent water changes were used to remove residual HFIP and methanol. An organic respirator mask was used for the first few rinses as HFIP has a strong odor and should not be inhaled. After 6 rinses, blanks were safely removed with no residual odor. The blanks were then removed and allowed to dry in a fume hood for ~4 days, followed by drying in a 60°C oven for ~ 4 days before being autoclaved and ready for machining.

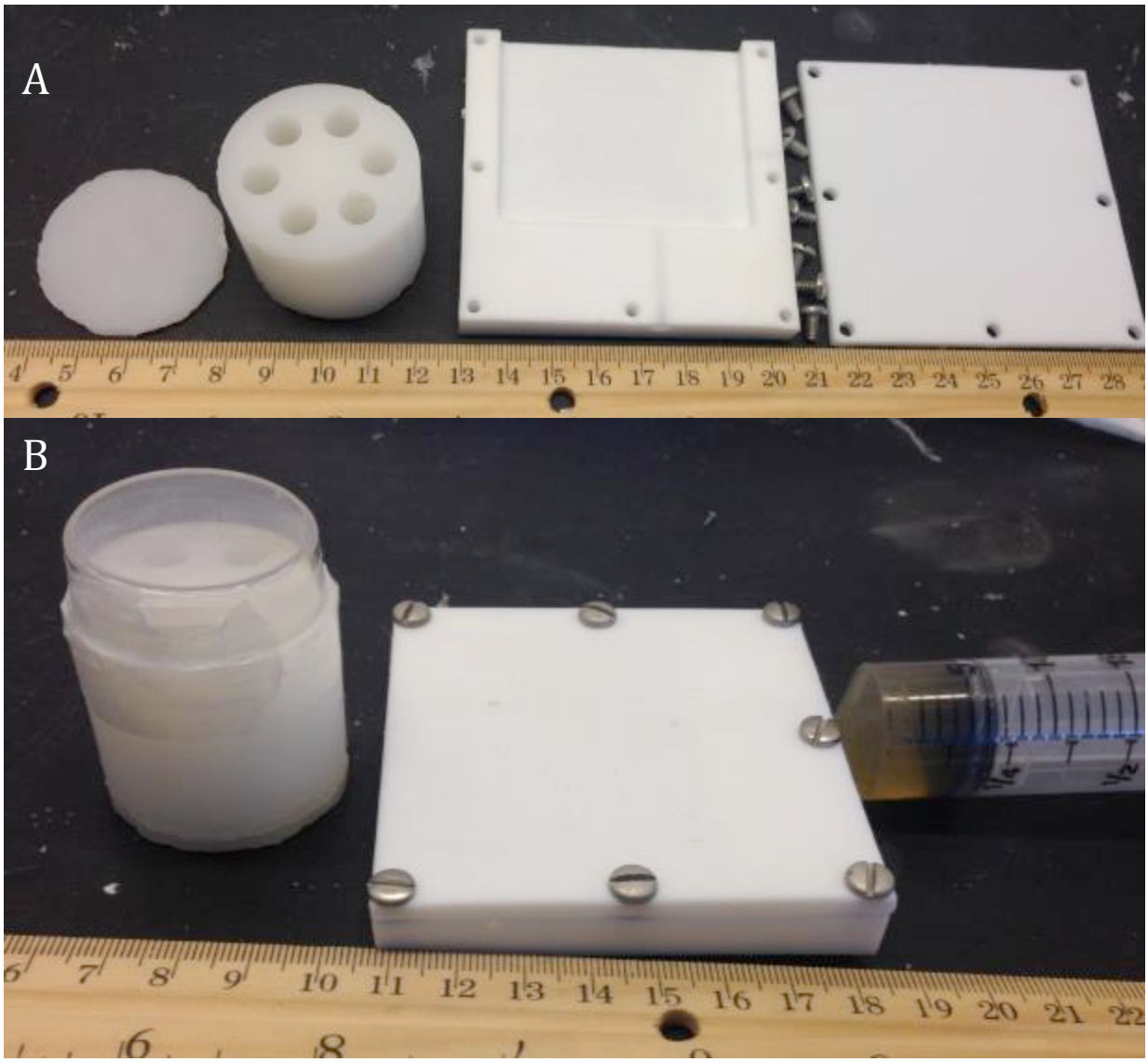

Figure 8 A) Wax molds for cylindrical plugs an Teflon molds for plate blanks; B) Wax mold with cap and parafilm to release bubbles and plate mold with fitted syringe for filling (metric ruler, markings in cm)

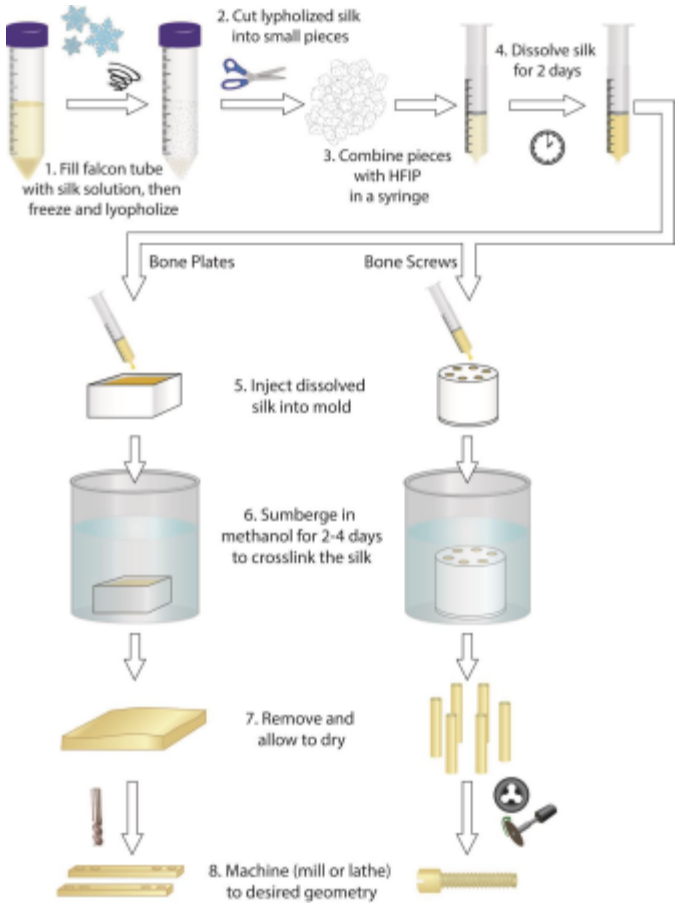

Figure 9 Process Diagram for creation of silk bone screws and plates from aqueous silk solution.[72]

4.3 Preparation of Aqueous-Based Silk

In order to avoid the use of highly-toxic HFIP or other organic solvents, aqueous based silk solutions were pursued. Candidates were chosen based on potential to form dense, rigid structures that could be machined and would have strong mechanical properties. All variations were examined for machinability and imaged using Scaning Electron Microscopy (SEM) for surface morphology.

4.3.1 Lithium Bromide/Formic Acid Silk Solution

In work by Feng Zhang reported a two step method for electrospinning silk fibroin nanofibers that was able to maintain the native nanofibrillar structure of native

silk. Preservation of the nanofiber structure resulted in excellent mechanical strength compared to traditional electrospun fibers. The ability to maintain this structure was related to the preparation of the doping solution for electrospinning. It was hypothesized that this doping solution could be manipulated with post treatments other than electrospinning, that would result in a machinable material with strong mechanical properties. The spin dope solution was prepared by boiling *B mori* cocoons for 60 minutes in 0.02 M sodium carbonate followed by rinsing and drying as described in section 3.1. The dried silk was then dissolved in a lithium bromide-formic acid solution with a LiBr concentration of 2% (w/v) in formic acid. The silk was dissolved for 3 hours at room temperature to prepare a 10% (w/v) silk solution . Once solution was prepared, multiple post treatments were attempted including the use of crosslinking, heating, autoclaving and critical point drying. The treatments are summarized below in Table 9.

Table 9. Summary of Post Treatments to LiBr-FA silk solution. Methanol (MeOH) and Ethanol (EOH) were used as crosslinkers. Samples were then dried in ambient air conditions, in an oven or critical point dried (CPD) and then autoclaved.

Sample #	Treatment
1	MeOH crosslinking, air dry, oven dry, autoclave
2	MeOH-EOH crosslinking, CPD, autoclave
3	60°C oven for 3 days
4	EOH crosslinking, CPD, autoclave

4.3.2 High Concentration Silk Solution

High concentration silk solutions were pursued under the hypothesis that a higher content of silk and lower content of water could ultimately result in a strong and dense silk blank without the need of HFIP. Two sub-hypotheses that supported this thought were that a higher concentration of silk would allow a higher degree of silk-silk interactions during physical or chemical crosslinking and that a lower water content

would require less drying/water removal to achieve a pure silk blank. High concentration silk solution was generated in two ways. The first method used an aqueous silk solution prepared under the process described in section 3.1 with a 30 minute boil. The solution was then poured into small Eppendorf tubes and placed in a Centrivap Concentrator 10392 (Labconco) heated centrifuge. The solution was spun at 55°C allowing water to evaporate off the silk solution. Solution was centrifuged until a final concentration of 20% (w/v) silk solution was achieved. Three solution variations and two post treatment methods were attempted. The three solution variations included pure 20% aqueous silk solution, 20% silk solution with 5% w/v silk powder (5 micron particle size) and 20% silk solution with 5% hydroxyapetite particles (~10 micron particle size). Each of these variations were split into two groups of post-treatment. The first group was cross-linked with Methanol (MeOH) for 4 days, air dried for 4 days, oven dried at 60°C for 4 days and autoclaved. The second group was cross-linked with ethanol for 4 days, critical point dried and then autoclaved. Critical point drying was explored for its ability to extract solvents while preserving nanostructure by avoiding phase boundaries. Pressure and temperature are increased passed the critical point of the solvent and then dried [73].

The second method used to produce high concentration silk solution involved a slight variation on the standard silk processing protocol. Both 30 minute boil and 60 minute boil silk was extracted, rinsed, dried and dissolved in LiBr per the protocol described in section 3.1. Dialysis was then performed using the same Slide-a-Lyzer dialysis cassettes (MWCO 3,500) as previously mentioned. However, instead of dialyzing against deionized water, the silk solution was dialyzed against a solution of pH~10). Three solutions were created using this method; 30 minute boil 20%w/v silk

solution, 60 minute boil 24.1% w/v wilk solution and 60 minute 27.1% w/v silk solution. All three solutions were cross-linked with methanol for 4 days, air dried for 4 days, oven dried in a 60°C oven for 4 days and finally autoclaved. The high concentration silk solutions are summarized in Table 10.

Table 10. Summary of High Concentration Silk Solutions. Methanol (MeOH) and Ethanol (EOH) were used as crosslinkers. Samples were then dried in ambient air conditions, in an oven or critical point dried (CPD) and then autoclaved.

Method	Silk Solution description	Treatment
Heated Centrifugation	20%, 30 min	MeOH, air dry, oven dry, autoclave
		EOH, CPD, autoclave
	20%, 30 min, 5% Silk Powder	MeOH, air dry, oven dry, autoclave
		EOH, CPD, autoclave
	20%, 30 min, 5% Hydroxyapetite	MeOH, air dry, oven dry, autoclave
		EOH, CPD, autoclave
Dialyze against high pH	20%, 30 min	MeOH, air dry, oven dry, autoclave
	24.1%, 60 min	MeOH, air dry, oven dry, autoclave
	27.1%, 60min	MeOH, air dry, oven dry, autoclave

4.3.3 Silk Powder Pressing

Fine silk powder of 5 micron particle size was pursued under the hypothesis that such a fine particle size could be pressed under high pressure to create a solid machinable material similar to a ceramic. A hollow aluminum cylinder was filled with the silk powder and placed under a hydraulic press (Dake Model 7-001). A cylinder of equal diameter to the silk powder filled aluminum mold was attached to the press and aligned with the hollow mold. 20,000 psi was applied to the powder and held for about 5 minutes.

4.4 Machining of Silk Orthopedic Hardware

Silk blanks for screws or IM nails were machined using either a MicroLux True-Inch 7x16 Variable Speed Lathe (Micromark, Berkely Heights, NJ, USA) or CNC lathe (Trak TRL 1440 EX) as shown in Figure 10. For both screws and IM nails, the silk blank could be machined down to the desired outer diameter or head diameter. For IM nails, the nail blank was left on a CNC style lather once the desired diameter was reached and a needle type tip was placed on the end for insertion. For screws with mechanical screw threads, the screw blank (still attached to the lathe) was threaded by hand with the use of a 1-72 NF Die 13/16 OD (McMaster-Carr, Robbinsville, NJ, USA). For screws with bone screw threads a custom single point external cutter (Vargus USA) was used on the CNC lathe to cut screw threads by matching turning speed with horizontal speed of the cutter to cut a desired pitch length (length from thread peak to thread peak). The screw heads could be machined to have a cylindrical heads or conical heads by use of the CNC lathe. Once machined, the screw or IM nail was then cut off behind the head or length of nail. A diamond cutter was mounted to the lathe and used to cut a slot in the screw head for screw insertion.

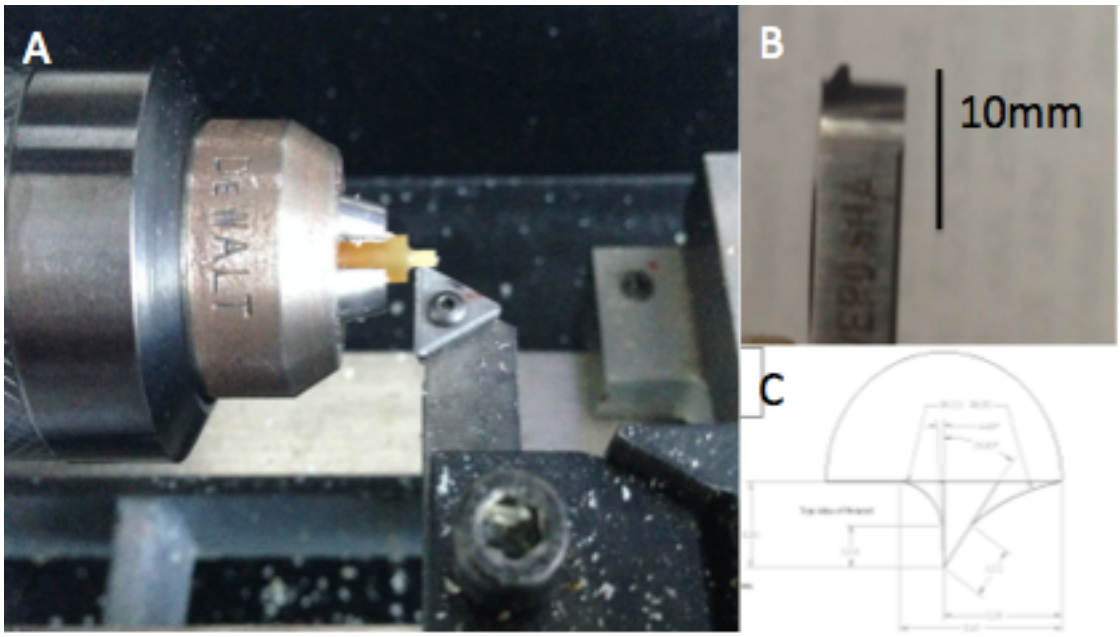

Figure 10. A) MicroLux True Inch 7X16 Variable Speed Lathe cutting a silk blank; B) External single point cutter with HA bone thread profile; C) HA bone screw thread profile.

For plates, rectangular silk blanks were machined using a CNC milling machine (Trak DPM). The milling machine was used both to cut the desired shape of the mold as well as the desired thickness. Once the plate was shaped and sized, cylindrical or conical screw holes were cut using a 90 degree Ford countersink. Plates were machined to two hole plates and four hole plates as shown in the drawing in Figure 11

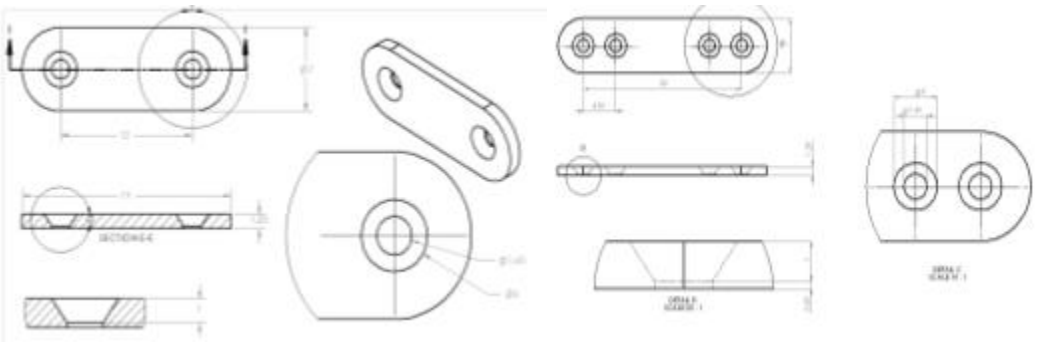

Figure 11. Drawings of 2-hole and 4-hole plates: 2 hole plates (19mm length, 7mm width, 1.2mm thickness, 1.6-3mm diameter holes placed 3.5mm from the end and 12mm apart), 4 hole plates (29mm length, 7mm width, 0.75-2mm thickness, 1.6-3mm diameter holes placed 3.5 mm from the end and 4.5mm apart).

4.5 Imaging of Silk Orthopedic Hardware

Various silk hardware formulations were imaged using Scanning Electron Microscopy (SEM) in order to observe surface morphology. Samples were sputter coated with a SC7620 Sputter Coater (Emitech) for 90 seconds to deposit a thin layer of gold. This allows the sample to be conductive and prevents it from accumulating charge while scanning. SEM images were taken using a ZEISS EVO MA10 and Smart SEM software.

4.5 Mechanical Properties

4.5.1 Pullout Strength Testing (dry, wet, cyclic)

Pullout strength testing was performed on an Instron 3366 test frame and tested to ASTM standard F2502-11 (ASTM standard F2502-11). Pilot holes were drilled into an artificial polyurethane bone block that was in accordance with ASTM standard F1839-08 (Standard Specification for Rigid Polyurethane Foam for Use as a Standard Material for Testing Orthopaedic Devices and Instruments). Polyurethane foam blocks (Pacific Research Laboratories, Inc. (Sawbones)) of varying densities were tested in order to investigate pullout strength in a range of bone quality. Polyurethane blocks were solid rigid polyurethane of 30pcf (0.48 g/cc) and 40pcf (0.64 g/cc). Standard 40pcf

polyurethane blocks were used for all groups unless otherwise specified. Screws were inserted into the pilot holes and screwed in to a depth at which at least 3 screw threads were engaged. Screws were able to self-tap in the polyurethane bone block so that no pre-tapping was required. A custom screw head holder (Figure 12A,B) was used to fasten the screw by the head to the Instron 3366 frame. In all tests a rate of 5 mm/min was used for extension rate of pullout (ASTM standard F2502-11). Tests were performed in both dry and hydrated conditions. For hydrated tests samples were incubated in PBS solution at 37°C for at least 24 hours and tests were then performed in a 37°C PBS solution bath with the use of a Biopuls temperature controlled bath. Cyclic testing was performed up to 10,000 cycles using a triangular loading regiment of 0 to 10N at 5mm/min. After 10,000 cycles screws were tested for maximum pullout strength. The loading scheme was based on previously reported work in testing of biodegradable bone fixation implants. Values of 10-100N correspond to bone loads borne by the fibula during normal weight bearing. 10,000 cycles corresponds to walking 10km[74]. Thus, 10,000 cycles at 10N for pullout strength in non-load bearing application should therefore be a worst-case scenario.

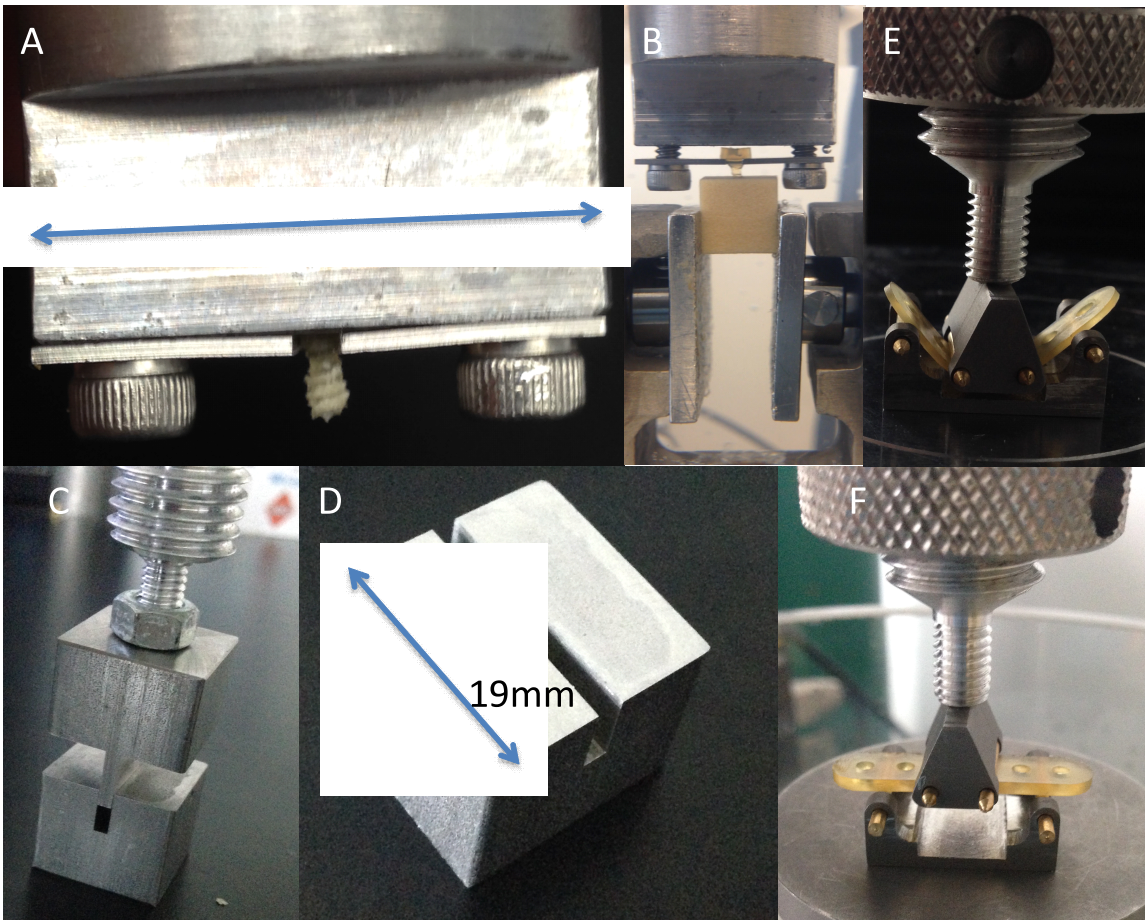

Figure 12. Testing Fixtures for Silk Orthopedic Hardware: A) Pullout strength test fixture with screw head locked in place, B) Pullout test fixture pulling a silk bone screw from polyurethane block secured by pneumatic grips; C) Top and bottom shear strength fixture; D) Bottom shear strength fixture with silk pin in place; E) Plate bending fixture with brass support rollers at maximum extension; F) Plate bending fixture pre-test.

4.5.2 Shear (dry, wet, cyclic)

Silk pins were machined to 1.5mm diameter and tested in a double lap shear test that consisted of three adjacent stainless steel plates (Figure 12C, D). Aligned holes of 1.5mm to 1.85mm were machined into the stainless steel fixtures for placement of the silk pins. The bottom fixture remained stationary while the top fixture was mounted to an Instron 3366 test frame and compressed at a rate of 5.00 mm/min until fracture of the silk pin (ASTM standard F2502-11). Maximum shear stress (MPa) was determined from maximum load at fracture and area of the silk pins. Tests were performed in both dry and hydrated conditions. For hydrated tests samples were incubated in PBS solution at 37°C

for at least 24 hours and tests were then performed in a 37°C PBS solution bath with the use of a Biopuls temperature controlled bath. Cyclic testing was performed up to 10,000 cycles using a triangular loading regiment of 0 to 100N at 5mm/min. After 10,000 cycles pins were tested for maximum shear stress. Loading scheme was based on previously reported work described in section 4.5.1.

4.5.3 Bending (dry, wet, cyclic, thickness)

Silk plates were machined to a width of 7mm, length of 29mm and a range of thickness from 0.75mm to 2mm and tested for 4 point bending strength. Plate thickness tested were 0.75mm, 1.2mm or 2mm. Plate geometry was also explored by machining plates with either a rectangular cross section or half I-beam cross section. Plate samples with a half I-beam cross section had a thickness of 1.2mm with 0.75mm by 2mm ridge machined down the center line of the plate. All plates were 4-hole plates with 2mm diameter holes. Holes were placed 3.5 mm from the ends of the plates with the nearest hole separated by 4.5 mm. The 2 center holes were separated by 13 mm. A 4-point bending fixture was machined from stainless steel with brass loading rollers (Figure 12E, F). Brass loading rollers and support rollers were used to allow rolling during testing to avoid frictional forces. The bending fixture was machined to ASTM standard F2502-11 with a loading span and center span of 6mm with support rollers placed directly between the 2 outer holes. Similar to double lap shear testing, the bottom fixture remained stationary while the top fixture was mounted to an Instron 3366 test frame and compressed at a rate of 5.00 mm/min until fracture or complete compression to the bottom fixture (Figure 12 E). A load vs load-point displacement curve was generated to

determine bending stiffness, bending structural stiffness and bending strength using methods described in ASTM standard F2502-11 (Figure 13).

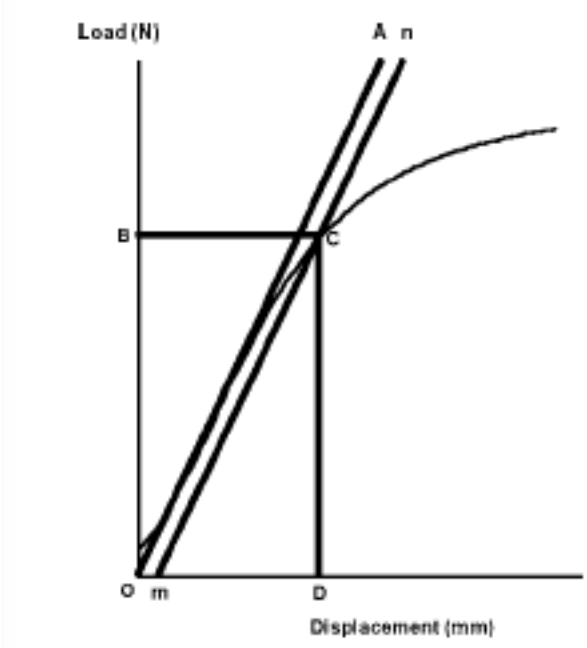

Figure 13. Load vs Displacement Curve for determining plate strength ASTM standard F2502-11.

Bending stiffness (N/mm) was determined by calculating the slope of the initial linear portion of the line OA. Bending structural stiffness was calculated using Equation 1. Bending structural stiffness is the normalized effective stiffness that takes the test set up configuration into consideration [75].

(1) $EI_e = \frac{(2h + 3a)Kh^2}{12}$

where:
EI_e = bending structural stiffness ($N - mm^2$)
K = bending stiffness (N/mm)
a = center span distance (mm)
h = loading span distance

Bending strength was determined using a 0.2% offset displacement line mn. A 0.2% offset was calculated using Equation 2.

(2) $q = 0.002a$

where:
q = offset displacement
a= center span distance (mm)

Bending strength of the plate was calculated using Equation 3 for plates that did not fracture or Equation 4 for plates that did fracture.

(3) $bendingstrength = \frac{Ph}{2}$

(4) $bendingstrength = \frac{F_{\max} h}{2}$

where:
P= proof load (N)
$F_{\max}$ = fracture load (N)
h = loading span distance (mm)

Proof load was determined by load at the intersection of the offset displacement line mn and the load vs load point displacement curve. Bending modulus was also determined using Equation 5 derived in published methods for three-point and four-point bending[76].

(5) $E_{4p} = \frac{m_{4p} L_0^3}{8wh^3}$

where:
E4p= 4-point bending modulus (MPa)
m4p= 4-point bending stiffness (N/mm)
L0= length between support rollers (mm)
w= width of plate (mm)
h=height of plate (mm)

Tests were performed in both dry and hydrated conditions. For hydrated tests samples were incubated in PBS solution at 37°C for at least 24 hours and tests were then performed in a 37°C PBS solution bath with the use of a Biopuls controlled temperature bath.

4.5.4 Compressive Modulus

Silk plugs were machined to 4mm on diameter and ~4mm in height. Plugs were then compressed between two flat plates at a rate of 5mm/min using an Instron 3366 test frame. Samples were compressed to an extension of 1mm. Load, extension and sample geometry were used to determine the compressive modulus.

4.6 In vitro enzymatic degradation

In vitro enzymatic degradation was performed using Protease XIV (Sigma-Aldirch, St Louis, MO) with an activity of 5 U/ml following previously published methods [72]. Silk pins were machined to 1.5mm major diameter and 3mm length and placed in 2 ml of PBS containing enzyme and PBS alone for control. Samples were incubated at 37°C and solution was replaced every 24-48 hours with freshly prepared solution. Pins were weighed for initial mass dry and after 4 days of incubation in 37°C PBS solution. Samples were then weighed at 1, 2, 4, 6, and 8 week time points while hydrated. All hydrated samples were wiped with a kimwipe and allowed to sit for ~10 minutes to ensure removal of surface moisture. Groups of double lap shear pins were enzymatically degraded under the same method and sacrificed at 3, 6 and 9 weeks in order to investigate the effect of degradation on shear strength.

4.7 Functionalization with BMP-2

In order to address current limitations in resorbable orthopedic hardware such as osseointegration and incomplete bone remodeling, the ability of silk orthopedic hardware to stabilize and release BMP-2 was studied. Functionalization with recombinant human BMP-2 (rhBMP-2) (Abcam) was initially investigated with the lead candidate silk screw formulation (30 minute boiled silk solution, lyophilized, dissolved in HFIP, cross-linked

with MeOH, dried and autoclaved 1 time). Due to the use of toxic HFIP immediately before cross-linking and drying, it was determined that successful incorporation of active BMP-2 would have to be done post-manufacturing. Two methods were initially proposed for BMP-2 functionalization; absorption/adsorption of BMP-2 solution into the silk hardware and coating of silk hardware with BMP-2 in silk solution. Absorption/adsorption was considered to be a potential loading regimen based on the swelling properties of silk hardware and previously published methods [54,77]. Silk coatings were proposed based on previously published work using BMP-2 stabilized in silk solution [55] and BMP-2 release from films [56]. However, only BMP-2 loading by absorption was investigated in the current work. It was felt that silk coatings may be immediately sheared off in the implantation of the screw. Target ranges for BMP-2 loading can be seen below in Table 11.

Table 11. Target Ranges for BMP-2

Host material	**Loading/coating (BMP-2)**	**Release rate (% initial amount)**
17% w/v HFIP derived porous silk scaffold [77]	7.2 ± 0.12 μg/g of scaffold	1 week: 75%
9 wt% silk fibroin solution [55]	3 μg/mg of silk solution	N/A
Silk fibroin films [56]	31.3 ± 0.86 ng/cm2 of film area	4 weeks: 50 - 90%
Hyaff-11 scaffold [78]	0.37 mg/ml of scaffold volume	4 weeks: 32%
Type I Collagen gel [78]	0.09 mg/ml of gel volume	2 weeks: 88%
PLGA microparticle/calcium phosphate (30:70) [79]	5.0 ± 0.4 μg per 75-mm3 disk	4 weeks: 3%

4.7.1 In vitro release

In vitro stabilization and release of BMP-2 was investigated for absorption/adsorption. For absorption of BMP-2, silk pins were machined to 1.5mm diameter and 3-4mm length. Pins were then placed in a solution of BMP-2 for 4 days at -

4°C in microtubes. After 4 days, the microtubes were weighed with solution and the silk pins. The pins were then removed and weighed twice; once with surface moisture and a second time with surface moisture removed. These measurements were used for mass balance to determine the quantity of BMP-2 solution that the silk pin absorbed and thus the quantity of BMP-2 absorbed. The assumption was made that the mass gained by absorbed solution would contain the loading concentration of BMP-2 in solution. Once the pins were dried, the BMP-2 would remain. A mass balance of initial screw mass and final screw mass was not used because the loading mass of BMP-2 (less than 1 μg) would be less than the error of the balance (0.002mg) (Mettler AT20). The loaded silk pins were dried for 4 days and then placed in 150μl PBS solution for release. PBS was removed for release data and replaced at 1 hour, 2 hour, 4 hour, 6 hour, 1 day, 2 day and 5 day time points. BMP-2 release was quantified by a BMP-2 human ELISA kit (Abcam) per manufacturers instructions.

4.7.2 In vivo implantation for osteointegration

Based on preliminary results, absorption of BMP-2 was chosen as the loading mechanism of silk orthopedic hardware for initial animal studies. Samples were sterilized prior to BMP-2 adsorption, by autoclaving with a dry gravity cycle with 25 minutes under pressure and steam followed by 15 minutes of drying. BMP-2 solution was filtered through a sterile filter before placing screws in the solution in sterile hood for 4 days. Screws were then allowed to dry for at least 4 days before implantation.

Animal studies were conducted under approved protocol #M2013-14 (Surgery Description: Part B. Femur Experiments) at Tufts University, with the help of surgeons from Beth Israel Deaconess Medical Center. For *in vivo* studies, 250 gram, 15 week old

female Sprague Dawley Rats were anesthetized with isofluorane and the incision area was shaved and disinfected with betadine. A 10mm longitudinal incision was made along the hind limb. The vastus lateralis and biceos femoris were then separated along the length of the femur. The distal end of the femur was exposed and a 1.5mm diameter, 3mm length uni-cortical hole was drilled with a Synthes Electric Pen Drive. The screw was then inserted with the use of standard flat head screwdriver. The incision was finally closed with a simple interrupted pattern with 5-0 Vicryl sutures.

Animals were sacrificed at 1 month, 3 month and 6 month time points. For each time point an N=5 was used. For 4 of the 5 rats per group, a control silk screw was placed in the right hind limb and a BMP-2 loaded silk screw was placed in the left hind limb. In the 5^{th} animal per group, a hole was placed with no screw in the left hind limb and a stainless steel screw was placed in the right hind limb for controls. Samples were explanted, fixed in 10% formalin solution and sent to Beth Israel Deaconess Medical Center for histology.

For histological preparation, samples were first decalcified by placement in Surgipath Decalcifier at room temperature for 8 hours or until the bone became flexible. Samples were then processed with ethanol and xylene and embedded in paraffin. Paraffin blocks were then sectioned along the long axis of the bone and cut through the screw. Sections were cut at 5 μm intervals and baked at 60°C on glass slides. The sectioned samples were then autostained with hematoxylin and eosin and Masson trichrome stains.

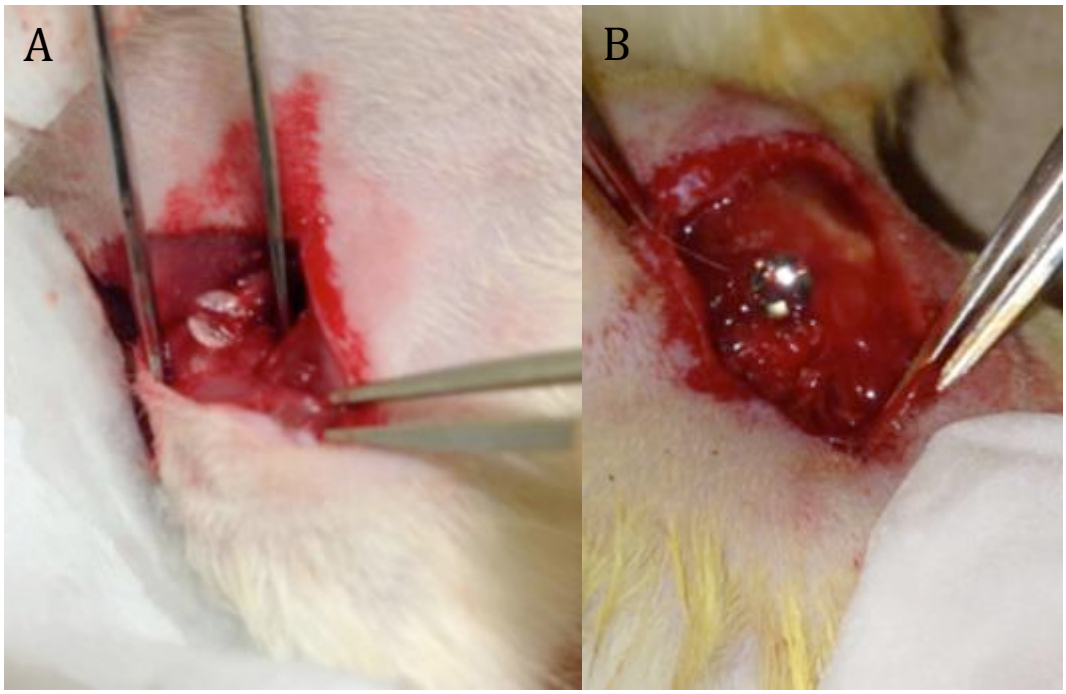

Figure 14. Implantation of BMP-2 loaded silk screw and stainless steel control screw.

4.8 In vivo implantation technique of screws/plates

Silk screws (1.5mm diameter, 3mm length) and plates (4 hole, 6mm width, 27mm length and 1.2mm thickness) were implanted for femur fracture fixation in a rat for feasibility and technique. Silk orthopedic hardware was sterilized by autoclaving with a dry gravity cycle with 25 minutes under pressure and steam followed by 15 minutes of drying. Animal studies were conducted under approved protocol #M2013-14 (Surgery Description: Part B. Femur Experiments) at Tufts University, with the help of surgeons from Beth Israel Deaconess Medical Center. For *in vivo* studies, 250 gram, 15 week old female Sprague Dawley Rats were anesthetized with isofluorane and the incision area was shaved and disinfected with betadine. A 10mm longitudinal incision was made along the hind limb. The vastus lateralis and biceos femoris were then separated along the length of the femur. A full femur incision was made mid-diaphysis with the use of a Synthes Electric Pen Drive and saw attachment. Pilot holes were then placed with the

use of the plate as a template and drilled with a Synthes Electric Pen Drive. Screws were then inserted with a traditional driver to secure the plate and fracture in place. The incision was finally closed with a simple interrupted pattern with 5-0 Vicryl sutures. One animal was implanted with a silk screw and plate system and a control animal was implanted with a titanium plate and screw system. Both animals were sacrificed at 1 month. Samples were explanted, fixed in 10% formalin solution and sent to Beth Israel Deaconess Medical Center for histological sectioning and imaging. Similar methods to those described in section 4.7.2 for histological preparation were used.

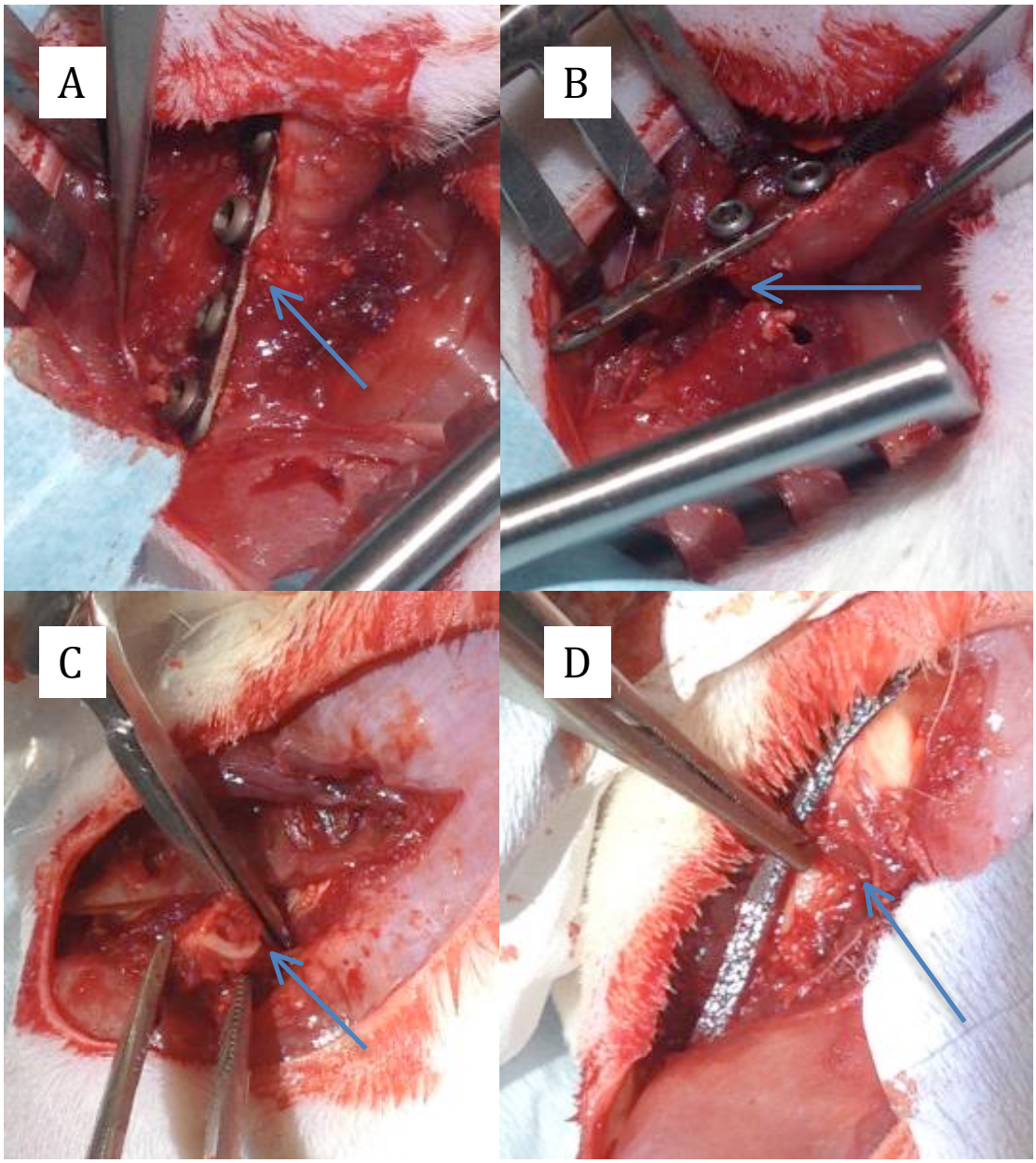

Figure 15. Implantation of Plate and Screw System for Fracture Fixation : A) Fixated rat femur with titanium system; B) Open fracture site with titanium system secured to one femur length; C) Open fracture site with silk system secured to one femur length; D) Fixated rat femur with silk system. Arrows are pointing to the fracture site in all pictures.

4.9 Resterilization

All silk samples were autoclaved using a GETINGE 400/500 LS Series Steam Sterilizer prior to machining to ensure dimensional stability. The standard autoclave

cycle used for materials in this work was a closed gravity cycle (25 minute autoclave, 15 minute drying).

The effect of autoclaving was investigated by using three different types of autoclave cycle as well as varying number of autoclave cycles. For this investigation a closed gravity cycle (25 minute autoclave, 15 minute drying), an open gravity cycle (25 minute autoclave, 15 minute drying) and a closed vacuum cycle (25 minute autoclave, 15 minute drying) were used. Open refers to samples being openly exposed to the environment while being autoclaved and closed refers to samples autoclaved while sealed in an autoclave bag. The difference in vacuum and gravity cycles is drying conditions. A vacuum cycle uses a ramped drying pressure while gravity cycle pressure remains constant during drying. Samples were tested for shear strength and enzymatic degradation. Dimensional stability after autoclaving was investigated for closed gravity cycle (25 minute autoclave, 15 minute drying) at 1X, 3X, 5X, 7X, 10X autoclave cycles. Autoclave cycles were investigated due to differences in appearance after autoclaving upon a change in autoclave equipment as well as to investigate the ability to resterilize.

4.10 Swelling Properties

Silk pins were machined to 1.5mm diameter and ~3-4mm length and immersed in a 37°C PBS solution bath for 4 days. Prior to immersion in PBS the dry mass of the samples were taken for dry weight (Wd). After 4 days, surface moisture was removed by wiping the samples with a Kimwipe and allowing to sit for ~10 minutes. Samples were

then weighed for swollen weight (Ws). The swelling ratio and water uptake (%) using Equation 5 and Equation 6.

(6) $$SwellRatio = \frac{Ws - Wd}{Wd}$$

(7) $$WaterUptake = \frac{Ws - Wd}{Ws} * 100$$

Four groups were tested for swelling. A 30 minute boiled, HFIP solution was used for all groups. Group 1 was a standard treated sample that was physically cross-linked with MeOH, dried and autoclave 1X. Group 2 was physically cross-linked with MeOH, dried and autoclaved 10X. Group 3 was physically cross-linked with MeOH, dried, autoclaved 1X and then soaked in EDTA for 4 days for further physically cross-linked, rinsed with RO/DI water and dried. Group 4 was chemically cross-linked with gluteraldehyde, rinsed with RO/DI water, physically cross-linked with MeOH, dried and autoclaved 1X. Gluteraldehyde was used for its widely studied use as a cross-linking agent and ability to react with lysine and glycine present in silk [80].

Chapter 5. Results

5.1 Fabrication of Orthopedic Hardware

A major issue with previous work on molding silk for orthopedic hardware was that a large quantity of material was wasted due to bubble formation while injecting. The use of a sealed cap and parafilm on molds and allowing bubbles to release for 1 day resulted in more consistent blanks with far less wasted material (Figure 16)

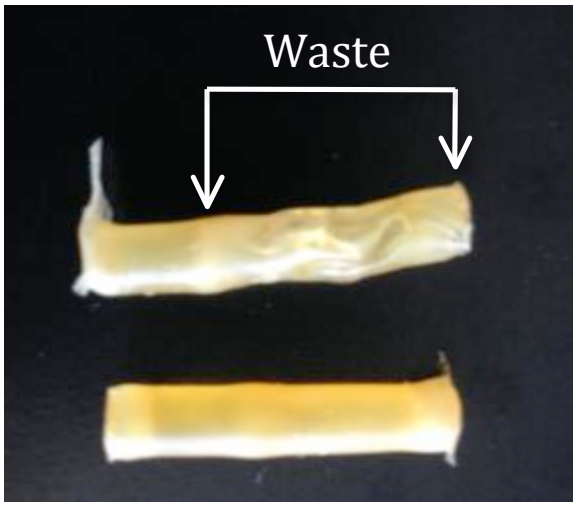

Figure 16. Old silk blank (top) with large portion of waste vs new silk blank (bottom).

After crosslinking and drying, silk blanks were observed to shrink and deform as a result of crosslinking and water removal. In the viscous state after dissolving with HFIP, the silk was a 25% silk solution in HFIP. HFIP induced alpha helix structure in the silk ([57,58]) which will not pack as tightly or densely as a β-sheet conformation that is induced by methanol. After crosslinking and rinsing in water, HFIP was removed and the silk blanks were swollen. During the 8 days of drying in a hood and oven, the silk blanks began to shrink and curl. This is most likely due to inconsisitent removal of water as a result of variation in temperature, air flow, humidity and air exposure. Blanks were then autoclaved to ensure dimensional stability and maximize water removal. Cylindrical screw blanks for pins and screws and rectangular screw blanks for plates were both observed to shrink similarly, however rectangular blanks for plates had a higher tendency to curl. This can be contributed to the fact the rectangular plates must be pulled out of the molds after crosslinking which slighlty curls the blank. The rectangular blanks also have a large surface that is exposed to the air and drying conditions and a large surface that will lay face down causing larger inconsistency during drying. This could be minimized by using a drying rack and rotating the blanks while drying. Prior to

machining, curled blanks could be hydrated, flattened under pressure and allowed to dry. After drying the blank remained uncurled.

Once silk blanks were dried and autoclaved, they remained dimensionally stable and were ready to be machined. Silk cylindrical blanks were easily machined on both a MicroLux True-Inch 7x16 Variable Speed Lathe (Micromark, Berkely Heights, NJ, USA) or CNC lathe and were threaded with a threading dye or external single point cutting tool on a CNC lathe. The material machinability was considered very good as bone screw threads were more easily placed on silk pins than Teflon pins. Screws were either machined to 1.5mm or 2mm diameter and length of 3-4mm with a pitch length (thread peak to thread peak) of 0.6mm to match dimensions of other current resorbable systems such as Synthes Rapidsorb. Figure 17 depicts the difference in thread profile of silk bone screws vs previous mechanical screw threads. Screws were also fitted with cylindrical heads or conical heads for countersinking into matching plates. Countersunk heads seen in Figure 17 would minimize palpability or the ability to be felt. Silk intramedullary nails were machined to a diameter of 2mm and length of 1-4 cm.

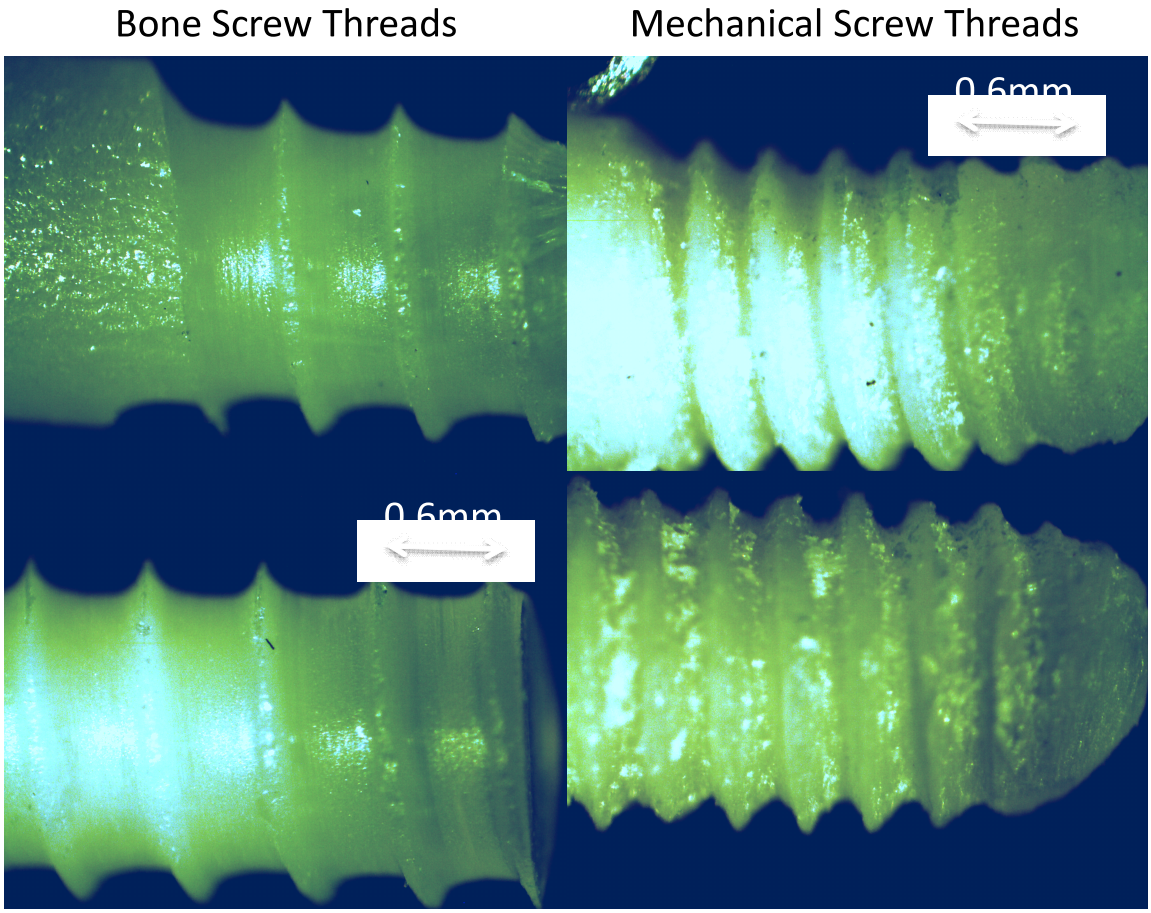

Figure 17. Bone Screw Threads vs Mechanical Screw Threads of Silk Screws. The two pictures on the left are silk blanks machined to have bone screw threads by an external single point cutting tool. The two pictures on the right are silk blanks machined with mechanical screw threads with the use of a threading dye.

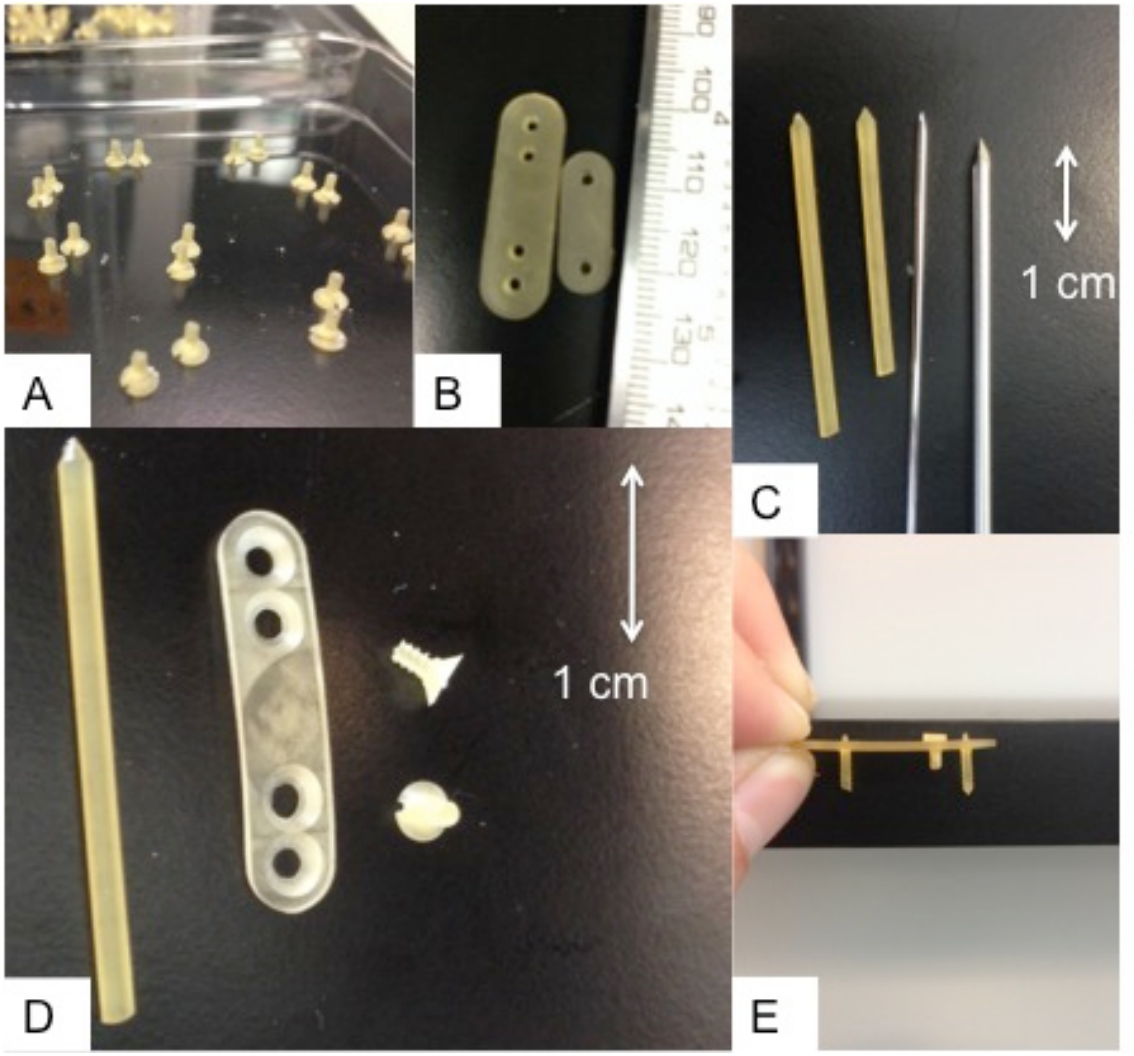

Figure 18. Silk Orthopedic Hardware: A) Silk screws with bone screw threads and countersunk head; B) 4-hole and 2-hole silk plates; C) Silk Intramedullary nails; D) Silk hardware devices; E) Silk plate and screws with countersunk head fitting vs conical head

Rectangular silk blanks were easily machined with the use of a CNC milling machine to various thickness and sizes. Two-hole plates were machined with a length of 19mm, 5mm width and 1.2mm thickness. Four-hole plates were machined with a length of 29mm, 6-7mm width and varying thickness of either 0.75mm, 1.2mm and 2mm. Different plate geometry was also achieved with a 4-hole plate with a half I beam cross section. Figure 18 depicts various plate sizes and geometry achieved.

The ability to easily machine silk intramedullary rods, bone screws and plates with various geometry, size and features using standard CNC tooling machines exhibits promising potential for the feasibility of scale up production.

5.2 Mechanical Properties

Different variations of silk processing and treatment were explored in the proposed research. These variations will be detailed in the sample description in the figures below. 20min, 30min and 40min refer to the boil time in minutes of silk fibroin. 1X, 5X and 10X autoclave refer to the number of autoclave cycles performed. Autoclave cycles are abbreviated as cycle 1 (closed gravity cycle), cycle 2 (closed vacuum cycle), cycle 3 (open gravity cycle). "CPD" refers to critically point dried silk and "heated" refers to the use of heated HFIP solution.

5.2.1 Screws: Pullout

A possible mode of failure for bone screws is to back out of the bone in which they are placed. For this reason, bone screws are often tested for pullout strength to determine loads at which the screw will be forced out of the bone. Silk screws of varying thread type and treatment were tested in hydrated and non-hydrated conditions and tested for pullout strength. Threads were either mechanical screws with designation 1-72 (MS) or HA bone screw threads (BS). Treatment types included 1X autoclave, 10X autoclave and heated HFIP. Screws were tested in 40 pcf (0.64 g/cc) and 30 pcf (0.48 g/cc) polyurethane blocks to explore pullout strength in different bone density. A lower density bone represents weaker or compromised bone. Screws were tested in 40pcf polyurethane unless otherwise stated. N=6 for all groups.

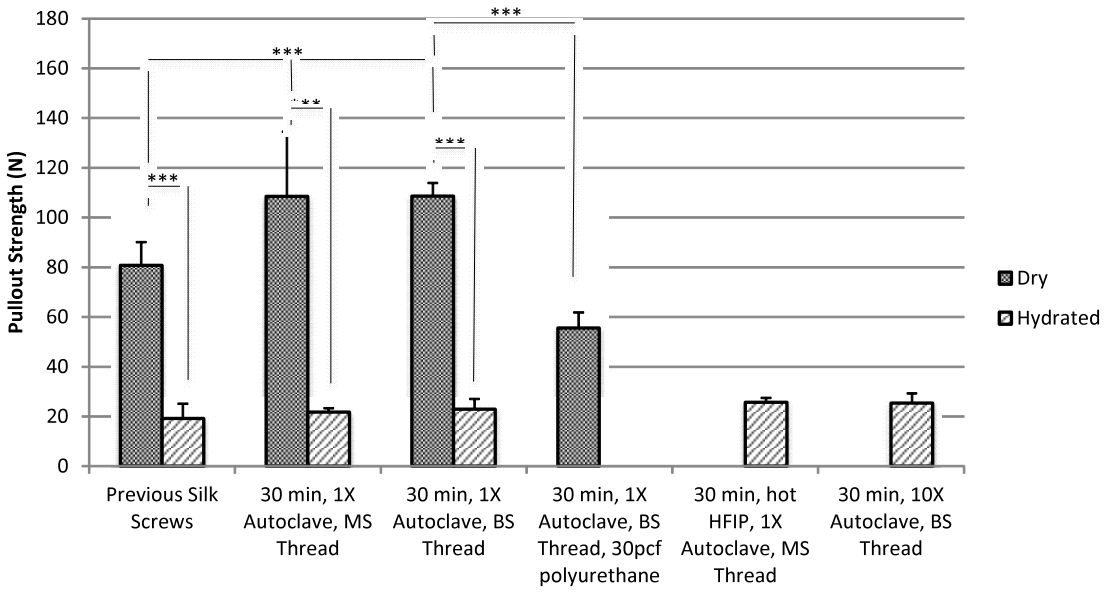

	Dry		Hydrated	
Sample Description	**Pullout**	**Std Dev**	**Pullout**	**Std Dev**
30 min, 1X Autoclave, MS Thread	108.44	26.06	21.66	1.67
30 min, 1X Autoclave, BS Thread	108.59	5.33	22.92	4.16
30 min, 1X Autoclave, BS Thread, 30pcf polyurethane	55.51	6.35	x	x
30 min, hot HFIP, 1X Autoclave, MS Thread	x	x	25.63	1.8
30 min, 10X Autoclave, BS Thread	x	x	25.33	3.94
Previous Silk Screws	80.7	9.38	19.18	5.98
Current Resorbable Hardware	95-175	x	x	x
Current Metallic Hardware	400	x	x	x

Figure 19. Pullout Strength Summary: The figure compares hydrated and dry pullout strength of silk screws with various thread type, treatment and polyurethane bone blocks. In each group that was tested in hydrated and dry conditions, pullout strength in dry vs hydrated was considered statistically different. There was no statistical difference between MS thread and BS thread. Pullout strength in 40pcf polyurethane was statistically higher than in 30pcf polyurethane. Standard MS thread and BS thread were statistically greater than previously measured silk screws. No statistical difference was seen in hydrated conditions with varying treatments. Strength was considered statistically different if $P<0.05$ using a one-way ANOVA and Tukey's multiple comparison test.Current silk screw formulation with bone screw threads is comparable to current resorbable systems and still far less than metallic system. Improvements have been made since previous work on silk screw. Hydrated pullout strength remains significantly low. (Abbreviations: 30 min=30 minute boiled silk, MS/BS= thread type (mechanical or bone screw), 1X autoclave= autoclaved once post machining, hot HFIP=heated HFIP silk)

Silk screws were also tested under cyclic loading. A load cycle regiment of 10,000 cycles of 10N loads was applied in dry and hydrated conditions. Screws were pulled out at less than 5,000 cycles while others were able to reach 10,000 cycles. This can most likely be attributed to the fact that pullout strength is a measure of both material

and geometry. Therefore any variability in machining of threads will affect the strength of pullout. Over 10,000 cycles, this variability will be more apparent than in a single cycle test.

Table 12. Cyclic Loading Pullout Summary: Cycle number reached by dry screws with bone screw threads varied from 4,372 cycles to >10,000 cycles. One screw was tested for maximum pullout strength after 10,000 cycles and maintained a pullout strength of 62.29 N. A hydrated bone screw thread screw was tested for cyclic loading and failed after 1,742 cycles. (Abbreviations: 30 min=30 minute boiled silk, MS/BS= thread type (mechanical or bone screw), 1X autoclave= autoclaved once post machining, dry/hydrated=testing conditions)

Sample Description	Sample #	Load of Cycle	#of Cycles	Pullout After Cycle (N)
30 min, 1X Autoclave, BS Thread, Dry	1	10 N	10000	N/A
	2	10 N	10000	62.29
	3	10 N	6793	N/A
	4	10N	4372	N/A
30 min, 1X Autoclave, BS Thread, Hydrated	1	10N	1742	N/A

5.2.2 Screws/IM Nail: Shear

One of the most common forces experienced by both silk screws and intramedullary nails is shear force. Maximum shear strength was tested on silk pins with a diameter of 1.5-2mm. Shear strength was tested in hydrated and dry conditions and is applicable to both screws and intramedullary nails. Silk pins tested for shear strength were used to compare the strength effects of treatments to silk hardware during processing, the effect of boil time of silk and the effect of autoclave cycle type and number. N=6 was used for each group.

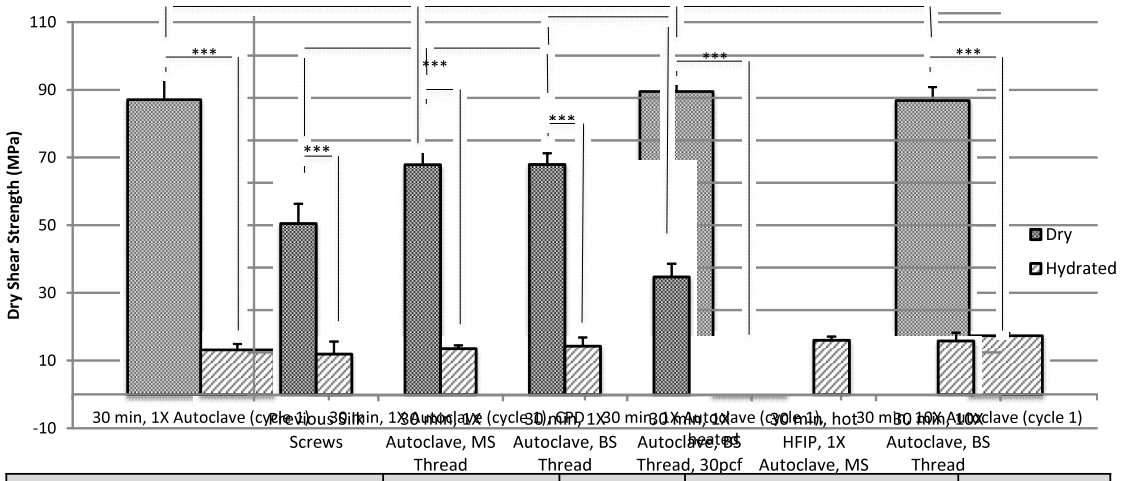

Description	Dry Shear (Mpa)	Std Dev	Hydrated Shear (Mpa)	Std Dev
30 min, 1				
30 min, 1X Autoclave (cycle 1), CPD	62.01	2.74	x	x
30 min, 1X Autoclave (cycle 1), heated	89.51	2.73	14.99	3.31
30 min, 10X Autoclave (cycle 1)	86.89	3.93	17.35	0.74

Sample Description	Dry Pullout	Dry Std Dev	Hydrated Pullout	Hydrated Std Dev
30 min, 1X Autoclave, MS Thread	108.44	26.06	21.66	1.67
30 min, 1X Autoclave, BS Thread	108.59	5.38	22.92	4.16
30 min, 1X Autoclave, BS Thread, 30pcf polyurethane	55.51	6.35	x	x
MS Thread	x	x	25.63	1.8

Figure 20. Effect of processing treatments on shear strength: In each group that was tested in hydrated and dry conditions, shear strength in dry vs hydrated was considered statistically different. In dry conditions, shear strength of critical point dried silk was statistically lower than all other treatment. 1X autoclaved silk, 10X autoclaved silk and heated HFIP silk showed no statistical difference when compared in dry or hydrated conditions. Strength was considered statistically different if P<0.05 using a one-way ANOVA and Tukey's multiple comparison test. (Abbreviations: XX min= XX minute boiled silk, 1X autoclave= autoclaved once post machining, cycle 1= autoclave cycle type described in section 5.2, CPD=critical point dried, heated= heated HFIP solution)

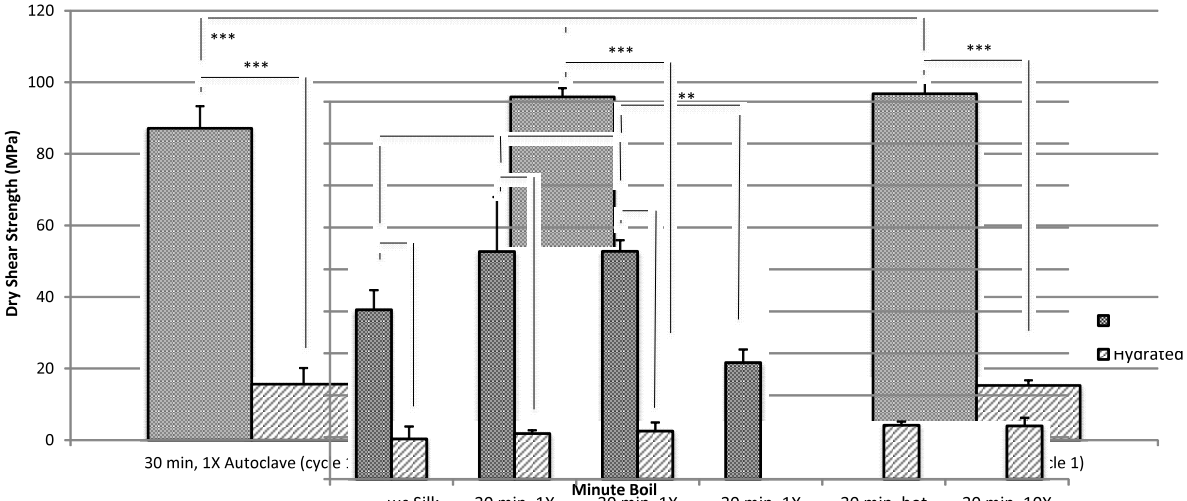

Description	Dry Shear (Mpa)	Std Dev	Hydrated Shear (Mpa)	Std Dev
30 min, 1X Autoclave (cycle 1)	87.11	6.17	15.65	4.49
20 min, 1X Auto-				
40 min, 1X Autoclave (cycle 1)	96.77	4.09	15.27	1.44

Sample Description	Dry Pullout	Dry Std Dev	Hydrated Pullout	Hydrated Std Dev
30 min, 1X Autoclave, MS Thread	108.44	26.06	21.66	1.67

Figure 21. Effect of boil time on shear strength: In each group that was tested in hydrated and dry conditions, shear strength in dry vs hydrated was considered statistically different. In dry conditions, 20 minute and 40 minute boil were significantly stronger in shear than 30 minute boil silk. No significance was observed in 20, 30 or 40 minute boiled silk for hydrated conditions or between 20 and 40 minute boiled silk in dry conditions. Strength was considered statistically different if P<0.05 using a one-way ANOVA and Tukey's multiple comparison test. (Abbreviations: XX min= XX minute boiled silk, 1X autoclave= autoclaved once post machining, cycle 1= autoclave cycle type described in section 5.2)

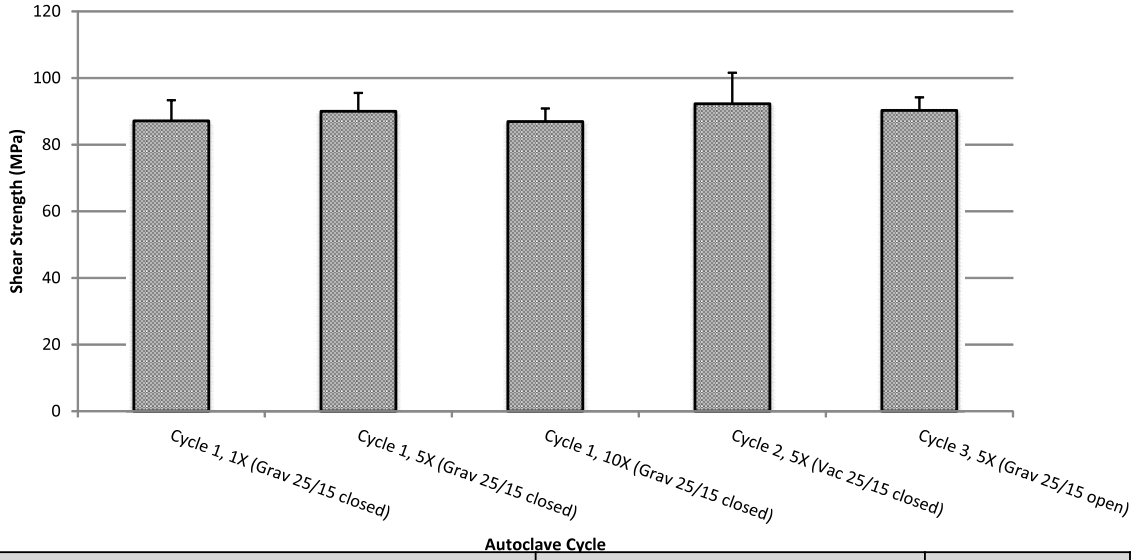

Description	Dry Shear (Mpa)	Std Dev
30 min, 1X Autoclave (cycle 1)	87.11	6.17
30 min, 5X Autoclave (cycle 1)	89.97	5.55
30 min, 10X Autoclave (cycle 1)	86.89	3.93
30 min, 5X Autoclave (cycle 2)	92.21	9.33
30 min, 5X Autoclave (cycle 3)	90.24	3.93

Figure 22. Effect of autoclave cycles on shear strength: No statistical difference was observed in any group using a one-way ANOVA and Tukey's multiple comparison test with a $P<0.05$ to determine statistical significance. (Abbreviations: 30 min= 30 minute boiled silk, _X autoclave= _ times autoclaved post machining, cycle X= autoclave cycle type X described in section 5.2)

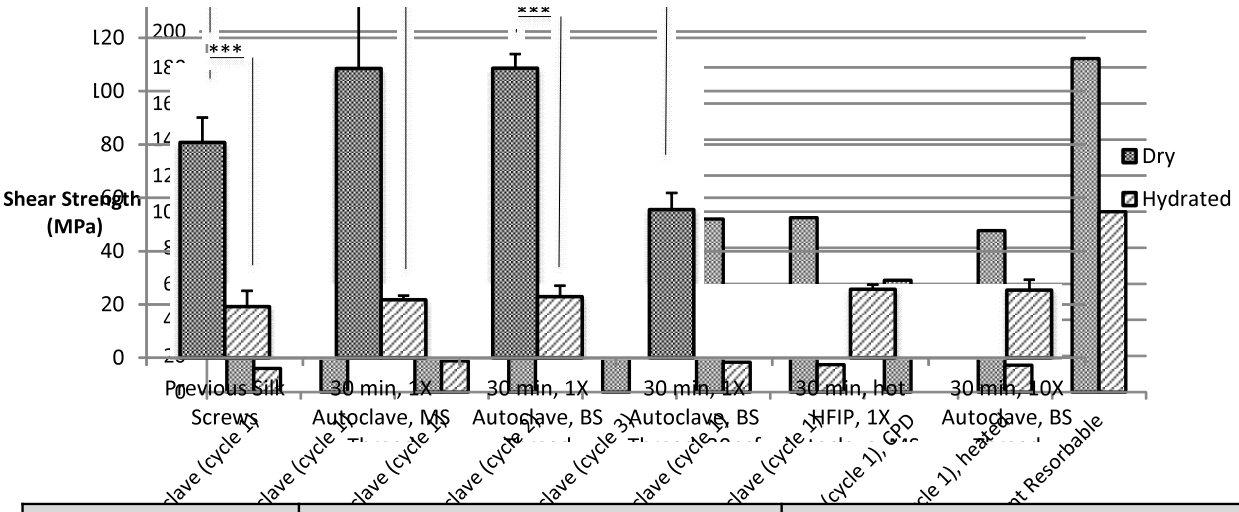

	Dry		Hydrated	
Sample Description	**Pullout**	**Std Dev**	**Pullout**	**Std Dev**
30 min, 1X Autoclave, MS Thread	108.44	26.06	21.66	1.67
30 min, 1X Autoclave, BS Thread	108.59	5.33	22.92	4.16
30 min, 1X Autoclave, BS Thread, 30pcf polyurethane	55.51	6.35		
hot HFIP, 1X Autoclave, MS Thread	x	x	25.63	1.8
30 min, 10X Autoclave, BS Thread	x	x	25.33	X 3.94 X
Previous Silk Screws	86.7	8.38	19.18	17.35 5.98 0.74
Current Resorbable Hardware	95-175	x	x	X x X
Current Metallic Hardware	400	x	2.4	x 16.51 x 0.52

Description	Dry Shear (Mpa)	Std Dev	Hydrated Shear (Mpa)	Std Dev
30 min, 1X Autoclave (cycle 1)	87.11	6.17	15.65	4.49
30 min, 5X Autoclave (cycle 1)	89.97	5.55	X	3.94 X
30 min, 10X Autoclave (cycle 1)	86.89	3.93	X	X
30 min, 5X Autoclave (cycle 2)	92.21	9.33	X	X
30 min, 5X Autoclave (cycle 3)	90.24	3.93	X	X
20 min, 1X Autoclave (cycle 1)	95.92	2.4	16.51	0.52
40 min, 1X Autoclave (cycle 1)	96.77	4.09	15.27	1.44
30 min, 1X Autoclave (cycle 1), CPD	62.01	2.74	X	X
30 min, 1X Autoclave (cycle 1), heated	89.51	2.73	14.99	3.31
Current Resorbable	~100-185	X	X	X
Current Metal	~550	X	X	X

Figure 23. Shear Strength Summary of Silk Orthopedic Hardware (Variations) and Current Resorbable and Metal Hardware. Silk shows comparable shear strength to current resorbable hardware in the dry condition but is significantly weaker in hydrated conditions. (Abbreviations: XX min= XX minute boiled silk, _X autoclave= _ times autoclaved post machining, cycle X= autoclave cycle type X described in section 5.2, CPD=critical point dried, heated= heated HFIP solution)

As shown by Figure 23 none of the processing treatments statistically improved shear strength of dry or hydrated mechanics. Changing the boil time of silk from 30 minutes to 20 or 40 minutes did not have an effect on hydrated mechanics but slightly increase dry shear strength. This can be attributed to a balance between density of

protein packing and degree to which the silk molecular weight is reduced. The boiling process is designed to remove sericin from the silk fibroin but has also been shown to affect the silk fibroin itself. . Silk protein is comprised of a heavy chain (390kDa) and light chain (26kDa). Silk that is boiled for longer periods of time will be further broken down to low molecular weight silk protein and thus will be able to pack more tightly and with smaller pore size. Previously published reports showed that 30 minute boiled silk had a peak in molecular weight distribution near 100 kDa while 5 minute boiled silk showed a distribution near the molecular weight of the heavy chain and 60 minute boiled silk had a molecular weight distribution peak near that of the light chain (~50kDa)[81]. Between 20, 30 and 40 minute boil there may be a tradeoff between the low and high molecular weight silk (light chain and heavy chain) and the ability to densely pack that will affect shear strength. Another likely explanation is that small variations in processing and testing conditions rendered the 30 minute boil slightly weaker. For example, if tested in more humid conditions, shear strength could be slightly lower, while the samples were dried in slightly different conditions while drying in ambient conditions (uncontrollable), the degree to which they dried may be different. Autoclave cycle type and number showed no effect on the shear strength of silk orthopedic hardware. Unfortunately, strength was not increased by any of the cycles in dry or hydrated conditions. However, this supports the ability of silk hardware to be resterilized which is an important advantage over current resorbable systems.

Standard formulation (30 minute boil, HFIP dissolve, MeOH physical cross-linked, 1X autoclave) silk pins were also tested in cyclic loading. A load cycle regiment of 10,000 cycles of 100N loads was applied in dry conditions on two silk pins. Both silk

pins were able to withstand all 10,000 cycles. One silk pin was tested for maximum shear strength after 10,000 cycles and achieved shear strength of 91.09 MPa. This value is comparable to values with no cyclic loading and showed lack of fatigue in strength even after 10,000 cycles. Future testing will need to be performed in order to support the lack of fatigue as well as to test hydrated mechanics.

Table 13. Summary of Shear Cyclic Loading. (Abbreviations: 30 min= 30 minute boiled silk, 1X autoclave= 1 times autoclaved post machining, dry=testing conditions)

Sample Description	Sample #	OD (mm)	Load of Cycle	#of Cycles	Shear After Cycle (MPa)
30 min, 1X Autoclave, Dry	1	1.52	100 N	10,000	X
	2	1.52	100N	10,000	91.09

5.2.3 Plates: Bend

For the fixation of fractures by internal fixation devices it is import that fixation plates have adequate bending strength and stiffness so that the fracture will be held in place and allowed to heal properly. Silk plates were tested in 4-point bending in order to produce a load vs load-displacement curve. From this curve, bending stiffness, structural stiffness and bending strength were calculated using methods described in ASTM standard F2502-11. Bending modulus was also calculated. Plate dimensions and bending properties are summarized in Table 14.

Table 14. Plate Dimensions of Silk Orthopedic Hardware for Plate Strength Testing

Plate Thickness (mm)	Plate Width (mm)	Plate Length (mm)	Cross Section Type
0.75	7	29	Rectangular
1.2	7	29	Rectangular
2	7	29	Rectangular
0.75/1.2	7 (2mm center line had thickness 0.75mm)	29	Half I Beam

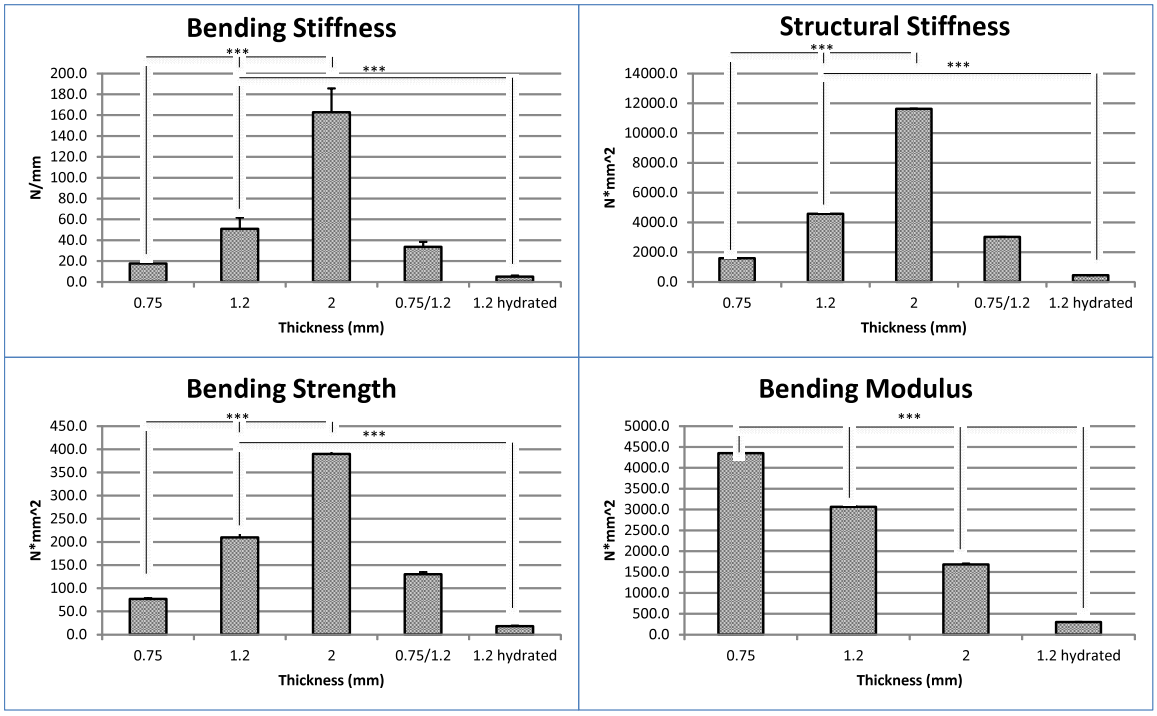

Figure 24. Bending Properties Summary of Silk Plates: For bending stiffness, bending strength and structural stiffness and bending modulus, the hydrated mechanics of 1.2mm plate were statistically lower than that of a dry 1.2mm plate. For bending stiffness and structural stiffness, incremental increases in plate thickness resulted in statistically different properties except between the 0.75/1.2 mm half I-beam plate and the 0.75mm plate or the 1.2 mm plate. For bending strength, incremental increases in plate thickness resulted in statistically different properties except between the 0.75/1.2 mm half I-beam plate and the 0.75mm plate. All bending moduli were statistically different. Properties were considered statistically different if $P<0.05$ using a one-way ANOVA and Tukey's multiple comparison test.

Table 15. Summary of Bending Properties of Silk Orthopedic Hardware and other Current Resorbable/Metallic Systems

Plate Material	Plate Thickness (mm)	Bend Stiffness(N/mm)		Structural Stiffness (N*mm^2)		Bending Strength (N-mm)		Bending Modulus (GPa)	
		Average	Std dev	Average	Std dev	Average	Std Dev	Average	Std Dev
Silk	0.75	17.6	1.6	1586.7	142.0	76.7	2.3	4.4	0.4
Silk	1.2	50.8	10.9	4569.9	982.8	209.6	38.9	3.1	0.7
Silk	2	162.8	23.0	11621.7	2068.7	389.6	56.4	1.7	0.3
Silk	0.75/1.2	33.5	4.9	3018.2	445.2	130.0	19.9		
Silk	1.2 hydrated	5.0	1.2	447.3	107.8	18.0	9.6	0.3	0.1
PLGA [18]	1.6 mm (Pin)	~10						~7	
PLLA [20]	1.2							5	
PLA [87]	2.5	~100							
Titanium [20,87]	2	~270						~5-7	

Increasing the thickness of plates resulted in increased strength and stiffness but a decrease in bending modulus. The use of a half I beam cross section exhibited properties between that of a 0.75mm plate and 1.2mm plate. This geometry was explored in order to examine the ability to use less material and decrease palpability by changing geometry to have a larger moment of area in bending. The 2mm thick plates showed comparable bending stiffness to current resorbable systems such as PLA and PLGA. Hydrated mechanics are a limitation as stiffness is significantly decreased, which will have an impact on the ability of a fracture to set correctly.

5.2.4 Elastic Modulus

The standard formulation silk for silk orthopedic hardware was tested for compressive elastic modulus. The compressive modulus was determined to be 2.17 ± 0.27 GPa. This is a much closer match to that of bone (~20 GPa) than metallic systems (>105 GPa). A closer match in elastic modulus will reduce stress shielding that is commonly seen with current metallic systems.

5.3 Resterilization of Silk Hardware

A major cost advantage of metallic systems over current resorbable systems is the ability to be resterilize and reuse the devices if not used during surgery. The term reused in this sense refers to a device that was opened in the operating room (or elsewhere) and is considered no longer sterile. The ability to reuse this device depends on the ability to be resterilized. Silk orthopedic devices were investigated for the ability to be resterilized by autoclaving. Sample cylindrical plugs were autoclaved 1X, 3X, 5X, 7X and 10X. Mass, height and outer diameter were measured to determine the dimensional stability of the silk screws.

No statistical difference was found in height, diameter or mass using a one-way ANOVA and Tukey's multiple comparison test. Dimensions were considered statistically different if $P>0.05$. Silk screws and plugs were also tested for shear strength after undergoing three types of autoclave cycle as well as 1X, 5X and 10X cycles. No statistical difference was observed. The stability of both hardware dimensions and strength after multiple autoclave cycles showed that silk orthopedic hardware can be resterilized and reused.

5.4 Enzymatic Degradation

In vitro degradation using 5U/ml Protease XIV at 37°C was performed on different silk variations and treatments in order to determine the effect of different autoclave cycles on degradation, the effect of different boil times of silk on degradation and to determine preliminary relationships between degradation and strength retention of silk orthopedic hardware. **Error! Reference source not found.** represents the groups and time points that were investigated.

Table 16. Degradation Groups and Time Points.

Autoclave Cycle	Fibroin Boil Time	Time Points
Cycle 1, 1 X	30 Min, Cycle 1, 1 X	Time 0
Cycle 1, 1 X (control)	30 Min, Cycle 1, 1 X (control)	1 week
Cycle 1, 5 X	20 Min, Cycle 1, 1 X	2 week
Cycle 1, 5 X (control)	20 Min, Cycle 1, 1 X (control)	4 week
Cycle 1, 10 X	40 Min boil, cycle 1, 1 X	6 week
Cycle 1, 10 X (control)	40 Min, Cycle 1, 1 X (control)	8 week
Cycle 2, 5 X		
Cycle 2, 5 X (control)		
Cycle 3, 5 X		
Cycle 3, 5 X (control)		

The autoclave cycles were the same as those described in section 4.3. All autoclave cycle groups were prepared from 30 minute boiled silk. Silk plugs were machined to similar sizes as the screws in order to correlate in vitro degradation to in vivo resorption. N=6 was used for each group. Degradation was tracked by mass and is reported as percent mass remaining. Samples were weighed in the swollen state for all time points. All samples were initially weighed dry, swelled for 4 days in PBS and weighed again to determine the swell ratio. The swell ratio of each sample was then used to determine dry weight.

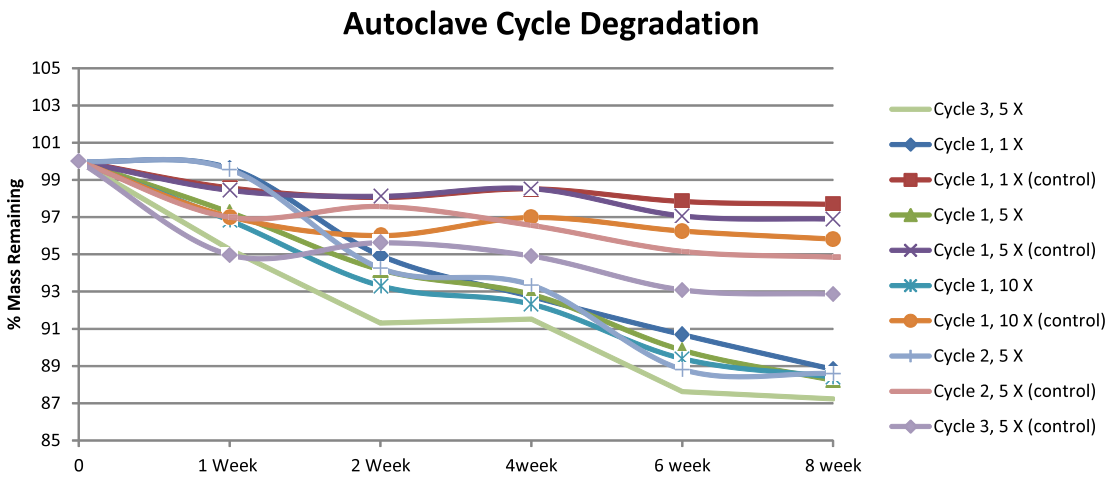

Figure 25. Summary Graph: % Mass Remaining of Autoclave Cycle Variations over 8 Weeks. (Abbreviations: _X autoclave= _ times autoclaved post machining, cycle X= autoclave cycle type X described in section 5.2, control=incubated in PBS, non-controls=incubated in Protease XIV)

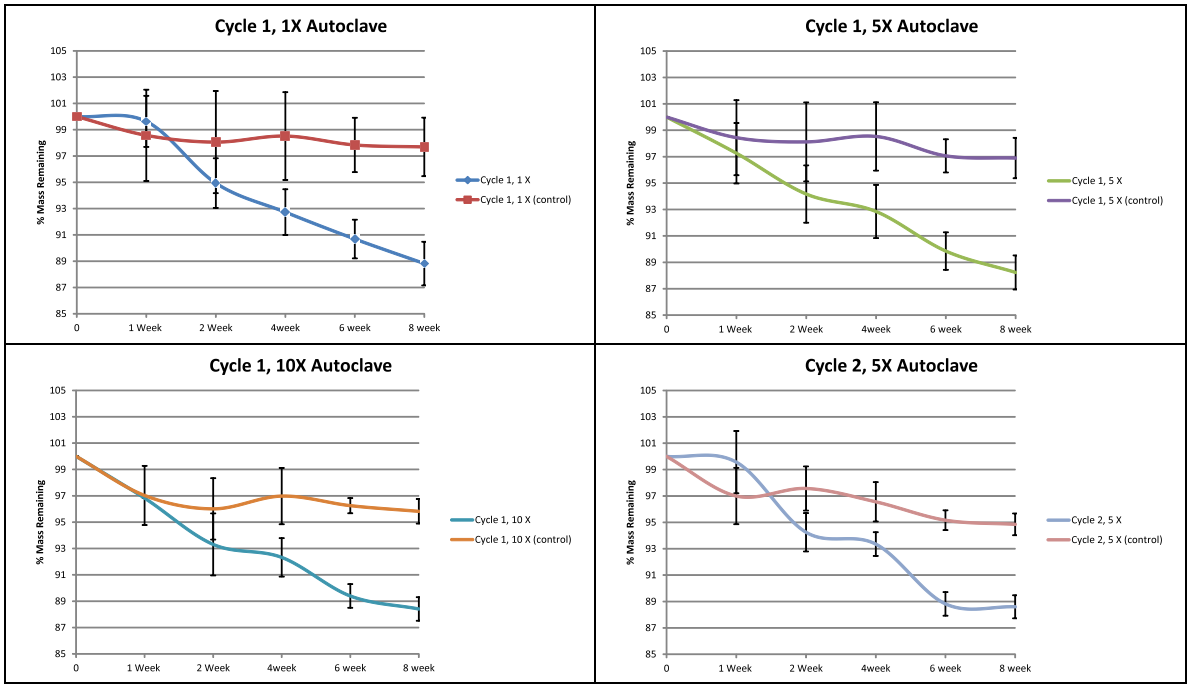

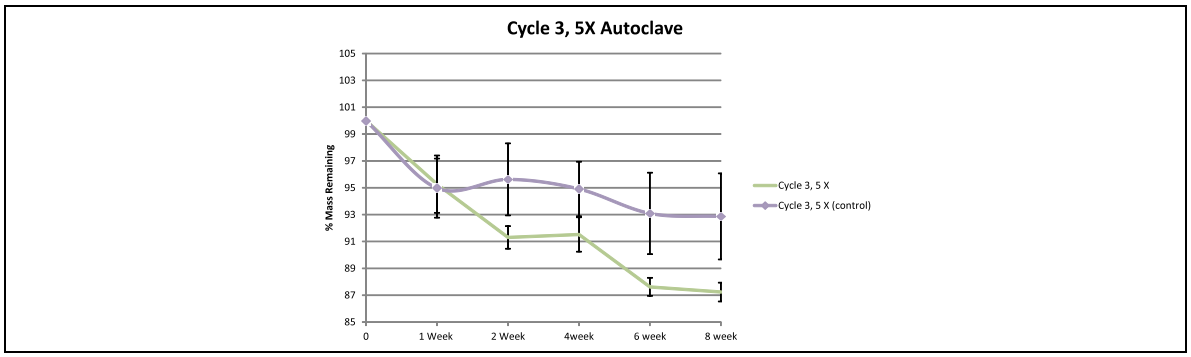

Figure 26. Degradation Comparison of Control (PBS) Silk Pin to Protease Degraded Silk Pin for all Autoclave Cycle groups. For each autoclave cycle, the treatment group showed statistically significant decreases in % mass between almost every consecutive time point. Control groups showed no statistically different changes between consecutive time points other than 0 and 1 week. Little statistical significance was observed between groups at the same time point. (Abbreviations: _X autoclave= _ times autoclaved post machining, cycle X= autoclave cycle type X described in section 5.2, control=incubated in PBS, non-controls=incubated in Protease XIV)

For each autoclave cycle group, the Protease XIV treatment group showed statistical significance between consecutive time points in almost all cases. Cycle 1, 1X had no statistical difference between 6 week and 8 week. Cycle 1, 5X and 10X and Cycle 2, 5X and Cycle 3, 5X showed no significant difference in 2 week to 4 week or 6 week to 8 week. Control groups showed no statistical differences in percent mass remaining between consecutive time points other than time 0 to 1 week. The variability in time 0 to 1 week degradation in control samples is most likely due to loss of particulate debris on the samples that remained from machining. Soaking screws in PBS most likely removed this debris causing an apparent drop in mass.

In comparing the degradation profile of the different treatments, there was no statistical difference between groups at time 0 or 1 week other than the 1 week percent mass remaining of Cycle 3, 5X appeared significantly less than Cycle 1, 1X and Cycle 2, 5X. This is most likely due to loss of surface particulate debris, which will cause variability. At 2 weeks, there were little statistical differences amongst any of the groups. For time points of 4 weeks or later, all groups showed significant differences between the

control group and the protease group. However, there was no statistical difference between treatments.

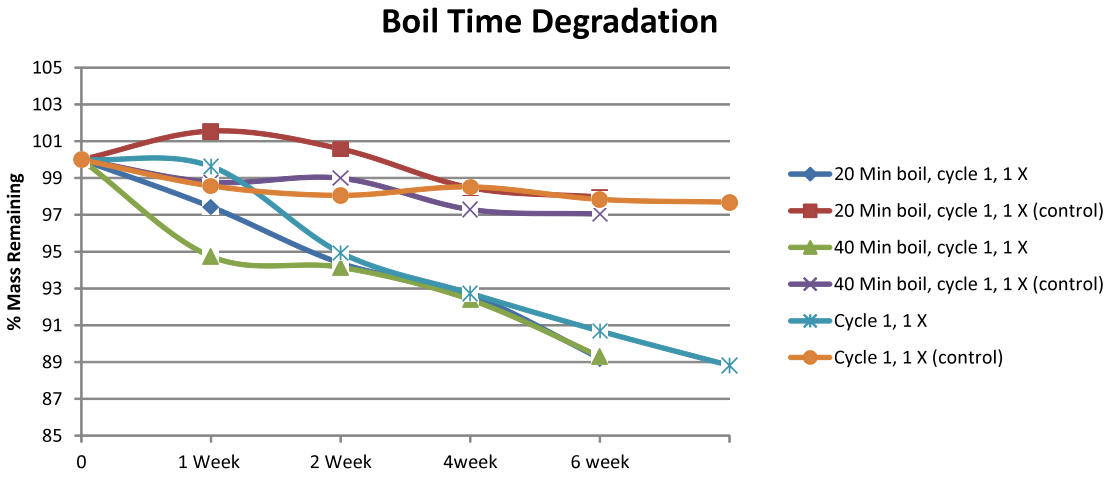

Figure 27. Summary Graph % Mass Remaining of Boil Time Variations over 8 Weeks. (Abbreviations: XX min= XX minute boiled silk, _X autoclave= _ times autoclaved post machining, cycle X= autoclave cycle type X described in section 5.2, control=incubated in PBS, non-controls=incubated in Protease XIV)

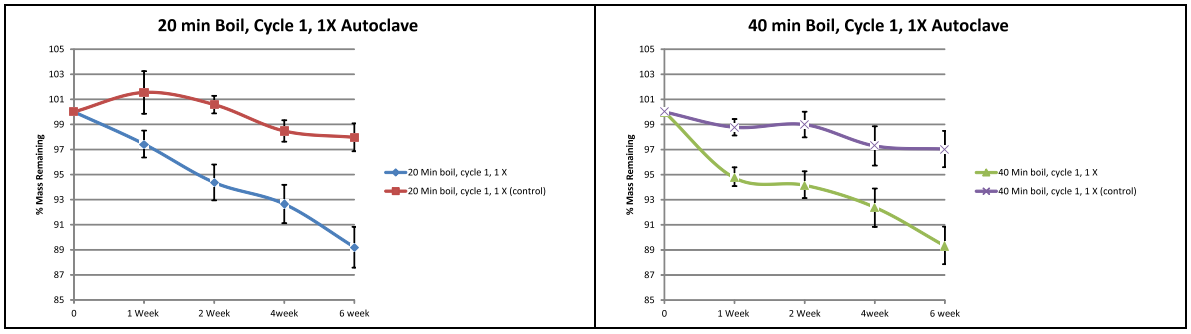

Figure 28. Degradation Comparison of Control (PBS) Silk Pin to Protease Degraded Silk Pin for Boil Time groups. For each boil time, the treatment group showed statistically significant decreases in % mass between almost every consecutive time point. Control groups showed no statistically different changes between consecutive time points other than 0 and 1 week. Little statistical significance was observed between groups at the same time point.(Abbreviations: XX min= XX minute boiled silk, _X autoclave= _ times autoclaved post machining, cycle X= autoclave cycle type X described in section 5.2, control=incubated in PBS, non-controls=incubated in Protease XIV)

In the investigation of the effect of boil time on degradation Cycle 1, 1X will represent the 30 minute boil group. For each autoclave cycle group, the Protease XIV treatment group showed statistical significance between consecutive time points in almost

all cases. The 30 minute, cycle 1, 1X had no statistical difference between 6 week and 8 week while 40 minute, cycle1, 1X had no statistical difference between 1 week and 2 week. Comparison of percent mass remaining between time points for the control group showed no statistical difference besides a difference in 0 and 1 week for 30 minute and 20 minute and a difference in 2 week and 4 week for 40 minute and 20 minute.

Degradation profile comparisons showed significant differences between the control group and protease group for 20 minute and 40 minute after 1 week while 30 minute boiled silk did not show significant difference in degradation than its control until week 4. No statistical difference was detected between treatments. Linear trends were fit to the protease degradation groups with moderately high R^2 values. Linear trends were used to extrapolate the time in weeks of full degradation (resorption) shown in Table 17. All groups were extrapolated to degrade in 38-43 weeks or 6-7 months.

Table 17. Projected Degradation for in vitro Degradation Groups

Group	Linear Trendline	Projected Degradation (weeks)
Cycle 1, 1 X	y = -2.4269x + 102.96	42.42
	R^2 = 0.966	
Cycle 1, 5 X	y = -2.3539x + 101.97	43.32
	R^2 = 0.9893	
Cycle 1, 10 X	y = -2.3204x + 101.5	43.74
	R^2 = 0.9678	
Cycle 2, 5 X	y = -2.5757x + 103.11	40.03
	R^2 = 0.9406	
Cycle 3, 5 X	y = -2.4728x + 100.81	40.77
	R^2 = 0.9136	
20 Min boil, cycle 1, 1 X	y = -2.6366x + 102.64	38.93
	R^2 = 0.9928	
40 Min boil, cycle 1, 1 X	y = -2.3724x + 101.24	42.67
	R^2 = 0.9217	

For all statistical analysis, a two-way Anova with Tukey's multiple comparison was performed. A P>0.05 was considered significant.

Three groups (N=5) of shear plugs were enzymatically degraded for 3 weeks, 6 weeks and 9 weeks in 5U/mL of Protease XIV. Post-degradation, samples were weighed to determine degradation by mass and then tested in hydrated shear in order to correlate degradation and strength retention. Figure 29 shows the effect of degradation on shear strength of the standard processed silk pins.

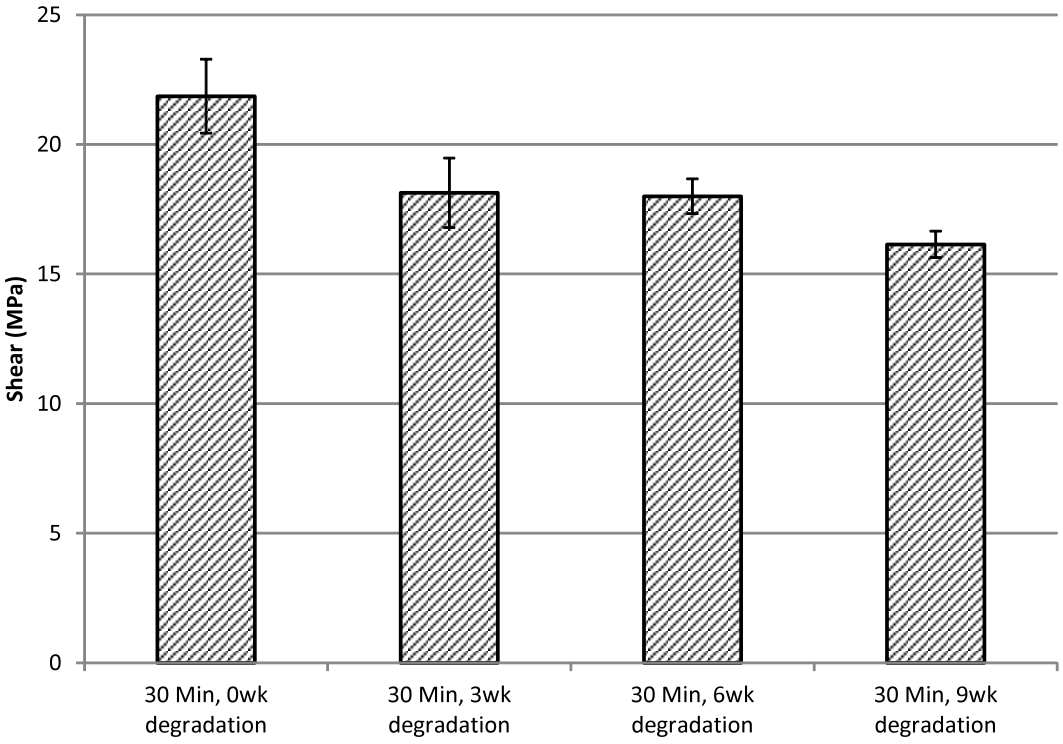

Description	Hydrated Shear (MPa)	Std Dev	% Mass loss
30 Min, 0wk degradation	21.86	1.43	
30 Min, 3wk degradation	18.13	1.34	10.36
30 Min, 6wk degradation	18	0.67	13.41
30 Min, 9wk degradation	16.14	0.51	15.25

Figure 29. Hydrated Shear of 0, 3, 6 and 9 week degradation samples. After 9 weeks (15% degradation), shear strength had significantly decreased. Only between 3 and 6 weeks was loss of strength not significantly different. (Abbreviations: 30 min= 30 minute boiled silk)

Degradation resulted in a statistically significant decrease in hydrated shear strength between time 0 and 9 weeks (~15% degradation by mass). All groups were

statistically different besides 3 and 6 week shear samples. Differences were considered significant if P>0.05 using a one-way ANOVA and Tukeys multiple comparison test.

5.5 Functionalization with BMP-2

5.5.1 In vitro

In vitro absorption and release of BMP-2 was performed in order to investigate feasibility of absorption as a loading mechanism as well as to determine a loading concentration for in vivo studies. A set of 1.5mm diameter by ~3mm length pins were weighed dry and placed in a microtube with 100 µl of 10 µg/ml BMP-2 solution for 4 days to allow full swelling. Upon removal from the BMP-2 solution, mass measurements were recorded on the loading tube, solution, and silk pin at each step of the removal process (e.g,. tube with and without silk pin, pin with and without surface moisture). provides the mass measurements and mass balance to determine loading of BMP-2.

Table 18. In Vitro BMP-2 Mass Balance. Mettler AT20 balance was used with accuracy of 0.002mg. Column A is the initial mass of the silk screw before any treatment, column B is the loading quantity and concentration of BMP-2 solution add to the silk screw, column C is the sum of the mass of the tube the screw was being loaded in and the screw and BMP-2 solution, column D is the mass of the hydrated/loaded screw with residual surface moisture, column E is the mass of the hydrated/loaded screw without residual moisture (wiped off), column F is the mass of the tube used for loading and remaining BMP-2 solution after the screw was removed, column G is the mass of the loaded screw after drying.

	A	B	C	D	E	F	G
sample	mass initial (mg)	BMP-2 added to absorb	Mass Tube + BMP-2 Solution+Screw (mg)	Mass Screw +Wet Residue (mg)	Mass Soaked screw (mg)	Mass of Tube +BMP/PBS (mg)	Screw Mass Dried(mg)
1	14.882	100uL of 10ug/mL	615.856	21.37	17.28	590.322	15.494
2	21.384	100uL of 10ug/mL	622.094	31.53	25.25	589.68	22.308
3	18.53	100uL of 10ug/mL	621.394	25.45	22.01	595.518	19.26

Mass Balance: Total Mass

	F+D	C
1	611.692	615.856
2	621.21	622.094
3	620.968	621.394

Mass of Solution Lost by Swelling

	C-(F+G+(D-E)) mg	C-(F+G+(D-E)) ml (assume 1 g/mL solution)	E-G mg	E-G ml (assume 1 g/mL solution)
1	5.95	0.00595	1.786	0.001786
2	3.826	0.003826	2.942	0.002942
3	3.176	0.003176	2.75	0.00275

Load BMP-2: assume volume of solution absorbed contains the concentration of BMP-2 in stock

Values highlighted in equivalent colors should theoretically be equal. However, determining the mass of solution that was lost from the loading solution to swelling (or gained by the screw) involved assumptions and possible inaccuracies resulting in a mass balance that is not equal. Possible error could arise in small differences in the weight of the silk pins due to humidity, balance error and the degree to which surface moisture was removed. All of these variables would result in small error but the order of magnitude of mass that is being determined was small enough to be affected. It was assumed that the mass that was gained by the absorbing solution would contain a concentration of BMP-2 equal to that in the loading solution. Therefore, the loading concentration of BMP-2

solution and the mass gained by absorption were used to determine a theoretical load (**Error! Reference source not found.**).

Once dry, the BMP-2 loaded silk pins were placed in 150 µl of PBS for release. PBS was sampled and replaced at 1, 2, 4, 6 and 24 hour, 2 and 5 days. Samples were then tested for BMP-2 using a BMP-2 ELISA kit to manufacturer's instructions. Release data can be seen in Table 19 and is represented as both quantity of BMP-2 released in µg as well as percent release based on the theoretical load.

Table 19. In Vitro release of BMP-2 from Silk Pins as determined by BMP-2 ELISA. The top three sample rows represent BMP-2 release as a quantity of mass (ug) while the bottom three sample rows represent release as a % of total BMP-2 release. The "Total Theoretical" column on the right represents the quantity of BMP-2 that was theoretically loaded using mass balance and loading assumptions.

	Sample	1hr	2hr	4hr	6hr	1D	2D	5D	Total Release (ug)	Total Theoretical (ug)
ug released	1	0.010	0.012	0.000	0.000	0.000	0.000	0.000	0.023	0.059
	2	0.010	0.004	0.000	0.000	0.000	0.000	0.000	0.015	0.038
	3	0.008	0.009	0.000	0.000	0.000	0.000	0.000	0.017	0.032
		1hr	2hr	4hr	6hr	1D	2D	5D	Total % Release	
% release	1	17.507	19.710	0.159	0.131	0.133	0.121	0.110	37.873	
	2	27.410	11.601	0.141	0.325	0.244	0.140	0.281	25.812	
	3	25.290	27.165	0.290	0.268	0.365	0.107	0.147	28.627	

Table 20. Summary of Scaffold Loading with BMP-2.

Sample	Loading Solution	mass initial (mg)	Total Release (ug)	Total Theoretical (ug)	Scaffold Loading	
					Released Based (ug/g)	Theoretical Based (ug/g)
1	100uL of 10ug/mL	14.88	0.02	0.06	1.51	4.00
2	100uL of 10ug/mL	21.38	0.02	0.04	0.72	1.79
3	100uL of 10ug/mL	18.53	0.02	0.03	0.92	1.71

As seen in **Error! Reference source not found.**, scaffold loading was determined based on initial mass, release data and theoretical loading. Considering that the scaffold

loading based on release data was more accurate and a more conservative estimate, this loading calculation was used to compare to other published loading concentrations. The loading based on release data was 1.05 ± .41 μg/g of scaffold. Loading concentration was compared to a 17% w/v HFIP derived porous silk scaffold in Table 11**Error! Reference source not found.** as this material most resembled the material in the current work. The loading quantity for the HFIP porous scaffold (7.2 ± .12 μg/g of scaffold) appeared to be within the scope of possible loading for the silk orthopedic hardware.

5.5.2 In vivo

Based on calculated loading quantity for initial in vitro trials and published loading quantities, the concentration of loading solution was increased from 100 μl of 10 μg/ml BMP-2 solution to 100 μl of 30 μg/ml BMP-2 solution for in vivo studies. Sprague Dawley rats were implanted and sacrificed at 1 month, 3 month and 6 month time points (N=5/time point). Screws were implanted similarly to metal systems by drilling a pilot hole and then insertion by self-tapping. Screws came in contact with blood and other bodily fluids but were able to maintain integrity for insertion. In all 15 animals, rats were mobile on all four legs immediately after the effects of anesthesia diminished post-operatively. None of the animals appeared to show signs of pain during examination for 3-4 days post-surgery or have issues with infection or wound dehiscence.

All samples were explanted at the designated time points and sent for histological evaluation. Histology sections were stained with hematoxylin and eosin (H&E) in order to evaluate the presence of cells and the level of cell infiltration. H&E staining will result in a pink color where tissue and extracellular matrix are present while nucleic acids and

the nuclei of cells have a darker, blue color [82]. Sections were also stained with Masson's trichrome stain (MTC) in order to evaluate the deposition of collagen and osteoid as well as cell infiltration. In MTC stained histology slides bone and collagen will appear blue, muscle will appear pink, nuclei (cells) will appear dark red or purple and cytoplasm will appear pink [83]. Cell infiltration and collagen/bone deposition are important observations for the evaluation and validation of osteoinduction by BMP-2. In the remodeling process of bone, the BMP family is known to promote cell proliferation, attract osteoblasts/osteoclasts and generate collagen deposition [31].

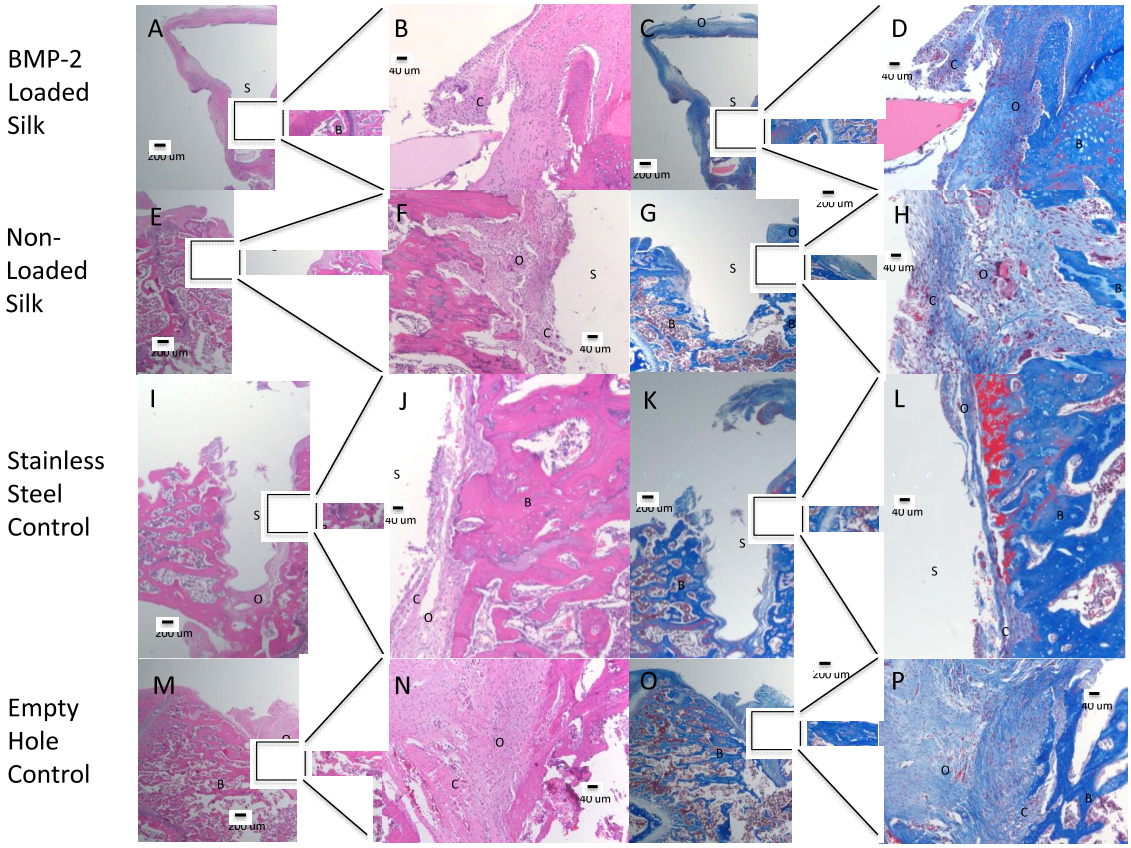

Figure 30. 1 Month Histological Cross Sections of Screws in Rat Femur: (A,E, I, M) 2X H&E stain, (B, F J, N) 10X H&E stain, (C, G, K, O) 2X MTC stain, (D, H, L, P) 10X MTC stain. Osteoclasts/osteoblasts/cells [C], screw placement [S], new bone/collagen/osteoid deposition [O] and bone [B] are marked in each image.

In all histological images, the silk screw, or void from stainless steel screw appears white. This signifies that the silk became removed during sectioning. Stainless steel screws were removed before sectioning and therefore should appear colorless. Sectioning of the distal end of the femur with silk implants was reported to be difficult. Sectioning was more difficult than previous work due to a more distal implantation of screws in the present work. The closer the implantation was to the distal end or knee joint, the harder the bone was and thus the more difficult sectioning became.

Figure 30(M-P) represent histological cross sections of a pilot hole that was drilled and not implanted with a device. The images provide a control reference as to how the empty space in bone will remodel if left alone. Unorganized collagen deposition with moderate cell density of osteoclasts and osteoblasts can be observed.

(I-L) shows histological cross sections from an implanted stainless steel screw that was removed prior to histological evaluation. The light blue region between the screw and the dark blue bone represents collagen deposition. The collagen/osteoid appears to be minimal and confined to the space between the screw and the bone due to pilot hole placement. Osteoblasts and osteoclasts are present in the collagen but in smaller concentration than other groups.

(E-H) in Figure 30, are cross sections of a non-loaded silk screw. Non-loaded silk screws were implanted in order to compare to BMP-2 loaded silk and justify that differences in improved remodeling in the BMP-2 group were a result of the BMP-2 and not the silk material. In the MTC stained images, new collagen was observed between the screw and the hard bone. The deposition appears fairly unorganized. A high density

of cells are visible in the 10X HE (F) and 10X MTC (H) that most likely represent osteoclast resorption of the silk material and osteoblast deposition of new bone matrix.

Figure 30(A-D) show histological staining of BMP-2 loaded screws in a rat femur at 1 month. In 2X HE and 2X MTC (Figure 30A and C), the pilot hole placement can be observed by the clear delineation between dark blue bone and light blue unorganized collagen/osteoid deposition. The width of the pilot hole appears wider at the top of the screw most likely due to drilling and insertion. It is clear in the MTC stains, that good collagen deposition has been induced between the screw and edge of the original pilot hole. Collagen around the periphery of the screw appears to be greatest and most organized in the BMP-2 loaded samples. Collagen has also been induced around the top of the screw head, which was only seen in the BMP-2 loaded sample. In Figure 30 B and C, osteoclasts and osteoblasts can be seen along the periphery of the silk screw as well as within the osteoid/collagen matrix. Cell density also appears highest in the BMP-2 loaded sample.

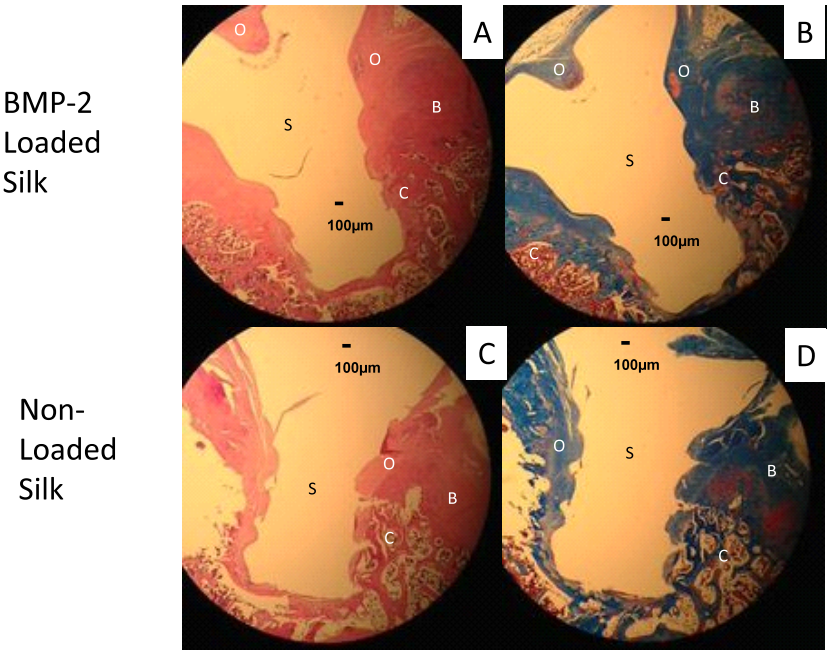

Figure 31 3 Month Histological Cross Sections of Screws in Rat Femur: (A,C) 2X H&E stain, (B,D) 2X MTC stain. Osteoclasts/osteoblasts/cells [C], screw placement [S], new bone/collagen/osteoid deposition [O] and bone [B] are marked in each image.

3 month histological cross sections further support the results observed in 1 month explants. It can be seen that at 3 months, the BMP-2 loaded silk screw (Figure 31 A,B) is surrounded by a thick layer of new collagen or osteoid labelled O. In comparison to the non-loaded silk screw (Figure 31 C,D), the BMP-2 sample has a higher degree of collagen deposition, the deposition is more ordered, and the new collagen has a darker color signifying it is further in the development process to mineralized bone.

No inflammation or negative host response was observed in any sample. The lack of any negative response supports the safety and biocompatibility of the silk hardware.

5.6 In vivo implantation

Plate and pilot hole placement along the fracture site were performed with comparable ease to the titanium system. Insertion of screws by self-tapping into rat

femur was also executed without difficulty. However, issues arose with fracture alignment and the ability of the screws to hold the plate tightly in place. Screws were designed as unicortical screws for CMF repair. A fracture fixation in the femur would normally require bicortical screws such as those of the titanium control system. With a unicortical screw, the screw was able to wiggle slightly. Another major issue related to fracture alignment was the stiffness of the plates. Soon after being hydrated, the plates were able to be molded to shape for placement which offers a good advantage over resorbable systems that require heat treatment. However, the plate swelling rendered it not stiff enough to hold the fracture in place and prevent bone misalignment. Implantation can be seen in Figure 32.

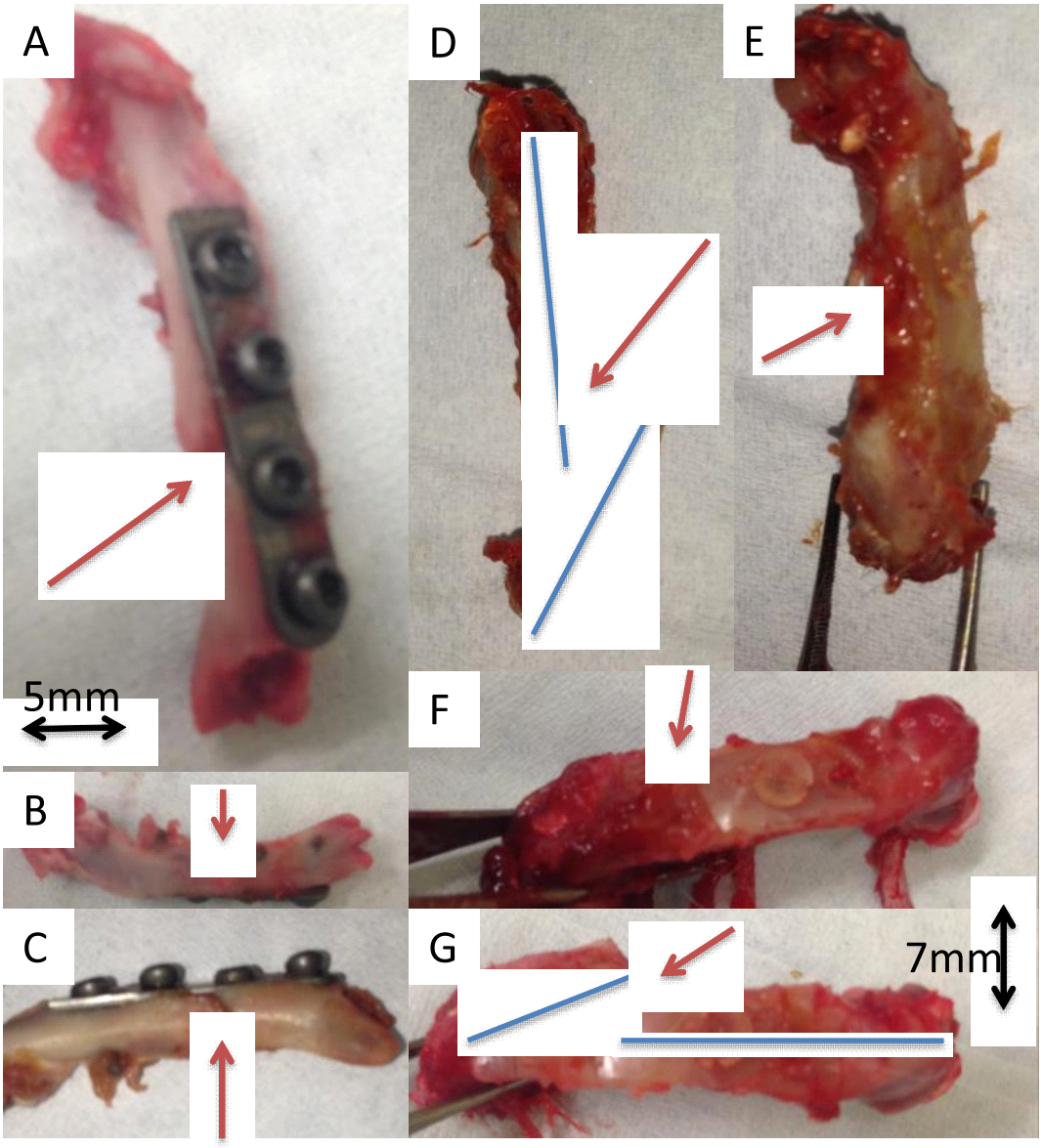

Figure 32 Explanted Fractured Rat Femur. (A-C) Titanium hardware; (D-G) silk hardware. Arrows point toward original fracture site and lines delineate bone alignment.

In both rats (titanium and silk), the animals attempted to keep weight off the surgically repaired leg. By 1 day post-op both rats were using the repaired limb, however, the rat with the silk implant was using it less and exhibited a higher degree of swelling. Both animals showed a decrease in pain over the first few days and increase in activity. Throughout the 1 month time period before sacrifice, the rat implanted with titanium hardware seemed to fully recover with minimal to no swelling. The silk

implanted rat showed increase in activity and weight bearing on the repaired limb but did not seem to fully recover as swelling was still noticeable. Both animals were sacrificed at 1 month time points and the entire femur was explanted and sent to Beth Israel Deaconness Medical Center for histology. Pictures immediate post-op explant showed that the titanium implant did set correctly while the silk implant was misaligned (Figure 32). It was concluded that in order to revisit this model with silk hardware bicortical screws must be used and screw head/plate fitting could be optimized. The main modification would be to increase the stiffness of hydrated plates. Another option that will be pursued is the use of a silk intramedullary nail rather than a plate and screw system.

5.7 Feasibility of Aqueous Based Hardware

All aqueous silk formulations were prepared and injected into the silk plug molds. Formulations were then exposed to various treatments such as critical point drying in the hope of preserving nano-structure or standard crosslinking and drying. The ability of each solution/treatment to form a silk plug blank was recorded. If the formulation was able to generate a blank, it was then tested for machinability on a lathe and threadability using a threading dye. The summary of these results are described in Table 21.

Table 21. Feasibility Summary of Aqueous Silk Solutions. High concentration silk solutions with no additive, cross-linked with methanol, dried and autoclaved show the greatest potential aqueous silk hardware.

Solution Description	Note	Treatment	Plug Formation Y/N	Machineable Y/N	Thread (w/ dye) Y/N
LiBr-FA Silk	N/A	MeOH crosslinking, air dry, oven dry, autoclave	Y	N	N
	N/A	MeOH-EOH crosslinking, CPD, autoclave	Y	N	N
	N/A	60°C oven for 3 days	N	N	N
	N/A	EOH crosslinking, CPD, autoclave	Y	N	N
High Concentration Silk Solution (Heated Centrifuge)	20%, 30 min	MeOH, air dry, oven dry, autoclave	Y	Y	N
		EOH, CPD, autoclave	Y	Y	N
	20%, 30 min, 5% Silk Powder	MeOH, air dry, oven dry, autoclave	Y	N	N
		EOH, CPD, autoclave	Y	N	N
	20%, 30 min, 5% Hydroxyapetite	MeOH, air dry, oven dry, autoclave	Y	N	N
		EOH, CPD, autoclave	Y	N	N
High Concentration Silk Solution (Dialyze vs High pH)	20%, 30 min	MeOH, air dry, oven dry, autoclave	Y	Y	N
	24.1%, 60 min	MeOH, air dry, oven dry, autoclave	Y	Y	N
	27.1%, 60min	MeOH, air dry, oven dry, autoclave	Y	Y	N
Pressed Silk Powder	N/A	N/A	Y	Y	N

Each formulation was also investigated for surface morphology through the use of SEM imaging (Figure 33-35).

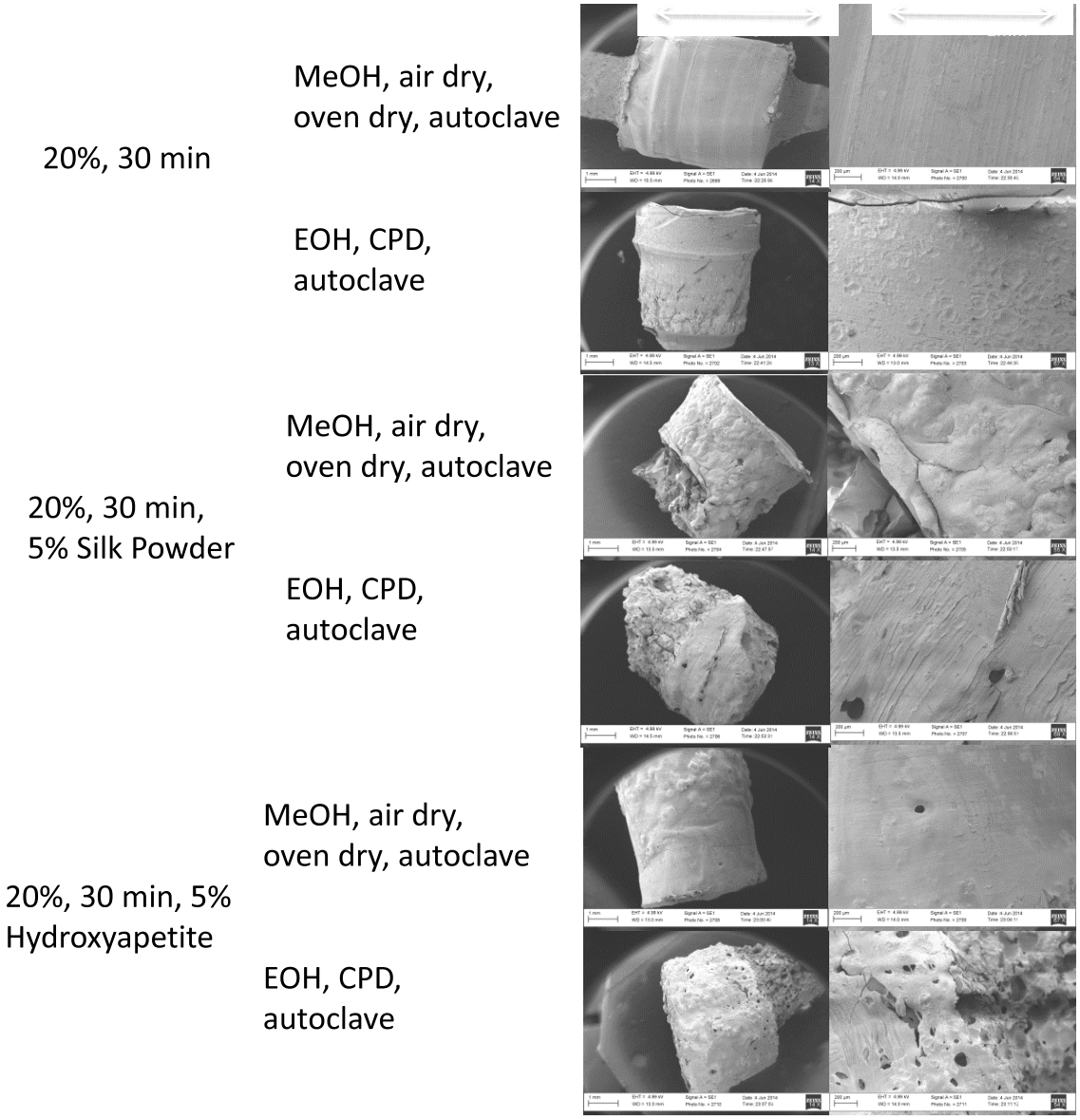

Figure 33. SEM images of aqueous silk formulations generated from high concentration silk, concentrated with a heated centrifuge. Scale bars at the top are applicable to each respective column of images.

20%, 30 min, MeOH, air dry, oven dry, autoclave

24.1%, 60 min, MeOH, air dry, oven dry, autoclave

27.1%, 60min, MeOH, air dry, oven dry, autoclave

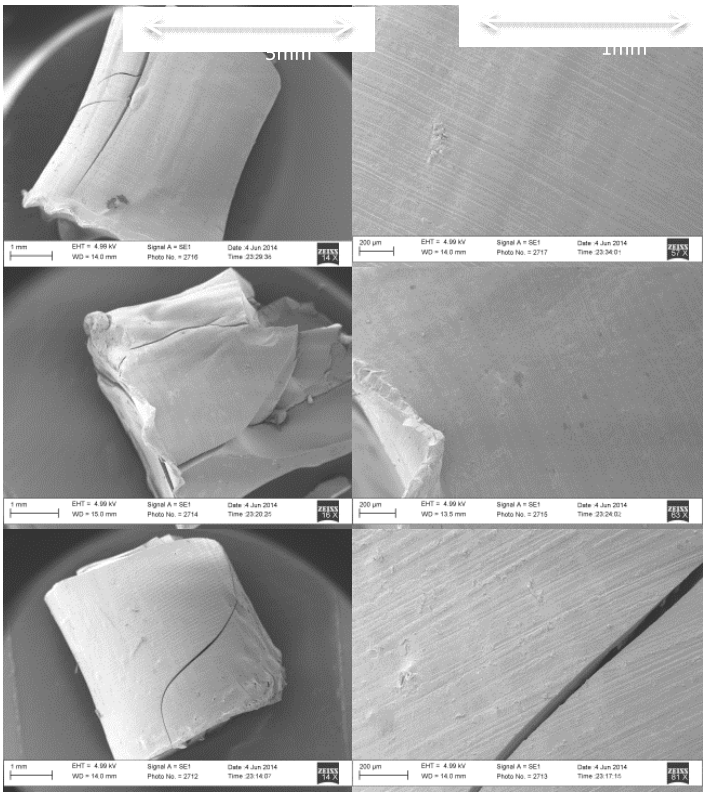

Figure 34. SEM images of aqueous silk formulations generated from high concentration silk, concentrated by dialysis against a high pH solution. Scale bars at the top are applicable to each respective column of images.

MeOH crosslinking, air dry, oven dry, autoclave

MeOH-EOH crosslinking, CPD, autoclave

EOH crosslinking, CPD, autoclave

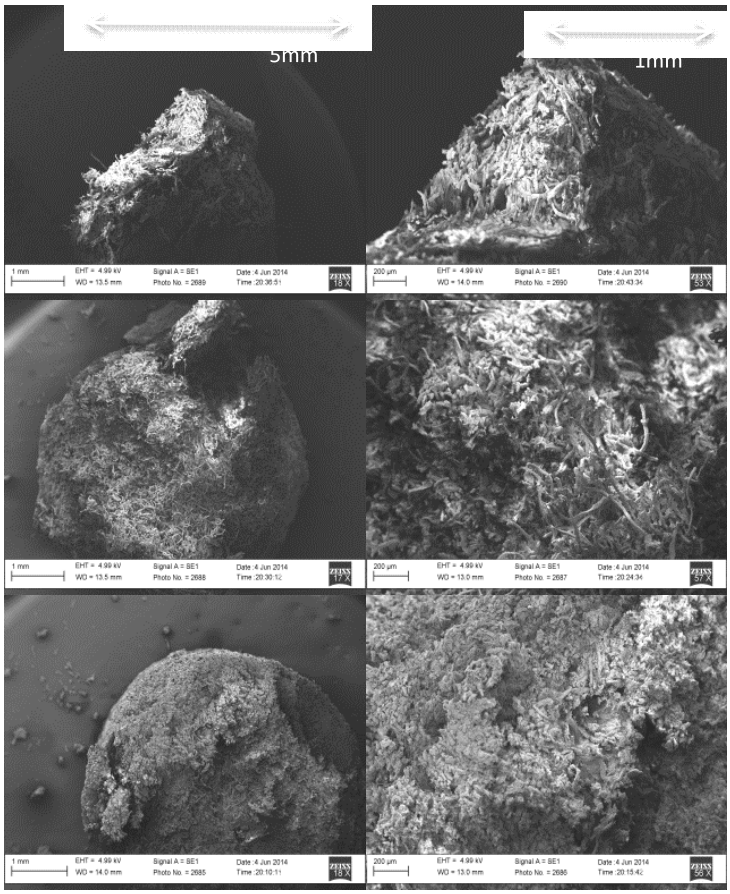

Figure 35. SEM images of aqueous silk formulations created from Lithium Bromide-Formic Acid solution. Scale bars at the top are applicable to each respective column of images.

Pressed Silk Powder

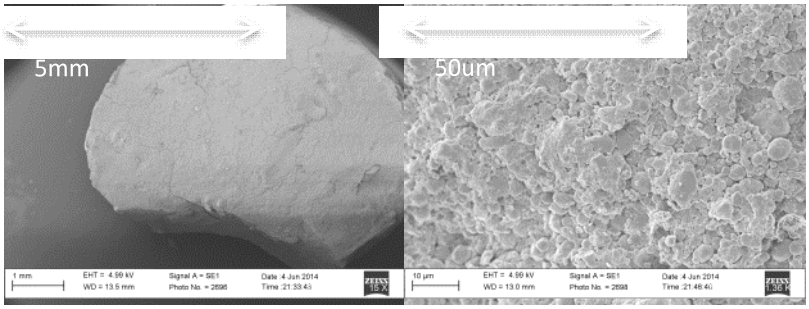

Figure 36. SEM images of aqueous silk formulations created from pressed silk powder (5 micron particle size). Scale bars at the top are applicable to each respective column of images.

High concentration silk solutions without particle additives appeared to be the lead candidate based on machinability. SEM images show that these formulations each have very similar, non-porous, smooth surface morphology. LiBr-FA silk formulations appear to be a tight bundle of silk nanofibrils. The material was similar to a tightly knit yarn

plug and therefore did not machine well and only frayed. The addition of silk powder particles and hydroxyapatite particles generated pores seen in SEM images. The pores resulted in chipping during machining. Critical point drying did not seem to have a major effect on surface morphology or machinability. Pressed silk powder had a unique morphology when imaged by SEM. The particles could be seen very tightly packed with little to no pores. Silk powder is another promising candidate for future investigation.

5.8 Swelling

A major issue with mechanical integrity as seen earlier is the poor hydrated mechanics. Cross-linking agents and autoclaving were investigated to reduce swelling and thus reduce the effect of hydration on mechanics. The swell ratio describes the ratio of water absorbed to dry weight of the screw and is intimately related to water uptake % which is the water % of the swollen sample. The control group of 30 minute boiled HFIP silk, cross-linked with MeOH and autoclaved 1X had a swell ratio of 0.16 ±0.006 and a water uptake of 13.88±0.46 %. The additional soak in EDTA did not statistically affect swelling with a swell ratio of 0.19 ±0.016 and water uptake of 15.64±1.15 %. Cross-linking with gluteraldehyde also did not improve swelling properties resulting in the highest swell ratio of 0.2 ±0.007 and water uptake of 17±0.47 %. Autoclaving did not effect the dimensional stability of silk devices, however it was hypothesized that the high temperature steam system may act to limit mobility of silk molecules and prevent hydration. 10 x autoclaved samples showed significantly lower swell ratio (0.11 ±0.002) and water uptake (9.7±0.18 %). However, hydrated mechanics addressed before were not improved. More autoclave cycles may be necessary.

Chapter 6. Discussion

The goals of the current project as described in Table 8. Summary of previous work on silk orthopedic hardware, were each addressed with a range of success. Great improvements were realized in the fabrication of silk hardware with the addition of bone screw threads, standard sized plates of different length and cross section, intramedullary nails, countersunk head fitting for less palpability and minimized material waste. Initial feasibility of aqueous processes was tested and showed potential for replacement of HFIP silk. Mechanical properties were further investigated for optimization of shear and pullout strength. Some improvements from previously reported work were made but increasing strength with variations in process and post process treatments was unsuccessful. Bending and fatigue properties were measured for the first time. Bending showed comparable modulus to current systems but a need for improvement in stiffness. Fatigue testing illustrated the resistance of silk to fatigue as silk hardware was able to withstand high load cycles that represented worst case scenarios. The elastic modulus was determined and found to be much closer to bone than metal (reduced stress shielding). Swelling proved to be a major concern in the initial work on silk hardware due to poor hydrated mechanics. Physical treatments and cross-linkers were investigated to reduce swell ratio and water uptake. Both swell ratio and water uptake were reduced but hydrated mechanics remained poor. Degradation was further investigated for various treatments and processing but little differences

were seen. With the insignificant differences in strength and degradation of the various treatments, it is hypothesized that the use of HFIP in the processing of silk is the most important determinant of physical properties. The resterilization of silk hardware was also confirmed with retention of strength, dimensional stability and no effect on degradation after 10 autoclave cycles. Feasibility and implantation technique was investigated for fracture fixation with silk hardware. Minor size modifications will need to be instituted for silk screws and plates as well as stiffening of the plates. Intramedullary nails were implanted in a sacrificed rat for feasibility and implantation but a live model will need to be used in order to determine the ability to fix a fracture. Silk hardware was successfully functionalized and able to release an osteoinductive molecule (BMP-2) *in vitro* and *in vivo*. This will offer a distinct advantage of not only being biodegradable and resorbable but actually promoting and inducing bone growth and remodeling.

Table 22. Summary of Goals and Results

Category	Previous Results	Goals	New Improvements
Fabrication	30 minute boil HFIP silk process	Screws with bone screw threads	Bone Screw Threads
	Machinable silk blanks	Bone plates (various geometry)	Bone Plates (varying length and cross section)
	1-72 mechanical screws	New application/device	Intramedullary Nail
	Proof of concept plates (strips of silk material)	Minimize material waste	Less wasted material with HFIP silk
		Minimize Palpability	Countersunk head fitting for screw/plate
		Aqueous process	Feasibility of aqueous processes
Silk Structure	High beta sheet content confirmed (49.3%)	N/A	N/A
Mechanical Properties	Shear (dry): 90.0±11.8 MPa	Shear (dry, hydrated), optimization	Bending properties of plates (stiffness, bending modulus)
	Shear (hydrated): 19.3±0.51 MPa	Pullout (dry, hydrated), optimization	Shear= ~90 MPa (dry), ~17 MPa (hydrated)
	Pullout (dry): 80.7±9.38N	Bending properties of plates	Pullout= 108.59 ± 5.33 N (dry), 22.92± 4.16 N (hydrated)
	Pullout(hydrated): 19.18 ± 5.98 N	Fatigue testing (cyclic)	Preliminary Fatigue testing in shear, pullout and bend
		Elastic Modulus	Elastic Modulus= 2.17 ± 0.27 Gpa
Swelling	Swell ratio: 0.22±0.03	Optimize (decrease) swell ratio/water uptake	Swell Ratio=0.11 ± 0.002
	Water uptake: 17.9±1.99%		Water Uptake= 9.7 ± 0.18 %
	No significant swelling in first 15 min		
Degradation	31% by week 23 (by surface erosion), ~ 7 months	Further investigate degradation with different treatments	Investigated/extrapolated degradation through 8 weeks for various boil time and autoclave cycle
		Shear strength after degradation	Shear strength at 3,6,9 week degradation
Ease of implantation	Proved self tapping (Vickers microhardness=40 kg/mm2)	N/A	
Resterilization	Dimensional stability proven after 1st autoclave	Determine feasibility of resterilization by dimensional stability and mechanics	Resterilization by autoclave confirm
	Some decrease in shear strength		
In vivo characterization and implantation technique	Plates malleable with spray of water	Fracture fixation: implantation of silk screw and plate	Implantation technique of silk screw and plate(feasibility)
	Self tapping in rat femur and human cadaver skull	Fracture fixation: implantation of silk IM nail	Implantation technique of IM nail (feasibility)
	Rats implanted with a screw were mobile post surgery on all 4 legs		
	Implanted rats showed minimal signs of complication/infection		
	Osteoclast/osteblast formation		
Functionalization	N/A	In vitro functionalization and release of BMP-2	In vitro functionalization and release of BMP-2
		In vivo implantation and release of BMP-2	In vivo implantation and release of BMP-2

6.1 Fabrication of Silk Hardware

The efficiency and consistency of silk blanks for machining was improved significantly. In the past, the high viscosity of HFIP-silk solution made the filling of narrow molds difficult without the formation of bubbles or gaps. Placement in MeOH for physical cross-linking soon after filling the molds generated large defects in the silk blanks that rendered much of the material unusable. The introduction of a bubble releasing step by sealing plug molds with lids, was successful in producing minimal bubble silk blanks that were nearly completely usable material for machining. A sealed

lid was necessary due to the fact that HFIP would quickly evaporate upon exposure to air creating a hard rubbery surface. Uniform plates were also generated through the use of Teflon molds that were injection-filled from bottom to top in order to minimize bubbles.

Silk blanks (cylinder plugs and rectangular plate molds) showed high machinability with both bench-top machining equipment as well as with CNC style machines. Silk screws and IM nails were machined to specified diameters with the use of a CNC lathe and screw threads were placed by replacing the cutting tool with a single point external cutting tool. The use of CNC machining to produce bone screws is promising for a number of reasons. First, screws were much more consistent when machined with CNC tooling. Previous silk screws cut with a threading dye relied on the user to place threads often resulting in thread inconsistencies and threads being placed on an angle. This was supported by mechanical pullout strength tests. The standard deviation in the bone screws threads was far less than that in screws with mechanical screw threads placed with a threading dye. CNC machining for bone screw formation also shows great potential in the possible scalability and manufacturability of the devices. Silk plates were also able to be machined with CNC milling machine. However, in order for machining on a lathe the material must be able to lie flat. Due to deformation and drying inconsistency, many of the plate molds had some degree of curling. In order to be machinable on the milling machine, molds were rehydrated, placed under significant weight and dried. This process rendered flat molds but were time consuming. Once flattened, plate holes were first placed in order to hold the mold in place. CNC milling was then used to cut the various plate geometries.

6.2 Material Properties

Mechanical strength and material properties including degradation and swelling were investigated for a variety of conditions, treatments and processing variations to optimize areas of weakness such as mechanics upon hydration, as well as to provide data that was not previously gathered such as plate strength, elastic modulus and fatique testing.

Pullout strength was investigated for screw thread geometry, post-silk processing treatments and polyurethane density. It was important to test and compare the strength of bone screw threads due to the fact that data from other systems is based on bone screw thread geometry and pullout strength is a geometry-dependent test. Testing showed no significant difference between bone screw thread and mechanical screw thread in dry or hydrated conditions. It is promising that the mechanics were maintained considering the fact that the bone screw threads were machined with a pitch length of 0.6 mm to match competitor screws while the mechanical screws had a smaller pitch length of around 0.4mm. A smaller pitch length (pitch peak to pitch peak) will result in a higher thread count and therefore should have higher pullout strength. The improved repeatability in machining by CNC placed bone screw threads is also supported by the small standard deviation in bone screws and large deviation in mechanical screw threads. The inconsistency in mechanical screws was most likely due to inconsistent thread placement. Treatments to the silk post-silk processing included heating the HFIP solution and autoclaving 10 times as opposed to once. Heated HFIP resulted amber plugs that were the most consistent plugs due to lower viscosity while filling. This was tested for hydrated strength under the hypothesis that a more consistent plug could be a result of

denser packer or some other physical change resulting in the amber color and that hydrated mechanics could possibly be increase. A 10X autoclave group was tested in the hypothesis that autoclaving 10X would result in the maximum amount of drying and that hydration would be limited. Average hydrated pullout strength in both treatments appeared slightly higher than the control silk mechanical and bone screws, however differences were not significant. Dry mechanics were ignored due to considerations with materials and machining as well as the fact that the hydrated mechanics are a larger concern at the current time. One group of screws was tested in a sample of 30 pcf (0.48g/cc) polyurethane provided by Sawbone. All other tests were performed in 40 pcf (0.64 g/cc) polyurethane. The lower density bone resulted in significantly lower pullout strength values due to the inability of the polyurethane to maintain structure. Threads were kept intact but pulled out at 30pcf at 55.5N as opposed to nearly 110N in 40 pcf polyurethane. The 40 pcf (0.64g/cc) was used although it has a lower density than that of human parietal bone (1.75-1.85 g/cc) which is commonly reported for the testing of bone screws ([34,63,65]. The reasoning for the use of 40 pcf polyurethane is that it is one of the highest density polyurethane blocks that are produced and polyurethane is used as the standard bone mimic for testing under ASTM standard F1839-08. Polyurethane is meant to mimic cancellous bone while parietal bone is dominated by more dense cortical bone. For cortical bone mimic, polyurethane can not be used and high strength fiber composite would be necessary. For these reasons, pullout strength in bone may be much higher than are reported here. Dry pullout strength was increased from previously reported strength of ~80N to 108N. These values compared favorably with reported resorbable system pullout strength between 95N and 100N. Metal systems remain much higher at 400N.

However, hydrated mechanics remain an unsolved issue with hydrated pullout strength of about 20N. Treatments were not able to significantly improve the hydrated mechanics. In order to address this issue, reinforcement by particles or fibers could be investigated as well as another treatment to potentially reduce hydration of silk hardware. Cyclic testing was performed in order to investigate the effect of fatigue by small loads. For example, placement of a screw in the mandible may experience repetitive loading due to chewing and talking. Screws were tested at 10N cycles up to 10,000 cycles based on a reported study that used 10,000 10-100N cycles to simulate the load of walking 10km on the fibula [74]. Reported cyclic loading of internal fixation devices was limited so a 10N, 10,000 cycle loading scheme was used as an extensive measure of the cyclic fatigue properties of silk screws. Two dry screws were able to remain in the polyurethane for all 10,000 cycles. One of these screws was tested for maximum pullout strength afterward and resulted in 62.29N pullout. This shows great potential for cyclic fatigue strength retention which will be important. However, two dry screws pulled out between 4,000 and 7,000 cycles and a hydrated screw pulled out after 1,742 cycles. The loading regiment was much greater than a device would experience in non-load bearing applications so the initial investigations into cyclic pullout strength are promising.

Shear strength (most applicable to screws and IM nails) was studied more extensively than pullout strength due to ease of machining and due to the lack of geometry dependence in correlation of sample group and strength. Process treatments, boil time of silk fibroin and autoclave cycle variation were investigated for improved shear properties. Processing treatments of heating HFIP solution, 10 times autoclaving and critical point drying were investigated. Processing treatments appeared to have no

effect on hydrated or dry shear strength other than critical point drying which resulted in decreased strength. Boil time was investigated due to the previously reported differences in molecular weight and scaffold assembly in silk prepared from varying time degumming [81]. Hydrated mechanics were unaffected while dry mechanics appeared statistically higher in the 20 and 40 minute boil than the 30 minute boil silk. Although the difference was statistically significant, the difference was relatively strong and can most likely be attributed to drying of the different silk plugs. If the 30 minute silk plugs were not as dry (humid conditions while testing or smaller driving force of drying while in ambient conditions) the strength would appear lower. Another explanation would be that there is a balance between molecular weight and the assembly/pore size during packing. Higher boil time would result in lower molecular weight silk which has potential to pack tighter with smaller pores [81]. There may be a tradeoff between 20 and 40 minutes at which molecular weight of the silk and structure of assembly render 30 minute boiled silk a weaker material. An array of autoclave cycle and cycle number were investigated for shear strength but neither hydrated or dry mechanics were significantly improved. Dry shear strength of lead candidate silk hardware tested was 87-95 MPa while hydrated mechanics were around 15 MPa. Other resorbable systems report strengths from 100-185 MPa [22,63,84] while titanium remains much higher at 550 MPa. Dry mechanics resemble similar strength to resorbable systems for non-load bearing applications but remain weak in hydrated conditions. Cyclic testing was performed on shear strength of the standard formulation silk for orthopedic hardware for similar reasons explained for cyclic pullout. Two samples were exposed to 10,000 cycles of 100N in dry conditions. Both samples remained intact after 10,000 cycles. One sample

was tested for maximum shear strength after cyclic testing and was found to be 91 MPa. It appears that an aggressive loading scheme of 10,000 cycles at 100N did not cause any significant fatigue in dry hydrated mechanics. More testing would need to be performed to validate these results as well as to investigate hydrated cyclic shear.

Bending strength of plates was investigated only for the standard 30 minute boil, HFIP silk formulation. Plate size was investigated for varying plate thickness and geometry. Increase in thickness of the plates resulted in an increase in bending stiffness, structural stiffness and bending strength as expected. These values are a reflection of the plates resistance to bending or deformation. The bending modulus, which takes plate size and area into account, appeared to decline with plate thickness. In theory, bending modulus and bending stiffness should be related. The stiffness should be the product of the modulus and the moment of cross section inertia [85]. However, the data says while stiffness increases, the modulus decreases. This makes sense looking at the equation for 4-point elastic modulus in which there is a second order negative relationship with thickness and a first order relationship with stiffness. The calculations made for stiffness were calculate based on ASTM standards and the calculations made for modulus were based on previously published work specific to the testing performed. More testing will have to be performed to better understand plate strength. Bending stiffness of current resorbable systems has been reported to be as low as 10N/mm in a PLGA pin and as high as 100N/mm in a PLA plate, while titanium plates are about 270N/mm [18,24,86,87] . The bending modulus of current resorbables and titanium have both been reported in the range of 5-7 GPa. Silk plates of 0.75, 1.2 and 2 mm showed dry stiffness of 17.6, 50.8 and 162.8 N/mm and bending modulus of 4.4, 3.1 and 1.7 GPa, respectively. These

numbers appear to match the other products for non-load bearing applications, however hydrated mechanics were significantly lower. A hydrated 1.2 mm thick plate had stiffness of 5 N/mm and modulus of 0.3 GPa. A half-I beam cross section was also investigated with wall thickness of 1.2 mm and center line thickness of 0.75 mm to determine if adequate strength could be met while limiting palpability. As expected the stiffness of this plate fell between that of the 0.75 and 1.2 mm plate. Further investigation is needed to determine what the acceptable stiffness would be.

The compressive elastic modulus was determined to be 2.17 ± 0.27 GPa. This value is much closer to that of bone (~20GPa) than titanium (>105GPa). The compressive modulus was determined in order to quantitatively support the concept of reduced stress shielding by more closely matching the elastic modulus [6]

Swelling properties were studied due to the issue of poor hydrated mechanics. A decrease in swelling properties (swell ratio and water uptake %) would mean that the degree of swelling decreased. The less the material swells, the better the hydrated mechanics. Four post machining treatments were investigated for effect on swell ratio and water uptake. The four treatments included two variations on autoclave cycle (1X or 10X) and variation of cross linking agents (methanol, EDTA and gluteraldehyde). MeOH crosslinking and 1X autoclave (swell ratio=0. 16±0.006), MeOH physical crosslinking and 10X autoclave (swell ratio=0. 11±0.002), MeOH crosslinking, EDTA and 1X autoclave (swell ratio=0. 19±0.016), and gluteraldehyde-MeOH crosslinking and 1X autoclave (swell ratio =0.2 ±0.007) showed significant differences in swelling. The 10X autoclaved group swelled the least with a swell ratio of 0.11. However, 10X

autoclaved samples were tested for shear and pullout and hydrated mechanics were not improved.

In vitro degradation with Protease XIV was studied to determine the effect of boil time and autoclave on degradation. Degradation data showed little statistically significant differences between treatments and boil time. Full degradation was extrapolated using a linear trend and it was determined that silk internal fixation devices will degrade in about 10 months. The hydrated shear strength was determined at 3, 6 and 9 weeks of degradation. Significant decreases were observed from 0 to 3 weeks and 6 to 9 weeks. However, by 9 weeks shear strength was still at 16 MPa which is not much less than the time 0 point and other hydrated formulations.

Silk hardware was also investigated for resterilization by autoclave. Various autoclave cycle types and cycle numbers did not affect mechanical strength, degradation or dimensional stability. In fact, autoclaving has the potential to improve properties of the silk hardware. For these reasons it was determined that silk devices can be resterilized by autoclaving which is a significant cost advantage over other resorbable systems.

The pullout strength of the bone screw thread silk screws showed a statistically significant increase compared to previously reported results. However, none of the variations of processing treatments or post treatments caused significant improvement. All samples were self tapping in polyurethane which provides for a significant advantage over current resorbable systems. Shear strength was also not significantly improved but similar to pullout strength, remained comparable to resorbable systems in the dry state. The current mechanics are still inadequate for load bearing applications when hydrated but may be sufficient for non-load bearing applications. Initial cyclic testing showed

thatthe material had good fatigue properties and strength which may be advantageous over other products. The elastic modulus was close to bone to minimize stress shielding and swelling properties decreased but remain an area for improvement. Based on material property testing including mechanical strength and degradation, it appeared that varying process conditions and treatments had little effect on the material. It is hypothesized that the role of HFIP alpha helix induction and methanol beta sheet conversion is of the highest importance to material properties.

6.3 Functionalization and Release of BMP-2

Neither current resorbable systems nor metallic systems provide functionality beyond the mechanical union to fix a fracture. Resorbable systems such as PLGA are promoted to improve bone remodeling through absorption and degradation, however, results have shown that remodeling has been incomplete and that the resorption is not osteoinductive [18,86]. Silk has been known for its stability and release of many different molecules including BMP-2 [51,54,56,77,88,89]. In the present work, silk orthopedic hardware was functionalized with BMP-2 through absorption of BMP-2 solution. Initial in vitro studies showed absorption in 100μL of 10μg/mL loading solution resulted in loading quantities of 0.75-1.5 μg/g scaffold. Based on loading quantities in previously published work, the concentration of loading solution was increased by a factor of 3 for in vivo studies. Sprague Dawley rats were implanted with non-loaded silk screws, BMP-2 loaded silk screws, an empty hole and stainless steel screws. At 1 and 3 months, histological evidence supported the release and activity of BMP-2. At 1 month the BMP-2 loaded implant histological sections showed the greatest quantity of new collagen

deposition with high cell density consisting of osteoclasts and osteoblasts. The deposition of collagen and osteoids extended even over the head of the screw. No inflammation or negative side effects were noticed in H&E and MTC stained slides. In order to quantitatively measure the effect of BMP-2, a method that observes mineralization and/or bone formation such as a von Kossa stain, would need to be utilized in conjugation with X-ray diffraction or FTIR [90]. The ability to be functionalized with BMP-2 and successfully show release in vitro and in vivo supports the feasibility of producing osteoinductive fixation devices and shows potential for the loading and release of other molecules. Potentially, antibiotics can also be loaded to minimize infections and inflammation or proteases could be loaded to facilitate more rapid degradation.

6.4 In Vivo Implantation

Previous reported work on silk orthopedic hardware investigated the implant technique of screws, showing that screws could be implanted by self-tapping and would be biocompatible. Self-tapping obviates the need of a two-step hole drilling process that is required for resorbable systems. In the current work, the feasibility of fracture fixation was examined in the fracture of a Sprague Dawley rat femur. Screw implantation was performed similarly to previous animal studies. Silk plates were used in conjunction with the silk screws in order to hold a mid-diaphysis fracture in place. During implantation it was noted that the screws would need to be made longer so that they would be bicortical screws. It was also observed that the plate was overhydrated and lacked sufficient stiffness. The plate was easy to handle and shape but the flexibility in the plate, along with loose unicortical screws resulted in a weak fracture fixation. The animal recovered

by a month and was able to bear weight but explantation photos showed that the fracture did not align correctly. Possible methods to stiffen the plates and avoid misaligned fracture repair include that the plates should not be fully hydrated when implanted and plates could be made thicker as illustrated by plate strength testing. Fiber reinforcement, particle reinforcement and other treatments/ additives could be investigated to reduce swelling and improve the stiffness. Screws will also need to be cut with a longer shank.

6.5 Aqueous Silk Feasibility

The current lead candidate silk formulation for silk orthopedic hardware involves the use of toxic HFIP. While biocompatibility tests in rats have shown no negative side effects or inflammation, sacrificial time points were only analyzed for short term studies. Long term effects are unclear. It would be advantageous to generate an aqueous based silk formulation in order to obviate the risks of using HFIP as well as to avoid any health concerns. Feasibility studies were performed on various aqueous based solutions to test for consistent blank formation, machinability and ability to be threaded. All LiBr/formic acid dissolved silk formulations appeared to be the least feasible option. The result was silk blanks that consisted of densely packed fibers. The material was difficult to machine as it would fray and it was not nearly as stiff as the other formulations.

Silk powder presented an interesting option when pressed to a solid material under high pressure. The pressed silk powder was comparable in look and feel to a ceramic. The plug was easily machined on a lathe to a specified diameter but would break upon thread placement due to being brittle. While plugs may not be feasible for screws, pressed silk powder could be explored for some applications, for example, silk

plates do not require the same torsion or deflection properties needed for threading. The stiffness of the pressed material would also be advantageous for plates.

The lead candidate aqueous silk solution is some variation of highly concentrated silk that is then physically cross-linked with methanol. All high concentration silk solutions produced machinable silk blanks besides those that had silk powder or hydroxyapatite. Plugs with particles may in fact be machinable to a plate or to a specified diameter but the addition of pores created by particles resulted in chipping during machining. High concentration silk produced from 30 minute and 60 minute boiled fibroin, 20-27% silk and concentrated by heat and by dialysis in high pH solution all generated machinable blanks. The blanks were very similar to HFIP silk solution blanks after methanol cross-linking. Drying in a hood and oven caused some shrinking and caused the color to darken to a gold/yellow color. Autoclaving resulted in final shrinking and dimensional stability. Threads were not easily placed with a threading dye but could be feasible with the use of the external single point cutter. The use of a threading dye relies heavily on torsional properties and the resistance to splinter while external cutting does not. Investigation into mechanical strength, degradation, and particle/fiber reinforcement will need to be performed in order to make silk hardware with the material properties necessary for internal fixation. Aqueous high concentration silk can be considered feasible and will hopefully allow for better control of material properties through variations in processing conditions.

Chapter 7. Conclusions

At present, material options for internal fixation devices can be categorized into two groups; metals (titanium, stainless steel) and resorbables (PLLA, PLGA, PGA). Metal systems provide unmatched mechanical strength for efficient fracture fixation but are permanent and associated with many side effects. Resorbables offer an option that will potentially degrade over time obviating need for hardware removal or long term adverse effects. Resorbables are limited by weaker mechanics and ease of use due to the need for pre-tapping and the inability to be resterilized. There exists a large unmet window inbetween these two systems for new materials that provide adequate mechanical strength, ease of use and implantation and also degrades over time to provide complete bone remodeling with limited long term side effects or a need for a secondary surgery. In prior work, silk screws were investigated for proof of concept and showed potential in mechanics, degradability and ease of use. In the current work, optimization of material properties was pursued. Optimization involved new design and manufacturing, varying process conditions of silk and post processing treatments. The manufacturability of not only screws but various geometries of plates and nails with the use of CNC machining was demonstrated and supported scalability. Mechanical strength was not significantly improved but a wider scope of mechanical properties was gathered including cyclic testing, elastic modulus and plate strength. Current strength appears comparable to current resorbable systems for non-load bearing applications but hydrated mechanics remain the drawback. Degradation was extrapolated for full resorption at 10 months with retention of mechanical properties at 3, 6 and 9 weeks. The ability to be resterilized by autoclave without effecting hardware integrity was also demonstrated.

The possibility of functionalization of silk hardware with osteoinductive molecules was also investigated. BMP-2 was successfully loaded into silk screws and released in vitro and in vivo. BMP-2 loaded screws in vivo supported previous results of safety and compatibility with no negative host response. BMP-2 appeared to be successfully release resulting in increased collagen deposition and cell density. The release of BMP-2 would allow silk hardware to facilitate osteoinduction and result in more complete bone remodeling. Functionalization is not limited to BMP-2 but could potentially be an approach utilized to minimize infection rate and other side effects by the incorporation of antibiotics and other therapeutic compounds.

The feasibility of an aqueous process to produce silk hardware was also studied. Results showed formulations with promising potential to produce bone screws. Materials feasible for screws will also need to be investigated for plate formation. Plates may need to be produced through a different formulation than screws so all formulations should be investigated. The mechanical strength of feasible aqueous materials is still unknown.

Error! Reference source not found.summarizes the current progress that has been made on silk hardware in comparison to resorbable systems, metal systems and the target goals for such systems. The potential has now been demonstrated by the combined ability to self-tap, be resterilized for re –use, be functionalized for osteoinduction or other added benefits, resorb in a reasonable time frame and have adequate mechanical properties.

Table 23. Summary of Work [3,6–8,18,22,24,46,48,63–71]

Category	Metal		Resorbable		Ideal New System	Silk
Implantation	Self Tapping (pilot hole)		Pre-drill pilot hole and tapping required		Self Tapping (pilot hole)	Self Tapping (pilot hole)
	In situ plate shaping		Heat to shape plates		In situ plate shaping	Hydrate to shape plates
Mechanical Properties	Pullout:	~ 400 N [69]	Pullout:	95-175 N ([63],[69])	Pullout:~100-200N (non-load bearing, >200N (load bearing)	Pullout:~108N
	Shear:	~550Mpa [68]	Shear:	100-185MPa ([63-66])	Shear: ~100-200 Mpa (non-load bearing), > 200MPa (load-bearing)	Shear:~90MPa
	Bending Mod:	~7GPa [18,24]	Bending Mod:	~7GPa [18,24]	Bending Mod:	Bending: 1-4 Gpa
Degradation	N/A, Permanent		Time: PLLA (over 1 year), PGA (6-12 months), PLGA (~1 year to more than 1.5 years), P(L/DL)LA (2-3 Years) (c,k,r)		Time: Maintain strength for ~3 months, degrade quickly after (~6-12 months)	Time:10 months (maintains 75% strength at 9 weeks)
			Degradation Products: acidic components (inflammatory response) (l,m)		Degradation Products: Biocompatible/biodegradable with no inflammatory response	Degradation Products: amino acids (no inflammatory response) (n-p)
Biocompatability	yes		yes		yes	yes
Resterilization	yes (any method)		no		yes	yes (autoclave)
Elastic Modulus	> 105 Gpa [6]				Close to bone (20 Gpa) [6]	Comp: 2.17 +/- 0.27 GPa
Complications/ Weaknesses (a,q)	Stress Shielding		Inflammatory reaction		None	No inflammatory reaction
	Temperature Sensitivity		Sterile sinus formation			Poor hydrated mechanics
	Plate Exposure or Migration		Osteolysis			Limited applications
	Corrosion		Incomplete bone remodeling			
	Growth Disturbance in Children		Limited applications			
	Palpability					
	Interference with medical imaging					
	Infection					
	Cold sensitivity					
	Possible need for hardware removal					
Benefits	Robust Mechanical Properties		Biodegradable/obviate need for hardware removal		Robust Mechanical Properties	Biodegradable/obviate need for hardware removal
	Ease of Implantation		Avoid stress shielding with close modulus to bone		Ease of Implantation	Avoid stress shielding with close modulus to bone
	Resterilization				Resterilization	Ease of Implantation
					Biodegradable/obviate need for hardware removal	Resterilization
					No complications	
					Match degradation to strength required for fixation	

Chapter 8. Future Work

8.1 Continuation of current lead candidate silk hardware formulation

While improvements and additional data for lead candidate silk hardware formulation (30 minute boiled silk with HFIP processing) show great potential to meet the needs of an ideal fixation system, further characterization and improvements are necessary. Hydrated mechanics remain one of the biggest downfalls for silk devices. Silk hardware must be optimized to either increase overall strength so that hydrated mechanics are comparable to other systems, or to resist hydration and swelling. Swelling could possibly be reduced with a large number of autoclave cycles or possibly other cross-linkers. Fatigue testing will need further investigation, as sample numbers tested in the present work were very low. Silk hardware showed high potential in strength retention after being fatigued and in the ability to retain function after high cycle numbers but a large N value will be necessary for confirmation. Overall mechanical strength could also be increased through reinforcement by particles or fibers[91,92]. Torsional properties will need to be investigated for full mechanical characterization.

In vitro release of BMP-2 was successfully demonstrated but determination of loading quantity will need to be further investigated. An analytical method other than a mass balance must be used due to the very small masses being measured causing great difficulty and limiting specificty. This can be done using a BMP-2 ELISA and precise volume measurements to quantify the amount of BMP-2 in the loading solution before

and after the silk devices were loaded, or by re-dissolving a loaded scaffold and using an ELISA assay. Functionalization by silk coatings will also need to be investigated. Molecules can potentially be incorporated into a silk solution and deposited onto a silk device as a coating. Screws will need to be rotated on a lathe while solution is deposited and dried in order to ensure even deposition and avoid interference with the threads. Loading of other molecules including antibiotics must also be investigated. *In vivo* release of BMP-2 from loaded silk screws appeared to be successful in inducing more collagen deposition and cell activity than controls. However, increased osteoinduction will need to be confirmed by a staining or assay that can quantify bone deposition and mineralization. This can be done with the combined use of von Kosa staining and elctron microscopic analysis, X-ray diffraction or Fourier transform infrared spectroscopy[90].

Another major step in the advancement of silk hardware will be continued *in vivo* studies. The functionalization and release of osteoinductive molecules or antibiotics similarly to BMP-2 release, can be further investigated under current approved protocols in a rat model. Incorporation and release of these molecules will help mediate the healing process and remodeling of bone. Fracture fixation with a silk hardware system will also be essential to determine the ability to stabilize a fracture and retain strength for fracture healing despite weak hydrated mechanics. This may involve initial proof of concept models with silk screw and plate system or silk IM nail for the fixation of a rat femur [93]. A larger model should be investigated in order to better mimic non-load bearing applications in the CMF. This model could include rabbits[36,63,93,94], mini-pigs[95] or sheep[36,67,86,96].

8.2 Aqueous formulation of silk hardware

While HFIP processed silk shows great potential as a resorbable hardware system, it would be highly advantageous to develop an aqueous-based silk formulation. HFIP is a highly toxic organic solvent that would ideally be avoided for safety of the manufacturer as well as the patient. HFIP should be removed during cross-linking with methanol and with subsequent washes. However, one could not be sure that no residual HFIP was present without re-dissolving silk hardware and analyzing the solution by gas chromatography/mass spectrometry or another chemical analysis technique. This would need to be checked regularly under a system of quality control and could be both difficult and costly. The advent of an aqueous silk formulation to create orthopedic hardware with similar mechanical properties would eliminate great risk and concern over the use of toxic organic solvents. Not only would an aqueous system be more safe, but it may be more tunable. Silk has previously been reported as a tunable material but HFIP processed silk proved to have limited control over physical properties with insignificant differences after varying processing conditions and treatments. An aqueous formulation may allow better control of mechanical strength, degradation kinetics and more.

In the present work, aqueous processes were proposed and investigated for proof of concept. Moving forward, these formulations will need to be studied more in depth and other formulations may be attempted. The lead candidate formulation involved concentrating an aqueous silk solution to 20-30% silk protein, followed by cross-linking with methanol, drying and autoclaving. This formulation will need to be investigated for mechanical strength/capabilities, degradation kinetics and functionalization. The effect

of processing parameters should also be studied. For example, change in the boil time and silk concentration may offer great control over physical properties.

Although a high concentration, cross-linked silk formulation proved to have the most potential in the current work, feasibility was only tested for silk screws and IM nails that are machined on a lathe. Therefore, other formulations may be useful for silk plates that require high stiffness. Lithium bromide- formic acid silk formulations will most likely be insufficient for hardware as a stand-alone material; however, the creation of a tight nanofibril structure could be used in the reinforcement of another material. Pressed silk powder was easily machinable and resembled the look, feel and rigidity of a ceramic. Threading appeared to chip the material but machining into plates with a mill or a simple IM nail may be possible. High concentration silk with incorporated silk powder or hydroxyapatite showed high potential in the ability to form a rigid blank but particles created pores that caused chipping during machining. Investigation into loading concentration of the particles as well as particle size could very well lead to a high strength, stiff, machinable material. Although an aqueous process was not completely realized, there exists high potential that is ready to be explored.

References

[1] R. M. Slone, M. M. Heare, R. A. Vander Griend, W. J. Montgomery, *US Pat. …* **1991**, 823.

[2] M. S. Taljanovic, M. D. Jones, J. T. Ruth, J. B. Benjamin, J. E. Sheppard, T. B. Hunter, *Radiographics* **2003**, *23*, 1569.

[3] a Neumann, *Laryngorhinootologie*. **2009**, *88 Suppl 1*, S48.

[4] Inion, **n.d.**

[5] R. T. Adelson, R. J. DeFatta, Y. Ducic, *J. Oral Maxillofac. Surg.* **2007**, *65*, 940.

[6] M. S. Gilardino, M. Sc, E. Chen, S. P. Bartlett, **2009**, *19104*, 49.

[7] R. Suuronen, I. Kallela, C. Lindqvist, *J. Craniomaxillofac. Trauma* **2000**, *6*, 19.

[8] Imola, **2001**, *3*, 79.

[9] M. Suchenski, M. B. McCarthy, D. Chowaniec, D. Hansen, W. McKinnon, J. Apostolakos, R. Arciero, A. D. Mazzocca, *Arthroscopy* **2010**, *26*, 821.

[10] J. Zhang, N. Ebraheim, G. E. Lausé, B. Xiao, R. Xu, *J. Trauma Inj. Infect. Crit. Care* **2011**, *72*, 1.

[11] Biomet, "Lactosorb," can be found under http://www.biomet.com/microfixation/getFile.cfm?id=3174&rt=inline, **n.d.**

[12] CDC/NCHS, "National Hospital Discharge Survey," **2010**.

[13] Reportlinker. MediPoint, "Trauma Fixation-US Analysis and Market Forecasts," can be found under http://www.reportlinker.com/p01853474-summary/MediPoint-Trauma-Fixation-US-Analysis-and-Market-Forecasts.html, **n.d.**

[14] American Society of Plastic Surgeons, *ASPS Public Relations* **2013**.

[15] Synthes, "Rapidsorb," can be found under http://www.synthes.com/sites/NA/Products/Biomaterials/PorousPolyethyleneImplants/Pages/Rapid-Resorbable-Fixation-System.aspx, **n.d.**

[16] J. Simon, J. Ricci, P. Di Cesare, *Am. J. Orthop. (…* **1997**.

[17] B. L. Eppley, *J. Oral Maxillofac. Surg.* **2005**, *63*, 385.

[18] W. S. Pietrzak, D. S. Caminear, S. V Perns, *J. Foot Ankle Surg.* **2002**, *41*, 379.

[19] M. W. Larsen, *Am. J. Sports Med.* **2005**, *33*, 68.

[20] T. Iizuka, **1992**.

[21] R. R. M. Bos, G. Boering, F. R. Rozema, J. A. N. W. Leenslag, **1987**, 751.

[22] J. Simon, J. Ricci, P. Di Cesare, *Am. J. Orthop. (…* **1997**.

[23] Y. Weerakkody, R. et al Schubert, "Fracture Healing," can be found under http://radiopaedia.org/articles/fracture-healing, **n.d.**

[24] R. R. Bos, F. R. Rozema, G. Boering, a J. Nijenhuis, a J. Pennings, a B. Verwey, *Int. J. Oral Maxillofac. Surg.* **1989**, *18*, 365.

[25] R. R. Bos, F. R. Rozema, G. Boering, a J. Nijenhuis, a J. Pennings, a B. Verwey, P. Nieuwenhuis, H. W. Jansen, *Biomaterials* **1991**, *12*, 32.

[26] P. U. Rokkanen, O. Bo, E. Hirvensalo, E. A. Ma, E. K. Partio, S. Vainionpa, **2000**, *21*, 2607.

[27] C. Dumont, M. Fuchs, H. Burchhardt, D. Appelt, S. Bohr, K. M. Stürmer, **2007**, 491.

[28] A. Kumar, D. Staffenberg, … *Craniofacial Surg.* **1997**.

[29] J. Y. Rho, L. Kuhn-Spearing, P. Zioupos, *Med. Eng. Phys.* **1998**, *20*, 92.

[30] D. J. Hadjidakis, I. I. Androulakis, *Ann. N. Y. Acad. Sci.* **2006**, *1092*, 385.

[31] A. Schindeler, M. M. McDonald, P. Bokko, D. G. Little, *Semin. Cell Dev. Biol.* **2008**, *19*, 459.

[32] N. Kakudo, K. Kusumoto, A. Kuro, Y. Ogawa, *Wound Repair Regen.* **2006**, *14*, 336.

[33] M. Egermann, J. Goldhahn, E. Schneider, *Osteoporos. Int.* **2005**, *16 Suppl 2*, S129.

[34] J. Peterson, P. C. Dechow, *Anat. Rec. A. Discov. Mol. Cell. Evol. Biol.* **2003**, *274*, 785.

[35] D. E. Williams, R. L. Mason, B. B. Mcdonald, *J. Nutr.* **1964**, *84*, 373.

[36] a I. Pearce, R. G. Richards, S. Milz, E. Schneider, S. G. Pearce, *Eur. Cell. Mater.* **2007**, *13*, 1.

[37] P. P. Lelovas, T. T. Xanthos, S. E. Thoma, G. P. Lyritis, I. a Dontas, *Comp. Med.* **2008**, *58*, 424.

[38] J. Irish, A. S. Virdi, K. Sena, M. a McNulty, D. R. Sumner, *J. Orthop. Res.* **2013**, *31*, 800.

[39] D. N. Rockwood, E. Seok, S. Park, J. A. Kluge, W. Grayson, S. Bhumiratana, R. Rajkhowa, X. Wang, S. Jun, G. Vunjak-novakovic, D. L. Kaplan, *Acta Biomater.* **2011**, *7*, 144.

[40] C. Vepari, D. L. Kaplan, **2007**, *32*, 991.

[41] D. N. Rockwood, R. C. Preda, T. Yücel, X. Wang, M. L. Lovett, D. L. Kaplan, **2011**, DOI 10.1038/nprot.2011.379.

[42] G. H. Altman, F. Diaz, C. Jakuba, T. Calabro, R. L. Horan, J. Chen, H. Lu, J. Richmond, D. L. Kaplan, *Biomaterials* **2003**, *24*, 401.
[43] L. Zhou, X. Chen, Z. Shao, Y. Huang, D. P. Knight, *J. Phys. Chem. B* **2005**, *109*, 16937.
[44] D. Wilson, R. Valluzzi, D. Kaplan, *Biophys. J.* **2000**, *78*, 2690.
[45] R. L. Horan, K. Antle, A. L. Collette, Y. Wang, J. Huang, J. E. Moreau, V. Volloch, D. L. Kaplan, G. H. Altman, *Biomaterials* **2005**, *26*, 3385.
[46] K. Numata, P. Cebe, D. Kaplan, *Biomaterials* **2010**, *31*, 2926.
[47] B. Panilaitis, G. H. Altman, J. Chen, H. Jin, V. Karageorgiou, D. L. Kaplan, **2003**, *24*, 3079.
[48] Y. Wang, D. D. Rudym, A. Walsh, L. Abrahamsen, H. S. Kim, C. Kirker-head, D. L. Kaplan, **2008**, *29*, 3415.
[49] S. Hofmann, C. T. W. P. Foo, F. Rossetti, M. Textor, G. Vunjak-Novakovic, D. L. Kaplan, H. P. Merkle, L. Meinel, *J. Control. Release* **2006**, *111*, 219.
[50] D. J. Hines, D. L. Kaplan, *Biomacromolecules* **2011**, *12*, 804.
[51] Q. Lu, X. Wang, X. Hu, P. Cebe, F. Omenetto, D. L. Kaplan, *Macromol. Biosci.* **2010**, *10*, 359.
[52] S. Lu, X. Wang, Q. Lv, X. Hu, N. Uppal, D. L. Kaplan, *Biomacromolecules* **2010**, *10*, 1032.
[53] J. Zhang, E. Pritchard, X. Hu, T. Valentin, B. Panilaitis, F. G. Omenetto, D. L. Kaplan, *Proc. Natl. Acad. Sci. U. S. A.* **2012**, *109*, 11981.
[54] C. Kirker-Head, V. Karageorgiou, S. Hofmann, R. Fajardo, O. Betz, H. P. Merkle, M. Hilbe, B. von Rechenberg, J. McCool, L. Abrahamsen, A. Nazarian, E. Cory, M. Curtis, D. Kaplan, L. Meinel, *Bone* **2007**, *41*, 247.
[55] C. Li, C. Vepari, H.-J. Jin, H. J. Kim, D. L. Kaplan, *Biomaterials* **2006**, *27*, 3115.
[56] V. Karageorgiou, L. Meinel, S. Hofmann, A. Malhotra, V. Volloch, D. Kaplan, *J. Biomed. Mater. Res. A* **2004**, *71*, 528.
[57] D. Roccatano, M. Fioroni, M. Zacharias, G. Colombo, **2005**, 2582.
[58] N. Hirota, K. Mizuno, Y. Goto, *Protein Sci.* **1997**, *6*, 416.
[59] Z. H. Zhu, *eXPRESS Polym. Lett.* **2008**, *2*, 885.
[60] C. Zhao, J. Yao, H. Masuda, R. Kishore, T. Asakura, **2002**, 253.
[61] C. Chen, C. Chuanbao, M. Xilan, T. Yin, Z. Hesun, *Polymer (Guildf).* **2006**, *47*, 6322.
[62] U.-J. Kim, J. Park, H. J. Kim, M. Wada, D. L. Kaplan, *Biomaterials* **2005**, *26*, 2775.
[63] N. Ashammakhi, M. Veiranto, E. Suokas, J. Tiainen, S.-M. Niemelä, P. Törmälä, *J. Mater. Sci. Mater. Med.* **2006**, *17*, 1275.
[64] J. Tiainen, Y. Soini, P. To, T. Waris, N. Ashammakhi, **2004**, 49.
[65] J. Tiainen, S. Leinonen, J. Ilomäki, *J. …* **2002**.
[66] T. Mäkinen, M. Veiranto, J. Knuuti, J. Jalava, *Bone* **2005**, *36*, 292.
[67] C. a. Landes, A. Ballon, C. Roth, *J. Biomed. Mater. Res. Part B Appl. Biomater.* **2006**, *76B*, 403.
[68] MatWeb LLC, "Titanium Ti-6Al-4V (Grade 5)," **2014**.
[69] J. Wittenberg, R. Wittenberg, J. Hipp, *J. oral Maxillofac. …* **1991**, 512.
[70] H. K. Makadia, S. J. Siegel, *Polymers (Basel).* **2011**, *3*, 1377.
[71] Y. Cao, B. Wang, *Int. J. Mol. Sci.* **2009**, *10*, 1514.
[72] G. S. Perrone, G. G. Leisk, T. J. Lo, J. E. Moreau, D. S. Haas, B. J. Papenburg, E. B. Golden, B. P. Partlow, S. E. Fox, A. M. S. Ibrahim, S. J. Lin, D. L. Kaplan, *Nat. Commun.* **2014**, *5*, 3385.
[73] T. Metzger, **2011**, *3*.
[74] P. Vaananen, *Testing of Biodegradable Bone Fixation Implants In Vitro and Clinical Experiments*, **2009**.
[75] M. DeTora, K. Kraus, *Vet. Comp. Orthop. Traumatol.* **2008**, 318.
[76] F. Mujika, *Polym. Test.* **2006**, *25*, 214.
[77] V. Karageorgiou, M. Tomkins, … *Res. Part A* **2006**, DOI 10.1002/jbm.a.
[78] H. D. Kim, R. F. Valentini, **2001**, DOI 10.1002/jbm.10011.
[79] A. G. M. Ruhe, P.Q., E.L. Hedberg, N.T. Padron, P.H.M. Spauwen, J.A. Jansen, *J. Bone Jt. Surg.* **2003**, *85(suppl 3*, 75.
[80] I. Migneault, C. Dartiguenave, M. J. Bertrand, K. C. Waldron, *Biotechniques* **2004**, *37*, 790.
[81] L. S. Wray, X. Hu, J. Gallego, I. Georgakoudi, F. G. Omenetto, D. Schmidt, D. L. Kaplan, *J. Biomed. Mater. Res. B. Appl. Biomater.* **2011**, *99*, 89.
[82] A. H. Fischer, K. A. Jacobson, J. Rose, R. Zeller, **n.d.**, 9.
[83] M. L. Jones, H. T. Ascp, **2010**, 79.

[84] L. Ylikontiola, K. Sundqvuist, G. K. B. Sàndor, P. Törmälä, N. Ashammakhi, *Oral Surgery, Oral Med. Oral Pathol. Oral Radiol. Endodontology* **2004**, *97*, 312.
[85] E. Baumgart, *Injury* **2000**, *31 Suppl 2*, S.
[86] J. W. Leenslag, a J. Pennings, R. R. Bos, F. R. Rozema, G. Boering, *Biomaterials* **1987**, *8*, 70.
[87] K. J. Bozic, L. E. Perez, D. R. Wilson, P. G. Fitzgibbons, J. B. Jupiter, *J. Hand Surg. Am.* **2001**, *26*, 755.
[88] V. Karageorgiou, D. Kaplan, *Biomaterials* **2005**, *26*, 5474.
[89] E. M. Pritchard, T. Valentin, D. Boison, D. L. Kaplan, *Biomaterials* **2011**, *32*, 909.
[90] L. F. Bonewald, S. E. Harris, J. Rosser, M. R. Dallas, S. L. Dallas, N. P. Camacho, B. Boyan, a Boskey, *Calcif. Tissue Int.* **2003**, *72*, 537.
[91] B. B. Mandal, A. Grinberg, E. Seok, B. Panilaitis, D. L. Kaplan, **2012**, *109*, DOI 10.1073/pnas.1119474109.
[92] R. Rajkhowa, E. S. Gil, J. Kluge, K. Numata, L. Wang, X. Wang, D. L. Kaplan, **n.d.**, 599.
[93] J. T. Viljanen, H. K. Pihlajamäki, P. O. Törmälä, P. U. Rokkanen, *J. Orthop. Res.* **1997**, *15*, 398.
[94] O. M. Böstman, O. M. Laitinen, O. Tynninen, S. T. Salminen, H. K. Pihlajamäki, *J. Bone Joint Surg. Br.* **2005**, *87*, 1575.
[95] I. N. G. Springer, P. H. Warnke, H. Terheyden, Y. Açil, A. Bülhoff, S. Kuchenbecker, H. Bolte, P. a J. Russo, E. G. Vairaktaris, J. Wiltfang, *J. Craniomaxillofac. Surg.* **2007**, *35*, 177.
[96] J. E. Bergsma, W. C. de Bruijn, F. R. Rozema, R. R. Bos, G. Boering, *Biomaterials* **1995**, *16*, 25.